THERMOPOWER AND RESISTIVITY OF BINARY METALLIC GLASSES

by

Mario Norberto Baibich

A thesis submitted to the Faculty of Graduate Studies and Research of McGill University in partial fulfillment of the requirements for the Degree of Doctor of Philosophy

Rutherford Physics Building
Department of Physics
McGill University
Montreal, Quebec

January 1982

ABSTRACT

The resistivity and thermopower of two series of amorphous alloys have been measured between 4 and 300K. The alloys studied are MgZn and CuZr, both in the largest concentration range available as amorphous materials. The alloys were measured in both the 'as made' and 'relaxed' states, as well as some partial or totally crystallized samples. The simple Ziman theory was found at variance with the experimental results in both cases (even for MgZn, proven to be free-electron like as required by the theory). A simple two component model is proposed as an extreme simplification of the Faber-Ziman theory of liquid metallic alloys. The excellent agreement obtained indicates that metallic glasses should be considered as the alloys they really are. A full Faber-Ziman calculation is performed for CuZr and from this follows the conclusion that the term containing the energy dependence of the pseudopotential (r), usually assumed to be small, is probably of comparable magnitude to that of the disorder scattering (q). The suggested correlations between the electron-phonon mass-enhancement parameter λ (determined from superconductivity experiments) and the temperature dependence of the resistivity or the thermopowers are studied and both found not to be valid for CuZr amorphous alloys.

RESUME

La resistivité et le pouvoir thermoélectrique de deux séries d'alliages amorphes ont été mesurés entre 4 et 300K. L'étude a porté sur le MgZn et le CuZr, et dans les deux cas dans la plus vaste gamme de concentrations disponible pour ces materiaux amorphes. Les mesures ont été effectuées sur des échantillons d'abord tels que produits, puis soumis á relaxation et enfin partiellement ou totalement cristallisés.

La theorie simple de Ziman est trouvée en desaccord avec les resultats expérimentaux dans tous les cas traités (même pour la MgZn, dont le comportement électronique semble être du type d'un gaz d'electrons libres, ce qu'exige le modele). Une modéle simple à deux composantes, schématisant a l'extrême la théorie de Faber-Ziman sur les alliages métalliques liquides, est proposé. L'excellent accord obtenu indique que les verres métalliques doivent être considérés comme les alliages qu'ils sont de fait. Un calcul complet de Faber-Ziman est mené pour le CuZr; on en déduit que le terme contenant la dépendence energetique du pseudopotentiel (r), généralement consideré petit, est probablement de l'ordre de grandeur de celui de la "diffusion de désordre" (q).

Les corrélations suggérées entre le parametre λ d'augmentation de masse par interaction electron-phonon (determiné à partir d'expériences de supra-conductivité) et la dépendence en temperature de la resistivité et du pouvoir thermoélectrique sont étudiées. Elles semblent ne pas être acceptables pour les alliages amorphes de CuZr.

STATEMENT OF ORIGINALITY

This thesis describes original measurements, by the author, of electrical resistivity and thermopowers of two series of amorphous metallic alloys, namely MgZn and CuZr, in the widest range of compositions available in the amorphous state, The alloys were also measured in different stages of relaxation or crystallization.

The samples were provided, along with X-ray characterization, by Drs. Z. Altounian and Tu Guo-hua, of this laboratory. Part of the programming was done by P. Cotnoir and M. Olivier.

To the best of my knowledge, this work is the first systematic study of thermopower and resistivity in simple binary amorphous alloys. This thesis advances significantly the understanding of transport phenomena in metallic glasses.

ACKNOWLEDGEMENTS

I would like to thank my supervisor, W.B. Muir, for all of his help in this work.

My thanks also go to all those too numerous to list in the Physics Department who helped me in one way or another.

Discussions with Dr. C. Foiles were most helpful and stimulating.

To all of my friends in Montreal, my recognition for their friendship and hospitality.

Special thanks are due to Joanne Hay for her efficient and careful typing of this thesis.

Financial support from C.N.Pq. (Brazil) is gratefully acknowledged.

Finally, my eternal gratitude for the patience and understanding of my wife and son whose love made finishing this thesis possible.

TABLE OF CONTENTS

LIST OF FIGURES

CHAPTER V

NOTE ON UNITS

The majority of units in this thesis conform to the Systeme International (SI). Those that do not are used for consistency with other published work on the subject. Their SI equivalents are given below.

LENGTH	1cm	$= 10^{-2}$m
	1A	$= 10^{-10}$m
PRESSURE	1 atm	$= 1.013 \times 10^{2}$kPa
ENERGY	1 eV	$= 1.60219 \times 10^{-19}$ joules
RESISTIVITY	1$\mu\Omega$-cm	$= 10^{-8}\ \Omega$-m
THERMOPOWER	1μV/K	$= 10^{-6}$ V/K

I. INTRODUCTION

Amorphous materials have been extensively studied in the past few years. In particular, great interest has focused on metallic glasses. Those materials, in common with their non metallic counterparts, possess no long range structural order although a certain degree of short range order is preserved. For metallic amorphous alloys this short range order is limited to a much smaller distance than that found for amorphous covalent semiconductors or insulators[1].

The composition of metallic glasses can be classified into two groups:

(a) alloys of transition or noble metals with a metalloid of group IV or V acting as a glass former, e.g. $Fe_{80}B_{20}$

(b) alloys not containing glass formers, e.g. CuZr, MgZn, TbFe, etc.

The usual production techniques for metallic glasses include among others:

(a) deposition from a liquid solution

(b) rapid quenching from the melt

(c) evaporation

(d) sputtering

(e) chemical precipitation.

The magnetic properties of amorphous metals have been widely studied due to the potential commercial use of these materials as transformer cores, magnetic shielding and permanent magnets. The mechanical properties are also of interest as some of these materials possess tensile strength comparable to the strongest steels[2].

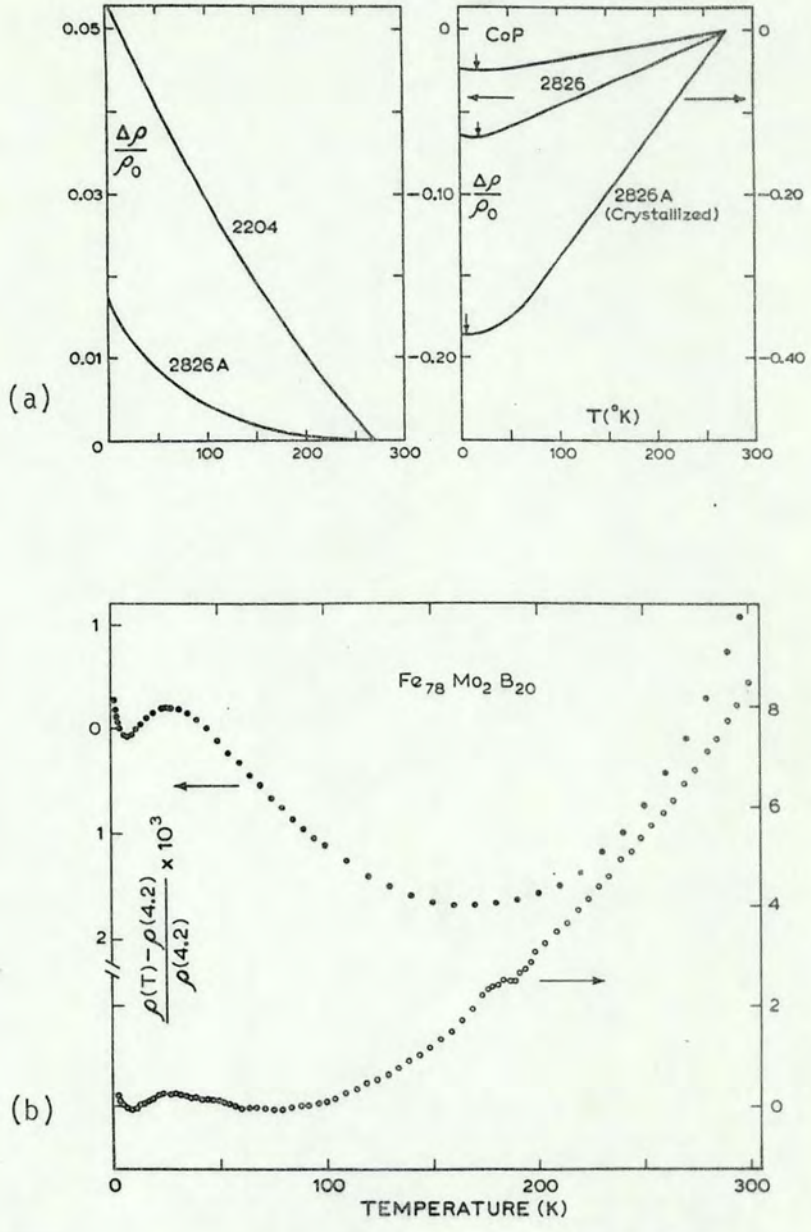

FIG. I - 1 - The electrical resistivities of some metallic glasses

(a) - the resistivities of some Metglas alloys and CoP, after R.W. Cochrane and J.O. Strom-Olsen[5].

(b) - the resistivities of two samples of Metglas 2605A, after R.W. Cochrane[1].

Soon after the first amorphous metallic alloys were made by Duwez[3], their resistivity and thermopower were measured in that laboratory[4]. Since that time the number of measurements of resistivity have grown in number at an ever increasing rate.

The conductivity of metallic glasses has been studied over four orders of magnitude on the temperature scale (∿50 mK to ∿700°C). The total change seen over this wide range of temperature does not exceed, in general, 10% of the total resistivity. A typical value for the resistivity of amorphous metals would be in the 100 to 300μΩ-cm range. Fig. I-1 shows some of the curves obtained experimentally for the resistivity of metallic glasses.

In most amorphous metals a region with negative temperature coefficient is present, whether followed by a minimum or not. Also, the functional form of the resistivity is not modified by the presence of a strong magnetic field (∿50 kG) although its magnitude may change due to domain effects and the normal orbital magnetoresistance. This holds even for the ferromagnetic amorphous alloys[5], precluding the simple application of the Kondo model[6] to explain the negative temperature coefficient of the resistivity. The Kondo effect is found in crystalline alloys of non magnetic hosts with small concentrations of magnetic impurities, and the model explains the rise in resistivity with lowering temperature by assigning the extra scattering needed to transitions between two spin states. The application of a strong magnetic field suppresses the extra scattering by aligning the spin of the isolated magnetic ion in the direction of the applied field giving a large change in $d\rho/dT$ in these alloys.

The structure (or lack of it) most probably plays an important role in the negative $d\rho/dT$ observed for some range of temperatures in the amorphous alloys. This lack of structure is a common property of all metallic glasses, as is the negative $d\rho/dT$. From these observations, two groups of theories have b proposed to explain the observed effects: one is based on extensions of the Kond theory and is applicable at low temperatures, and the other group is based on extensions of Ziman's theory of electron transport in liquid metals[7].

The extensions of the Kondo theory comprise a model where only some of the transition element atoms are in a negligibly small internal field, leading to a Kondo effect even when the sample is ferromagnetic[8,9], and an alternative model where the excess scattering is due to structural degrees of freedom inherent in the lack of atomic periodicity in the material[10]. In this model an ion is considered to be able to occupy either of two equivalent sites. The two tunneling levels can provide the necessary degrees of freedom which were provided by the spin orientations in the original Kondo effect.

The extensions of Ziman's theory are associated with the idea that the amorphous metal is merely a frozen liquid and therefore all the expressions derived for the liquid are valid for the metallic glass. Upon freezing of the liquid a relaxation time arises from the absence of translational symmetry in the ionic potential which produced incoherent electron scattering. This relaxation time, τ_z, is the only source of scattering considered in Ziman's theory of the resistivity of liquid metals.

The relaxation time can be written in terms of the ionic pseudo-potential and the liquid structure factor. The ionic pseudo-potential is derived from the potentials associated with individual ions. The liquid

structure factor may be inferred from X-ray and neutron diffraction experiments and it describes the scattering of electrons by the ion cores. For a totally random distribution of the ions, the structure factor would have a value of 1.

The temperature dependence of the structure factor, and the position of its first peak relative to the Fermi wave vector of the alloy ($2k_F \sim K_p$)[(a)], account for the negative temperature coefficients of the resistivity.

As seen above, more than one model is able to explain the results found in amorphous metals, so other electronic transport parameters should be used to test the theories in question. This implies changing the experimental boundary conditions: resistivity experiments are conducted at a constant temperature (no temperature gradients on the sample) with the application of an electric field.

By applying a thermal gradient only, we can study the thermal conductivity (κ), that relates the heat flow to the thermal gradient to the sample. Since the carriers of heat in this situation are mainly electrons, an electric current will be present and thus a voltage will develop between the ends of the sample. This difference of potential between the two points at different temperatures will be related to both the thermal gradient applied and the conductivity of the sample. This effect, called THERMOPOWER or SEEBECK EFFECT, relates the thermal gradient applied to the consequent electric field.[(b)]

Since the beginning of the studies of transport phenomena in amorphous metals, the thermopower has been used as a test for the proposed theories.

(a) this criterion is also used in a theory of the formation of amorphous metals[(11)]

(b) for a detailed discussion of thermopower see R.D. Barnard[(31)], chapter 1

This was done by Sinha[4] to whom we owe the first measurements of thermopower on amorphous metals; his results on NiPtP alloys were found to be positive and linear in temperature, in accordance with Ziman's theory for liquid metals.

About seven years later Korn and Mürer[12] published results on the measurement of the thermopower of SnCu vapor deposited amorphous and partially crystalline alloys. Their results, partly because of the material preparation method and partly on account of the evident crystallization taking place during the measurements, are to be regarded with caution. Somewhat later Nagel[13] published his results on a single TiBeZr alloy. His conclusion was that only the Ziman theory could explain the observed linear thermopower and negative temperature dependence of the resistivity. In 1979 Cote and Meisel[14] published the high temperature thermopower and resistivity results of amorphous NiP, and interpreted them in terms of liquid metal theory. In the same year the article by Baibich et al[15] appeared with the measurements on six metallic glasses. The results can be summarized as follows: the behaviour of the only non magnetic alloy (BeTiZr) among the samples is linear in temperature down to about 40K (see Fig. I-2); at lower temperatures it resumes a linear behaviour, pointing to zero as expected thermodynamically with a larger slope than at high temperatures. The 'magnetic'[(a)] samples, however, showed no consistent correlation between the experiment and any of the proposed theories. The other result was that the contribution from Kondo-type thermopowers (if there is any) to the total thermopower is greatly reduced

---

(a) not necessarily magnetic, but containing magnetic transition elements.

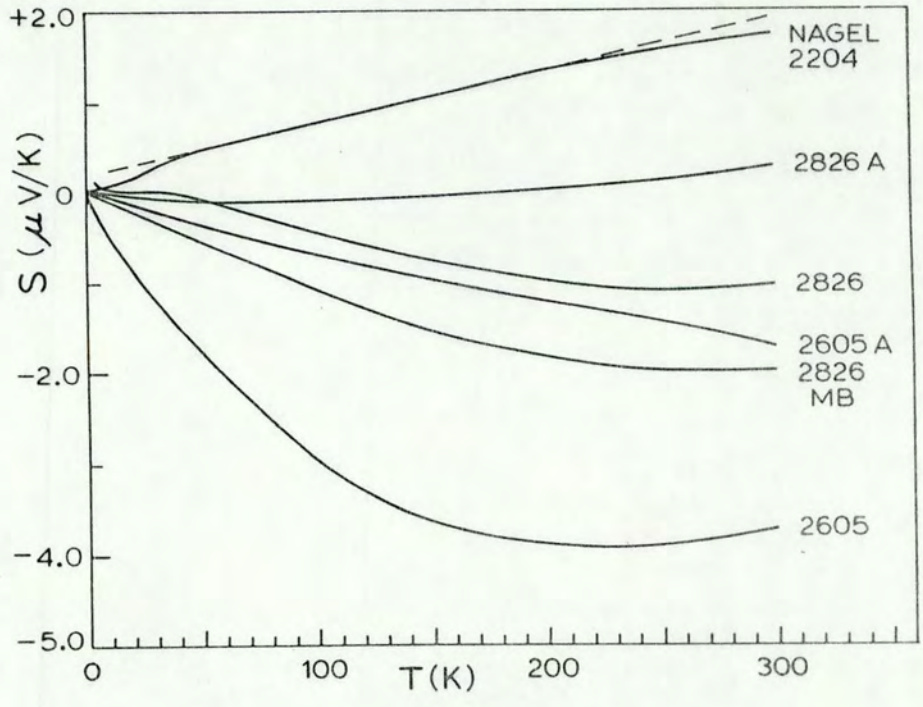

FIG. I - 2 - The thermopower of some metallic glasses, after M.N. Baibich et.al.[15].

in amorphous metals due to the large residual resistivities characteristic of these alloys, since these processes contribute to the thermopower through the Nordheim-Görter rule. This rule says that the total thermopower of a metal is the result of the resistivity weighted average of each of the processes involved.

In order to improve the understanding of thermoelectric effects in amorphous metals it is evident that a systematic study of the behaviour of the non-magnetic amorphous metallic alloys was needed to establish the role of the structural disorder in the transport phenomena of these alloys. Accordingly, we undertook the study presented in this thesis consisting of the measurements of the resistivity and thermopower of two series of amorphous metallic alloys. The alloy systems chosen were MgZn and CuZr. The first series was chosen for its free electron behaviour, as required by the Ziman liquid metal theory, but for which only one total structure factor is known; and the second because of the complete structural information available allowing us to conduct a thorough investigation of the structural aspects of the liquid metal theories.

The use of Kondo-type theories was restricted to studies of changes in thermopower and resistivity upon thermal relaxation of the alloys. This is because of the small thermopower contribution coming from Kondo-type processes, since there is a drastic reduction through the Nordheim-Görter rule[15].

During the course of this work, other publications on the subject have appeared. Namely a number of articles by Nagel and collaborators[16] basically confirming the findings of Baibich et al[15]; a note by Cochrane et al[17] on the systems PdSi, CuZr, MgZn (these are preliminary results on

some of the alloys studied in this thesis), and a letter by Gallagher[18] on three compositions of CuZr amorphous alloys. This later work suggested a correlation between the thermopowers at high and low temperatures with the electron-phonon mass-enhancement effects seen in superconductivity.

In accordance with the suggested mass enhancement correlation, a study of the relation between the thermopower and the known superconducting transition temperatures of CuZr alloys was undertaken.

In Chapter II we present the experimental procedures used in this thesis, as well as details of the sample preparation.

Chapter III is devoted to the outline of the theories to be used in the interpretation of the experimental results, presented in Chapter IV.

Chapter IV contains the analysis of the experimental results along the lines of different approaches to the Ziman theory. A simple two component model is proposed, which can be regarded as a simplification of the Faber-Ziman model for liquid metallic alloys[19]. The proposed contribution of the mass enhancement effects to the thermopower or temperature dependence of the resistivity are also discussed.

II - EXPERIMENTAL

The resistance and thermopower data reported in this thesis were measured using the probe shown schematically in Figure II-1.

After the samples are in place, the top clamp of the probe is wrapped in cotton to reduce convection effects. In operation, the probe is first completely submerged in liquid He and the value of the resistance at 4.2K is determined. At this point, the lock-in amplifier for the thermopower measurements is phase aligned by a method to be described later.

The probe is then raised so that the liquid helium level is about half way between the two clamps; power is then applied to the heater through a temperature controller. The thermal e.m.f. and resistance are continuously recorded as a function of temperature.

The temperature is measured with a calibrated carbon glass resistance thermometer[(a)] using a digital conductance bridge[(b)] modified so that an analog signal proportional to the thermometer conductivity can be obtained. This signal in conjunction with a ramp generator is used in a feedback configuration to provide a smooth and gradual temperature increase with time.

The sample resistance was measured using a four probe AC technique with a bridge described in detail by Cochrane et al[(20)]. The DC output of the lock-in amplified in this circuit, which is proportional to changes in sample resistance, is measured using a digital voltmeter.

The circuit used for the measurement of the thermopower is similar to that described by Edwards[(21)], and is schematically shown in Figure II-2.

(a) Lake Shore Cryotronics - CGR-200A-C1254

(b) SHE Corporation - Model PCB

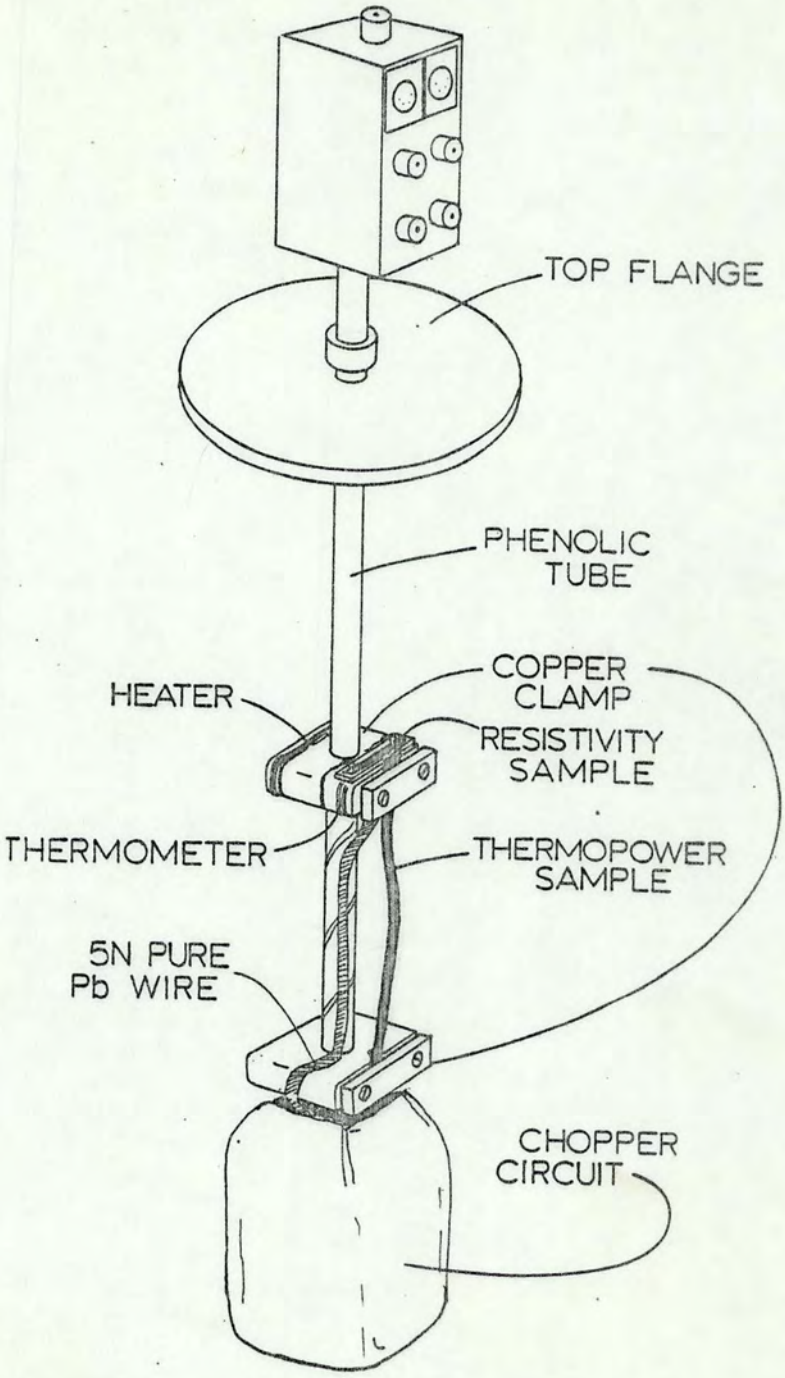

FIG. II - 1 - Schematic diagram of the apparatus

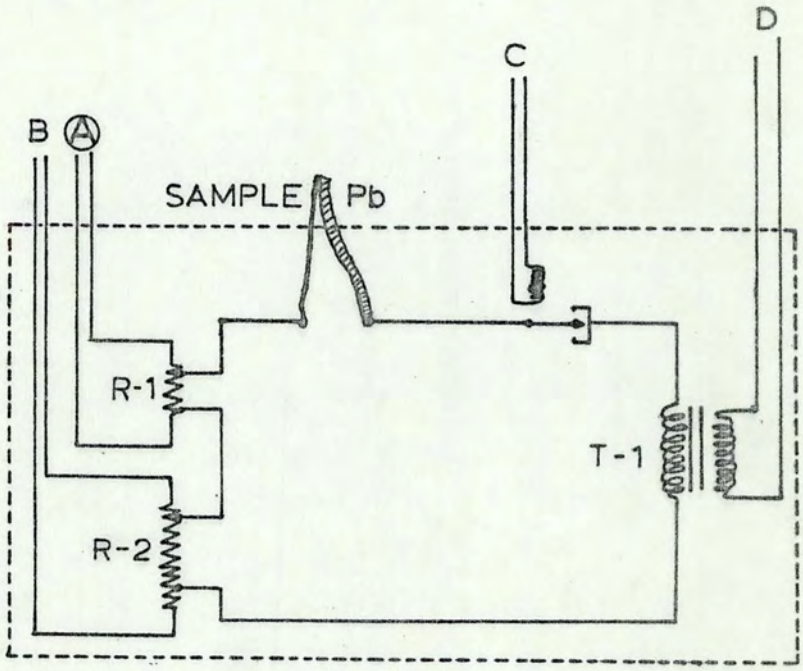

FIG. II - 2 - Thermopower Measuring Circuit

The section inside the broken lines is kept immersed in liquid helium. The method of operation is described in the text.

It consists basically of an electromechanical chopper[a] with its two stationary contacts connected together, placed in the circuit so as to modulate the current flowing through the primary of the transformer T-1[b].

The AC voltage across the transformer secondary is proportional to the difference between the e.m.f. of the sample-Pb thermocouple and the voltage developed by a D.C. current flowing through either resistor R_1 or R_2. This D.C. current is supplied from the output of the lock-in amplifier which is used to measure the AC voltage at the secondary of transformer T-1, thus completing the feedback loop. With the feedback connected, the system is an auto-null servo loop where the feedback current is proportional to the sample-Pb thermal e.m.f.

The lock-in amplifier is phase aligned by breaking the feedback loop at the current terminal of the low standard resistor (A in Fig. II-2) and driving the resistor with a battery thus providing a large signal at the input of the lock-in amplifier. The phase of the lock in amplifier can then be adjusted in the usual way.

With the chopper connected as shown, the signal frequency at the secondary T_1 is twice the chopper drive frequency. This greatly reduces the chance of mixing between the chopper drive and the signal circuit. In this respect it is worthwhile making the chopper drive as pure a sine wave as possible since any second harmonic will couple directly into the signal circuit.

As a further precaution against noise amplification both the chopper and the transformer are individually encased in Pb foil. The complete

---

(a) AIRPAX - Contact Modulator Model 30A

(b) U.T.C. Transformer Model O-1

circuit is also wrapped in Pb foil, as shown in Fig. II-1.

The sample-Pb thermal e.m.f. is obtained by measuring the feedback current through the standard resistor. This current is obtained by measuring the voltage developed across a 1 kΩ standard resistor[a] in the feedback loop using a digital voltmeter. The digital outputs of the voltmeters and the thermometer bridge form part of a computer based automatic data gathering system. This system reads the instruments simultaneously every 2 seconds providing, in our case, a density of experimental points of about 6 points/K.

All of the amorphous samples measured in these experiments were made in this laboratory[22,23] using a melt-spin technique in a reduced pressure argon atmosphere. The alloys measured had nominal compositions given by $Mg_{(1-x)}Zn_x$ (x = 0.20, 0.25, 0.30, 0.33, 0.35) and $Cu_{(1-y)}Zr_y$ (y = 0.30, 0.35, 0.40, 0.45, 0.50, 0.55, 0.60, 0.67, 0.70).

A sample of all of the resulting ribbons was examined by x-rays to ensure absence of crystalline lines. All of the ribbons were kept immersed in liquid nitrogen until measured.

The samples for thermopower measurements were simply cut to size from the ribbons; the resistance samples had six[b] copper wire contacts spot-welded using a simple home made capacitor dischange device. In the case of MgZn samples, contacts could not be permanently attached, thus a simple pressure contact apparatus was used (see Fig. II-3).

For each of the thermally treated samples, the room temperature

---

(a) General Radio Co., Cambridge, Mass. U.S.A.

(b) Six contacts were attached instead of the usual four on account of the fragility of the contacts, since the spot welding of the wire crystallizes a small region around it, which becomes very brittle.

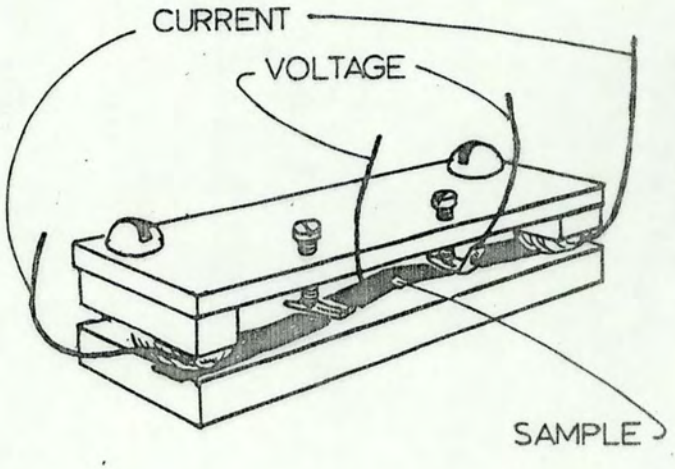

FIG. II - 3 - Pressure contact apparatus for resistance measurements.

resistances of all combinations of contacts were measured prior to heat treatment for later reference.

The thermal treatment was performed in sealed Pyrex tubes, each containing one resistance and one thermopower sample of the same composition. In the case of relaxation of CuZr or crystallization of MgZn, partial argon pressure ($\sim$ 0.85 atm) was used; for the partial crystallization experiment, partial pressure ($\sim$ 0.3 atm) of Helium obtained from the boil-off of a liquid Helium container was used[(a)].

The thermal relaxation of the amorphous CuZr samples was achieved by placing the sealed ampoules in a furnace set at 200°C for a period of 2 hours[(b)].

The crystallization of the MgZn samples followed a similar process, except for the temperature, now set around 120°C.

The partial crystallization of the $CuZr_2$ samples was performed following the results of Altounian et al[(22)]. Eight sealed ampoules were placed inside a furnace, set at 318°C, at the same time. They were left at that temperature for times as shown in the table below (Table II-1).

The composition and treatment of all the samples measured in these experiments are shown in Table II-2.

(a) this is to avoid any oxygen contamination[(22)]

(b) the temperature and time for relaxation were determined by independent mechanical stress relief experiments[(24)].

TABLE II-1

CRYSTALLIZATION OF $CuZr_2$

SAMPLE IDENTIFICATION	TIME OF ANNEAL* (hours)	EXPECTED CRYSTALLIZED FRACTION
EE	0	0
FF	**	
GG	8h 36min	12.5%
HH	10h 36min	25.0%
II	12h 24min	37.5%
JJ	14h	50.0%
KK	17h 35min	62.5%
LL	19h	75.0%
MM	23h 24min	87.5%
NN	50h	100.0%

* - at 318°C

** - at 200°C for 2 hours (relaxation)

TABLE II-2

MEASURED SAMPLES

SAMPLE	COMPOSITION		AS MADE		RELAXED		CRYSTALLIZED	
			R	S	R	S	R	S
	Cu	Zr						
	30	70	*	*		*		
EE	33	67						
FF					*	*		
GG							*	*
HH							*	*
II							*	*
JJ							*	*
KK							*	*
LL							*	*
MM							*	*
NN							*	*
	40	60	*	*	*	*		
	45	55	*	*	*	*		
	50	50	*	*	*	*		
	55	45	*	*		*		
	60	40	*	*	*	*		
	65	35	*	*	*	*		
	70	30	*	*	*	*		
	Mg	Zn						
	65	35	*	*				
	67	33	*	*				
	70	30	*	*			*	*
	75	25	*	*				
	80	20	*	*			*	*

R - RESISTANCE

S - THERMOPOWER

III - THEORY

In this chapter we present some of the details of the two groups of theories advanced for the understanding of the electronic transport phenomena in amorphous metals. The two groups of theories are 1) an extension of the theory developed by Faber and Ziman[19] to explain the behaviour of liquid metals and alloys and 2) a model where the Kondo-type scattering is due to structural degrees of freedom inherent in the lack of atomic periodicity in the material (magnetic Kondo or Kondo-like effects are not considered since our samples contain no magnetic impurities).

III - 1 The liquid metal model

It is claimed that in an amorphous solid the disordered structure resembles that of a liquid and that the time of interaction between the conduction electrons and the scattering centres is so small that the scattering in both liquid and solid are practically independent of ionic motion.

The basic assumption of Ziman's model[a] for liquid metals is that the electrons behave like a degenerate nearly free electron gas which is scattered by the irregular array of ionic cores. In this case, we can use the simple expression for the conductivity obtained from a linear

---

(a) This is presented as a condensation of various review articles by Ziman[25], Faber[26], and Bradley et al[27], as well as some of the original papers on the specific subjects.

response theory:

$$\sigma = \frac{1}{3} e^2 v_F^2 \tau \mathcal{N}(\varepsilon_F) \qquad (1)$$

where e is the electronic charge, v_F is the Fermi velocity, τ is the relaxation time and $\mathcal{N}(\varepsilon_F)$ is the electronic density of states at the Fermi energy.

The relaxation time is given by

$$\frac{1}{\tau} = \int (1 - \cos\theta) Q(\theta) d\Omega \qquad (2)$$

where $Q(\theta)$ represents the probability of scattering through an angle θ into the solid angle $d\Omega$.

The probability of scattering is given by the 'golden rule':

$$Q(\theta) = \frac{2\pi}{\hbar} |\langle \underset{\sim}{k}|U|\underset{\sim}{k}'\rangle|^2 \frac{1}{2} \frac{\mathcal{N}(\varepsilon_F)}{4\pi} \qquad (3)$$

the states $|\underset{\sim}{k}\rangle$ and $|\underset{\sim}{k}'\rangle$ are both on the Fermi surface, and the factor of 1/2 arises from the fact that the spin does not change on scattering (this makes 1/2 of the total available states forbidden after the transition). The potential $U(\underset{\sim}{r})$ is the result of the superposition of all ionic potentials at the point $\underset{\sim}{r}$:

$$U(\underset{\sim}{r}) = \sum_i u(\underset{\sim}{r} - \underset{\sim}{R}_i)$$

where R_i is the position of the i^{th} ion.

In evaluating the integral $\langle k|U|k'\rangle$ we follow Harrison[28] and use

Fourier transformations rather liberally to obtain the well known result:

$$|\langle k|U|k'\rangle|^2 = \frac{1}{N} |u(K)|^2 a(K) \quad , \tag{4}$$

where $K = k - k'$, N is the number of ions, a(K), the structure factor, is given by

$$a(K) = \frac{1}{N} \langle |\sum_i \exp(iK.R_i)|^2 \rangle \tag{5}$$

and u(K) is the pseudo potential that describes the ionic interaction in K space.

The integral $\langle k|U|k'\rangle$ can also be expressed in terms of scattering matrices[29] t such that

$$|\langle k|U|k'\rangle|^2 = \frac{1}{\Omega} |t(k,k')|^2 a(K) \tag{6}$$

For states on the Fermi surface ($|k\rangle$ and $|k'\rangle$ are defined as being at ε_F) we can use geometrical arguments to obtain

$$K = 2k_F \sin \tfrac{1}{2}\theta \tag{7}$$

The expression for the resistivity is obtained from the substitution of (2), (3) and (4) into (1), giving:[(a)]

$$\rho = \frac{3\pi}{\hbar e^2} \frac{1}{v_F^2} \frac{1}{N} \int_0^1 |u(K)|^2 a(K)\ 4\left(\frac{K}{2k_F}\right)^3 d\left(\frac{K}{2k_F}\right) \tag{8}$$

or

$$\rho = \frac{3\pi}{\hbar e^2} \frac{1}{v_F^2} \frac{V}{N} \langle |u(K)|^2 a(K) \rangle \tag{8a}$$

(a) The above expression for ρ assumes that thermal vibration (phonons) are unimportant. The effect of phonons on the resistivity has been calculated by Cote and Meisel[40].

From this, an expression for the thermopower can be obtained using the Mott relation, where $\sigma(\varepsilon)$ is an expression involving the relaxation time $\zeta(\varepsilon)$:

$$S \alpha \left|\frac{\partial \ell n \sigma(\varepsilon)}{\partial \varepsilon}\right|_{\varepsilon = \varepsilon_F} \tag{9}$$

We can define a dimensionless parameter containing the logarithmic derivative:

$$\xi = \varepsilon_F \left[\frac{\partial \ell n \sigma(\varepsilon)}{\partial \varepsilon}\right]_{\varepsilon = \varepsilon_F} \tag{10}$$

and

$$S_F = - \frac{\pi^2 k^2 T}{3|e|\varepsilon_F} \tag{11}$$

where S_F represents the "Fermi thermopower".

Thus we can write:

$$S = - \frac{\pi^2}{3} \frac{k^2 T}{|e|\varepsilon_F} \xi \quad , \tag{12}$$

We now concentrate on the analysis of the various expressions obtained for ξ upon evaluation of (10). Equation (12) is the general result used for the prediction of thermopowers of liquid and amorphous metals. Within the limits of validity of the NFE model, the bulk of the temperature dependence[(a)] comes explicitly from the factor T in (12). We therefore expect for the amorphous metals a linear thermopower with magnitude and sign governed by ξ.

(a) $\langle |u(K)|^2 a(K) \rangle$ has some T dependence which gives the temperature dependence of the resistivity. From this, a small T dependence in ξ is expected.

If the pseudopotential u(K) is K-dependent only, then (10) becomes:

$$\xi = \left[\frac{\partial \ell n k}{\partial \ell n \varepsilon}\left[2\,\frac{\partial \ell n v}{\partial \ell n k} + 4 - 4q\right]\right]_{\varepsilon = \varepsilon_F} \tag{13}$$

where

$$q = \frac{|u(2k_F)|^2\, a(2k_F)}{\langle |u(K)|^2 a(K)\rangle} \tag{14}$$

This result is greatly simplified if free electrons are considered[(a)]:

$$\xi = 3 - 2q \tag{15}$$

If the scattering is not well described by the simple Born approximation, the matrices are likely to be dependent on k as well as K which reflects some k dependence of the pseudopotential; then we have:

$$\xi = 3 - 2q - \frac{1}{2}\,r \tag{16}$$

where

$$r = \frac{k_F \left\langle \left(\frac{\partial |u(K)|}{\partial k}\right)_v a(K)\right\rangle}{\langle |u(K)|^2\, a(K)\rangle} \tag{17}$$

On the basis of this theory the general behaviour of both thermopower and resistivity can be understood by evaluating the integral $\langle |u(K)|^2 a(K)\rangle$.

(a) for free electrons $\frac{\partial \ell n k}{\partial \ell n \varepsilon} \equiv \frac{1}{2}$; $\frac{\partial \ell n v}{\partial \ell n k} \equiv 1$

In Figure III-1 a typical structure factor and pseudo-potential are shown, as well as the integrand $|u(K)|^2 a(K)$. The temperature dependence of the structure factor is shown in Figure III-2. Since the pseudo-potential is not expected to vary appreciably and we can safely consider it to be constant, all the changes in the thermopower and resistivity are attributed to the behaviour of $a(k)$[(a)].

The limit for the integration over K is $2k_F$, hence the temperature dependence of ρ and S will be determined by the relative position of $2k_F$ and K_p, which is the value for K at the first peak in the structure factor.

By inspection of Figures III-1 and III-2, we can see that for valences between $\sim$ 1.2 and $\sim$ 2 the integral $\langle|u(K)|^2 a(K)\rangle$ will <u>decrease</u> with increasing temperature, thus giving negative values for $d\rho/dT$ and positive values for the thermopower. This range of valencies is approximately the same range which is found in standard amorphous metals (this is used in a theory for the stability of amorphous metals by Nagel & Tauc[11] where the condition $2k_F \sim K_p$ is found to be a criterion for glass formation).

It should be pointed out that changing the effective valence within this range, one should obtain fairly sizeable changes in the thermo-ower and $d\rho/dT$.

Up to this point we have been dealing with the results of Ziman's theory for pure liquid metals. We should now recall that amorphous metals are only available as alloys, and therefore we should use the results for liquid alloys, as presented by Faber and Ziman[19].

(a) the structure factor should rigorously be the electron scattering structure factor; since this is generally unavailable, the x-ray or neutron determined a(k) is used.

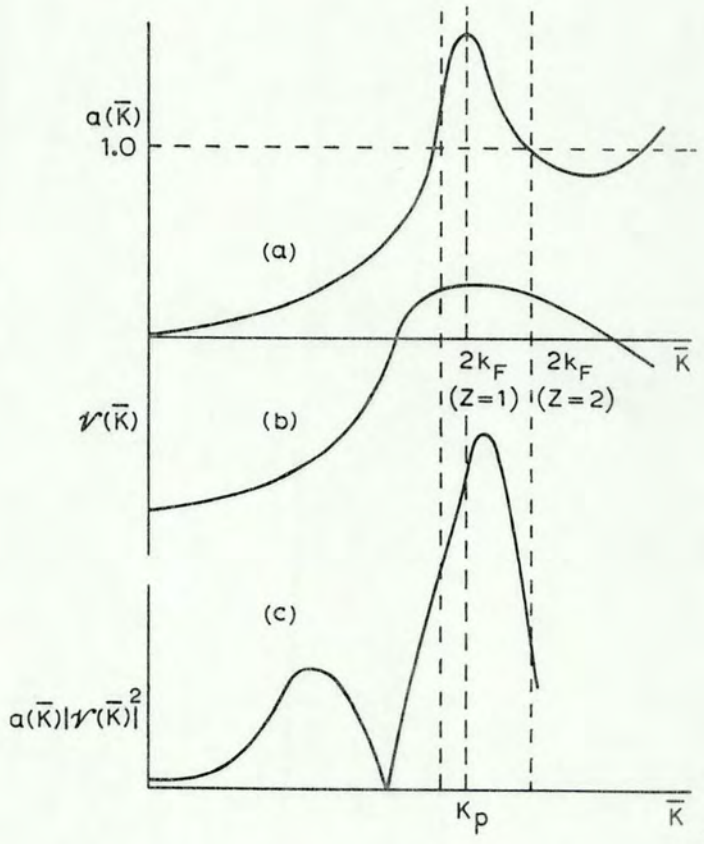

FIG. III - 1 - Schematic diagram showing the variation of
(a) - the liquid structure factor ($A(\underset{\sim}{K})$; $a(\underset{\sim}{K}) \equiv 1$ corresponds to a completely random array)
(b) - the ionic pseudopotential ($u(\underset{\sim}{K})$) and
(c) - the product $a(\underset{\sim}{K})|u(\underset{\sim}{K})|^2$ as functions of $\underset{\sim}{K}$, after R.D. Barnard[31].

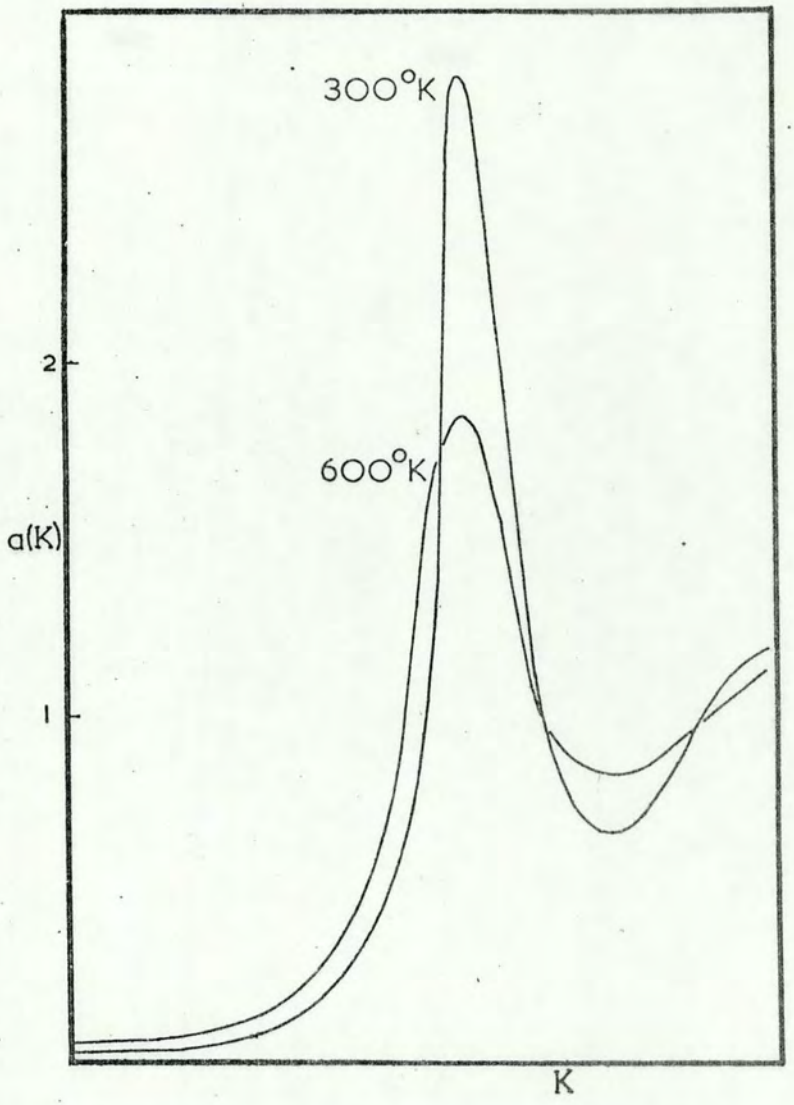

FIG. III - 2 - Temperature dependence of the structure factor (reproduced from J.M. Ziman[7]).

The basic assumption of the theory of liquid metallic alloys is that the electrons "see" the result of the proper combination of elements through the various partial structure factors $a_{ij}(K)$.

The expressions for the resistivity and thermopower then become:

$$\rho = \frac{3\pi}{e^2 \hbar v_F^2} \frac{N}{V} \langle F(K) \rangle \tag{18}$$

$$S = \frac{-\pi^2 k^2 T}{3|e|\varepsilon_F} \{3 - 2 \frac{F(2k_F)}{\langle F(K) \rangle}\} \tag{19}$$

where $\frac{N}{V}$ is the number of available electron per atom in the alloy and $\langle F(K) \rangle$ is defined by

$$\langle F(K) \rangle = \frac{1}{4k_F^4} \int_0^{2k_F} F(K) K^3 dK \tag{20}$$

For a binary alloy:

$$F(K) \equiv |u_1|^2 \{c(1-c) + c^2 a_{11}\} + |u_2|^2 \{c(1-c) + (1-c)^2 a_{22}\} +$$

$$+ 2u_1 u_2 \; c(1-c)(a_{12}-1) \tag{21}$$

where the pseudo-potentials of the two components are written as u_1 and u_2, and c is the atomic fraction of component 1. a_{11}, a_{12}, a_{22} represent the three partial structure factors for the different possible atomic pairs.

Using this formalism and a substitutional model[a] Enderby et al[30]

(a) In the substitutional model the two constituents have the same atomic volume and the same structure factor, so that replacement of one ion for another can occur at random without any distortions of the environment

were able to fit the variation of the thermopower with concentration for binary monovalent AgAu liquid alloys. The equivalent divalent MgCd liquid alloys could not be fit using the simple Faber-Ziman expression. An energy (k) dependent pseudopotential was then invoked.

In the case of amorphous alloys one should expect similar behaviour if the Ziman theory is applicable to metallic glasses. We must stress the fact that this test of the theory is somewhat hampered by the limited range of composition that one can obtain in the amorphous phase. Also one should note that the extended Ziman theory is valid at high temperatures and it can be only used down to around 50 K; below this temperature the inelastic scattering of electrons which is produced by ionic motion becomes important and it is not included in the theory in this first approximation.

In order to account for inelastic scattering, Cote and Meisel[40] have included in their formulation of the Ziman theory the effect of phonons through the introduction of dynamic structure factors. With this they were able to explain not only the high temperature resistivity, but also describe the low temperature behaviour which was formerly inaccessible through the static Ziman formalism.

It is worthy of note that an equivalent calculation in crystalline metals[31] gives values of ξ, the thermoelectric parameter, changing from 3 at low temperatures to 1 at high temperatures.

III - 2 The Kondo-type theory

An alternative group of theories has been developed for the low temperature region. They are similar to that advanced by Kondo[6] to explain the behaviour of the transport properties of dilute magnetic alloys. From these theories, the only one applicable to the type of metallic glass

studied in this work is that advanced by Cochrane et al[10]. It suggests that the anomalous negative $d\rho/dT$ could be due to electrons being scattered from structural degrees of freedom inherent in the lack of ionic periodicity in the material. In this model an ion is considered to be able to occupy either of two equivalent sites. The two tunnelling levels can provide the necessary degrees of freedom which were provided by the spin orientations in the original Kondo effect.

For all Kondo-like theories, one can write the resistivity as:

$$\rho = \rho_0 - C \ln (T^2 + \Delta^2) \qquad (22)$$

where C and Δ have different physical origins according to each of the theories. ρ_0 represents all temperature independent scattering.

In the tunnelling theory, C represents both the Coulomb interaction between the ion and the electron and the concentration of tunnelling states and Δ is the characteristic energy splitting for the levels of the double well potential of the tunnelling state.

Since the Hamiltonians describing the Kondo-like problems are identical to the original Kondo Hamiltonian, we expect all these models to have similar results for the thermopower. The original Kondo effect explains the "giant thermopower", seen in the Kondo alloys, which can be as large as 16 μV/K at 10K (this is about one order of magnitude larger than the normal diffusion thermopower).

In the case of metallic glasses, one should expect a similar behaviour. One important point to consider when comparing the experimental results to these theories is that the individual scattering mechanisms

contribute to the total thermopower with weight proportional to the relative contributions to the total resistivity (Nordheim-Görter rule). Because of the large residual resistivity which is a characteristic to metallic glasses, the relative contributions to the total thermopower coming from scattering described by one of the Kondo-like theories is greatly reduced (by a factor of nearly 1000!) - therefore the thermopower is not a good tool to test the validity of this theory[15].

One of the possible consequences of the tunnelling model is that thermal treatment of the amorphous metal should change the characteristics of the population and energy splitting of the double wells. This should have an effect on the electronic transport properties of these materials. Such an effect was seen for mechanical properties[32] and even some intriguing behaviour for the conductivity[33] which rises sharply after 100 minutes of annealing time at 200°C.

Recently Banville and Harris[34] published the results of a theoretical calculation, based on the two level systems model, where they simulate the effects of annealing by allowing their computer-generated structure to relax. Their results indicate that the annealing process should reduce the magnitudes of various low-temperature anomalies seen in metallic glasses.

On account of the Nordheim-Görter rule, even if the tunnelling model is valid, one should not expect detectable changes in the thermopower at low temperatures arising from relaxation effects. On the other hand, the temperature dependence of the resistivity should be affected quite noticeably, with the value of $d\rho/dT$ approaching zero as the time of annealing increases.

IV - EXPERIMENTAL RESULTS

We shall here describe the results obtained for the different systems studied, including a brief discussion, where pertinent, of their meaning.

The results for all the thermopower measurements were obtained using the apparatus described in Chapter II. The method used was an integral one and the processing of the data to obtain S(T) from the measured $\int_{4.2}^{T} S(T)dT$[(a)] was made using the programs MB0001.FOR and MB002.FOR, whose listings can be found in the Appendix. These programs read and translate the data files (MB0001) and then an average is established for each integer temperature affording 300 averaged data points for each experiment. The same program (MB0002) performs a numerical differentiation over variable range of points.

The results for the resistivities are presented as a reduced resistance ratio ((R(T) - R(4.2)/R(4.2)) which (if a small isotropic dilation is neglected) is the reduced resistivity ratio ($\rho(T)-\rho(4.2)/\rho(4.2)$). We also present the results for the resistivities based on room temperature measurements of each sample's resistance, length, density and mass. As is widely accepted[(35)] the geometrical factor is the largest source of error in the determination of the absolute values of the resistivity. In our case this difficulty was augmented by the small and irregular cross section of the ribbons.

This is why we used mass and density measurements to determine the average cross section of the samples. The density of the samples was obtained in this laboratory[(37)] by the Archimedes method, using toluene as the liquid.

(a) to obtain this, we have substracted the integrated thermopower of Pb published by Roberts[(36)]; this is done in program MB0001.FOR.

With the values of the room temperature resistivities all of the $\rho(T)$ could be determined from the reduced resistivity ratios.

The results for the reduced resistivity of a series of MgZn amorphous alloys is presented in Figure IV-1. An expansion of the low-temperature region is shown in Figure IV-2. The resistivities show negative slopes at around room temperature and a broad maximum around 40K, with the exception of $Mg_{80}Zn_{20}$ which has a broad maximum around 90K.

A plot of the room temperature resistivities and its temperature derivative against composition is shown in Figure IV-3.

The thermopower of the amorphous MgZn series is shown in Figure IV-4. The high temperature thermopowers can be described correctly by straight lines down to about 40K.[a] Linear regressions were performed and the parameters found are summarized in Table IV-1.

A plot of the thermopower of the alloys at room temperature against concentration is presented in Figure IV-5.

Earlier measurements of the thermopower of amorphous $Mg_{0.70}Zn_{0.30}$[17] give larger negative values than those measured in this work. We propose an explanation for such discrepancy based on the results of thermopower of a crystallized sample of the same composition. Applying the results obtained for the resistance and thermopower of composite materials by Airapetiants[38] one obtains 19% of crystallization for the early samples, if one considers the fresh sample as being entirely amorphous.

This indicates that the precaution of measuring absolutely fresh samples or keeping them in liquid nitrogen until measured is well founded. In Figure IV-6 we present the experimental results obtained for $Mg_{70}Zn_{30}$ in the crystallized and amorphous phases.

(a) The small deviation from linearity are probably due to the effect of phonons (Harris and Mulimani, private communication)

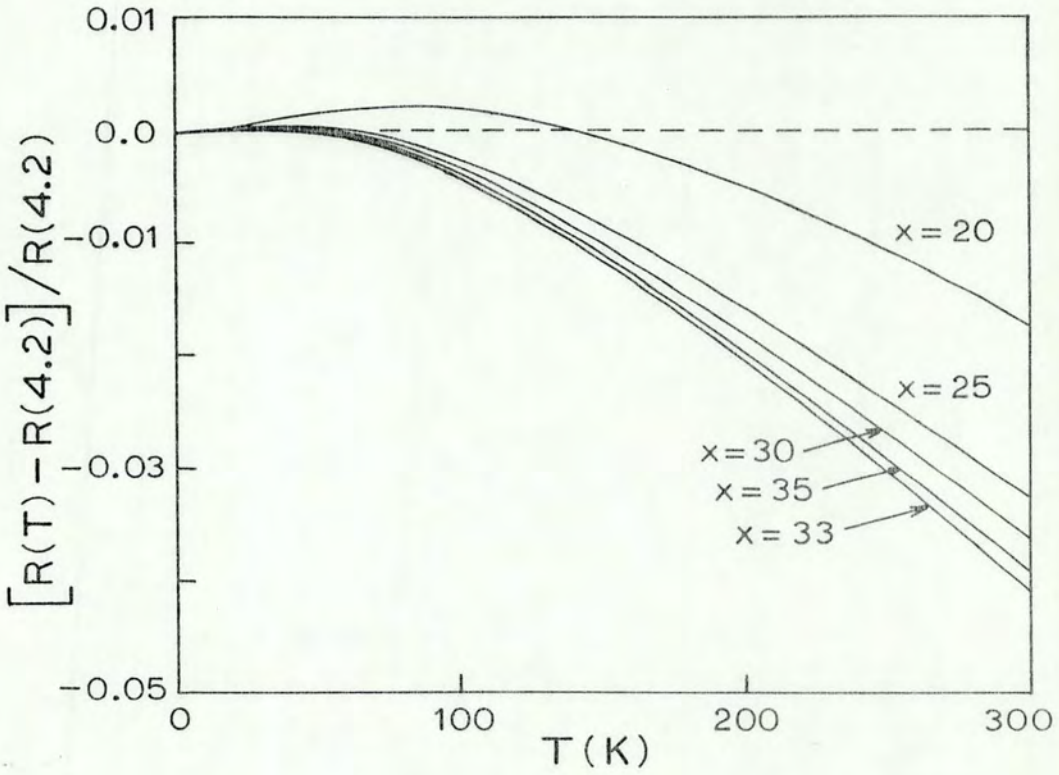

FIG. IV - 1 - Reduced resistance ratio of amorphous $Mg_{(1 - x)}Zn_{(x)}$ alloys.

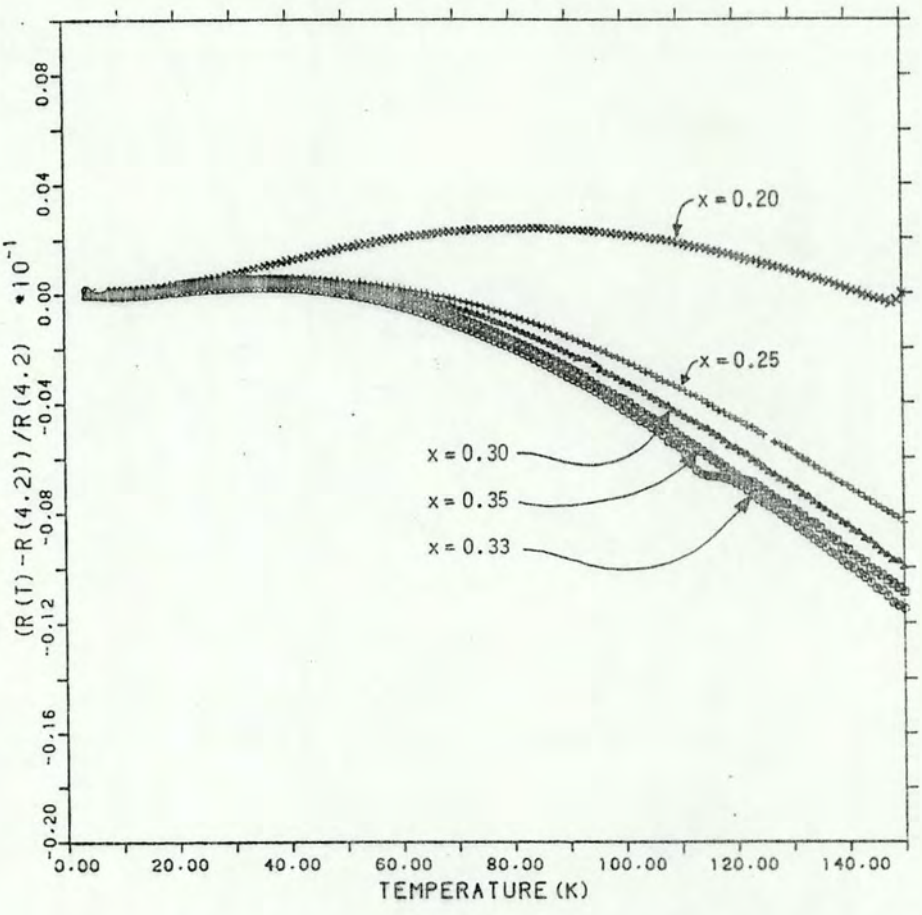

FIG. IV - 2 - Low temperature reduced resistance ratios of amorphous $Mg_{(1 - x)}Zn_{(x)}$ alloys.

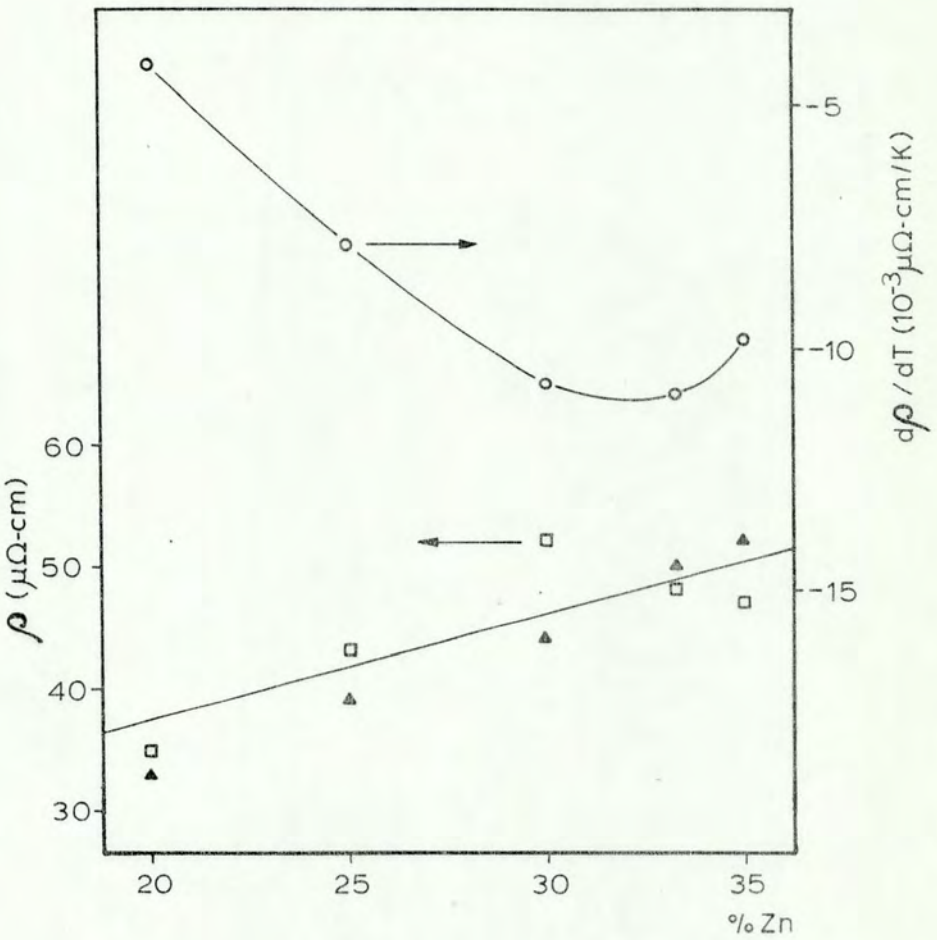

FIG. IV - 3 - Composition dependence of the room temperature resistivity (□) and its temperature dependence at room temperature (○), for MgZn alloys.

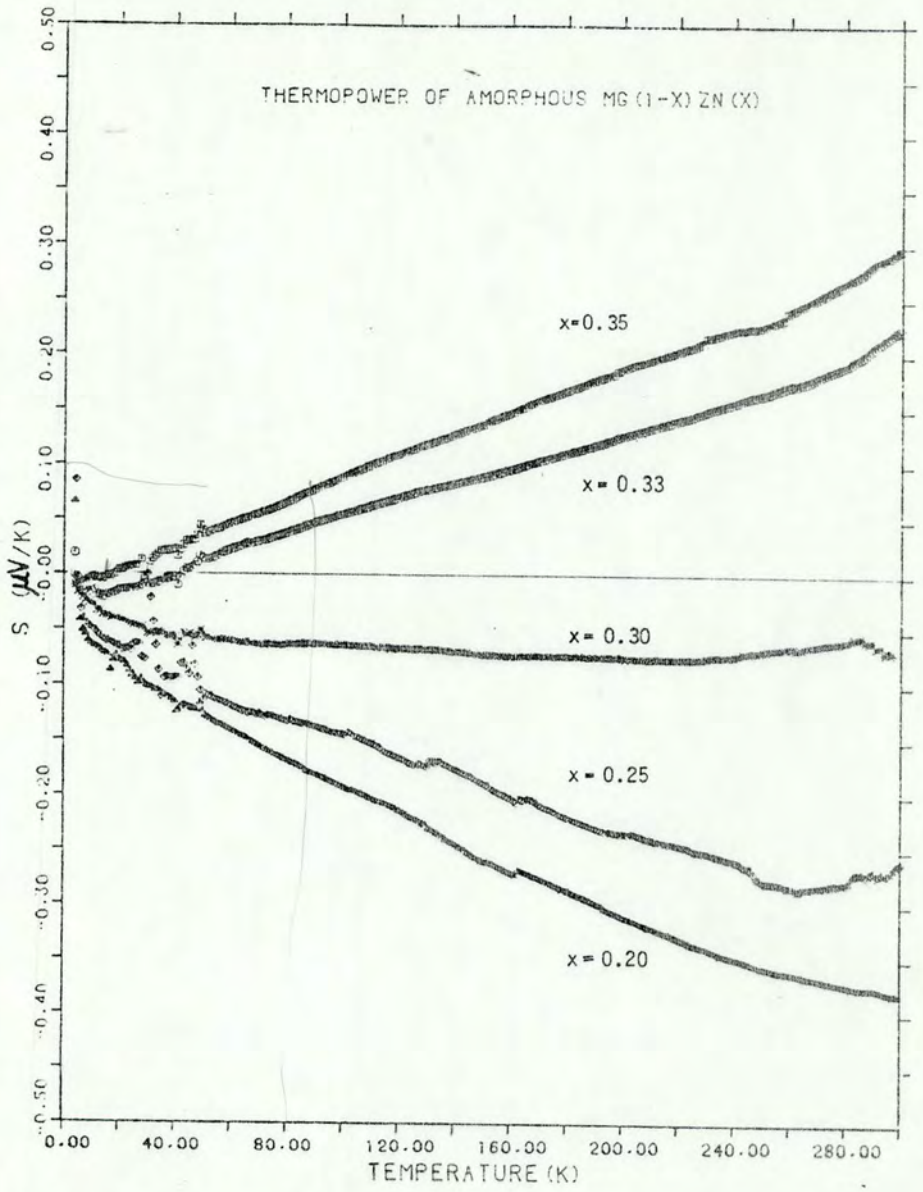

FIG. IV - 4 - Thermopower of amorphous $Mg_{(1-x)}Zn_{(x)}$ alloys.

TABLE IV-1

x	INTERCEPT	SLOPE
0.20	- 0.091	-10.6×10^{-4}
0.25	- 0.064	-8.3×10^{-4}
0.30	- 0.065	-2.1×10^{-5}
0.33	- 0.019	$+7.3 \times 10^{-4}$
0.35	- 0.004	$+9.5 \times 10^{-4}$

Linear regression parameters for the high temperature thermopower of amorphous $Mg_{(1-x)}Zn_x$ alloys.

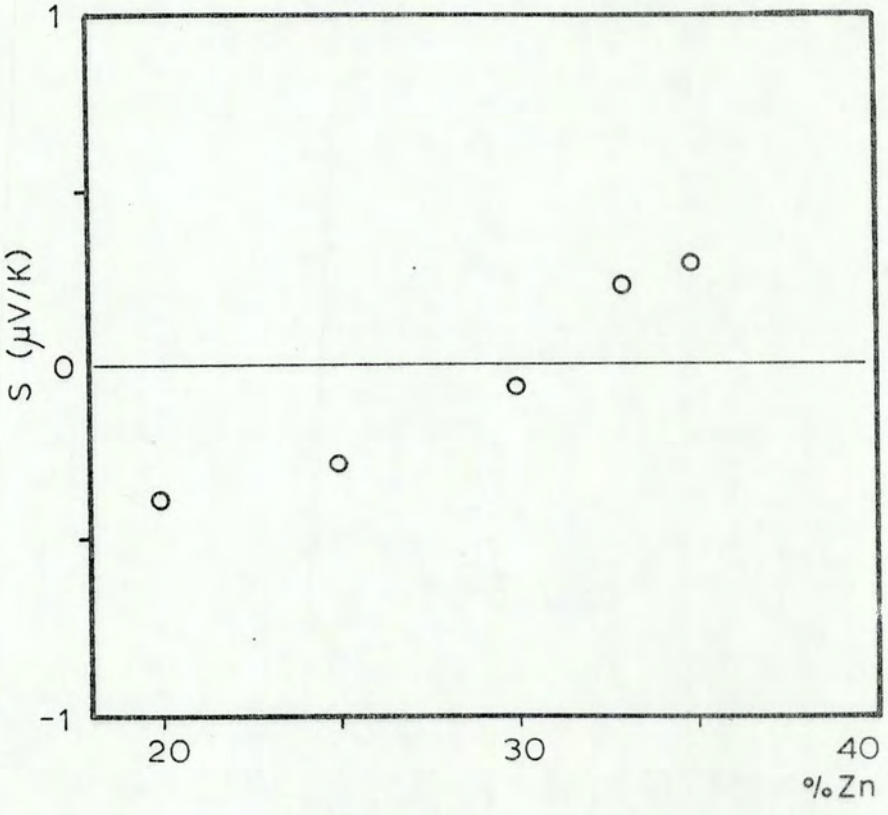

FIG. IV - 5 - The room temperature thermopower of MgZn alloys as a function of composition.

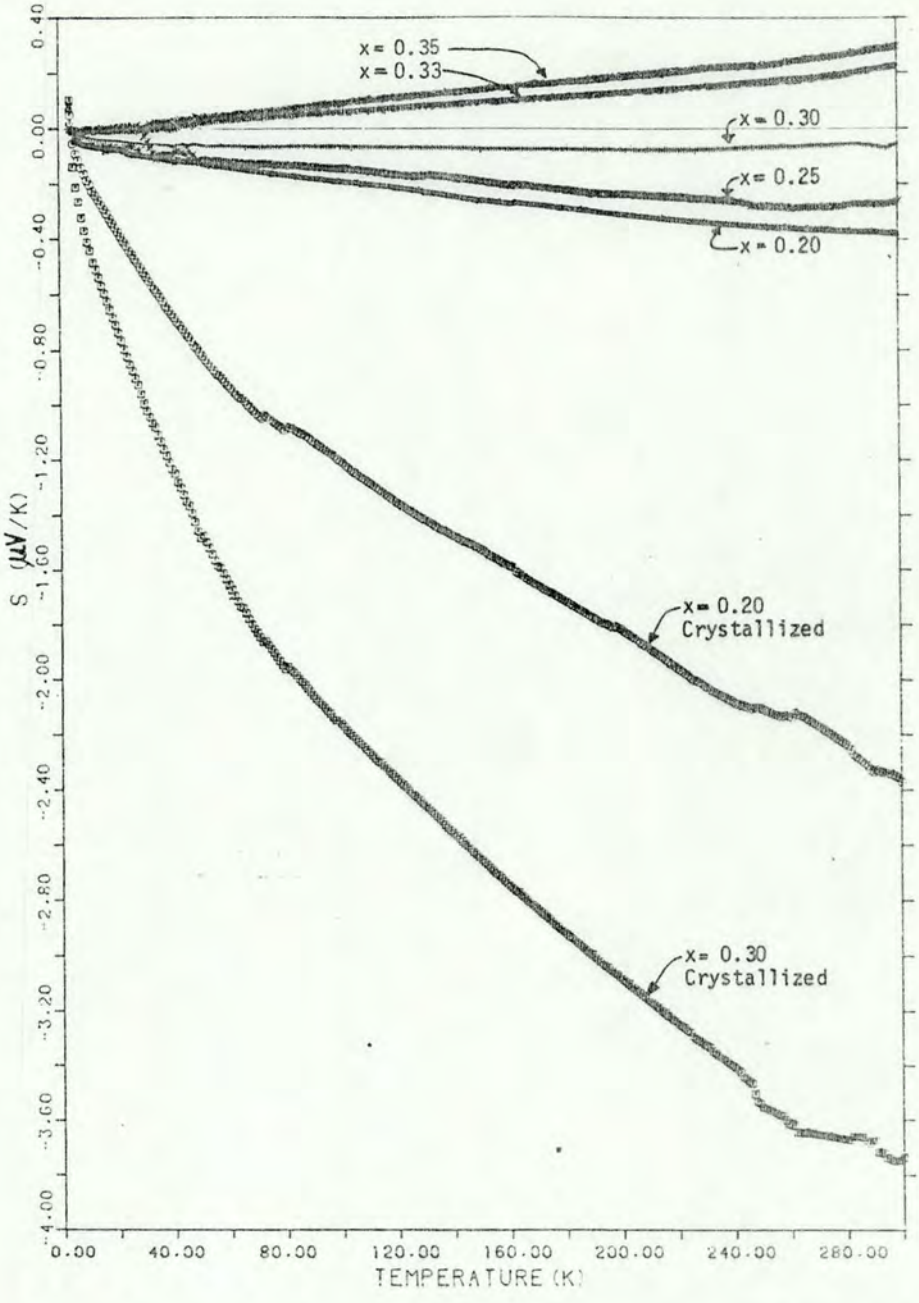

FIG. IV - 6 - The thermopower of amorphous and crystallized MgZn alloys.

The actual expressions used for this analysis were a modification of the original[38] so as to give the crystallization fraction and the theoretical value for the thermopower by using the reduced resistivity data, which in our case is always a more accurate measurement.

In the Appendix we show both the derivation of this alternate formulation, as well as the listing of the program used to perform this calculation (MBSAR.FOR).

The results for the thermopower of the "As Made" CuZr series is shown in Figure IV-7. It can be seen that, with the exception of $Cu_{70}Zr_{30}$, all of the samples show remarkably similar thermopowers. Numerical values for the constants of a linear regression over the high and low temperature regions are shown in Table IV-2.

In Figure IV-8 the low temperature thermopower of the same series can be seen. From this and Table IV-2 one can observe that all samples seem to fall in line with even less scattering in the points. This low temperature line is followed up to about 40K where the slope of the curve slowly changes into the slope of the high temperature region.

The reduced resistivities for the same series can be seen in Figure IV-9. It can be seen that the slope of the resistivity, which is always negative, changes slightly from low to high temperatures, and from one end of the concentration range to the other. This can be better appreciated in Figure IV-10 which shows the change in room temperature resistivity and $d\rho/dT$ with composition.

A similar set of results is given for the series of CuZr alloys after thermal relaxation: Figure IV-11 shows the thermopower from 4K to 300K; Figure IV-12 is a low temperature thermopower plot and the

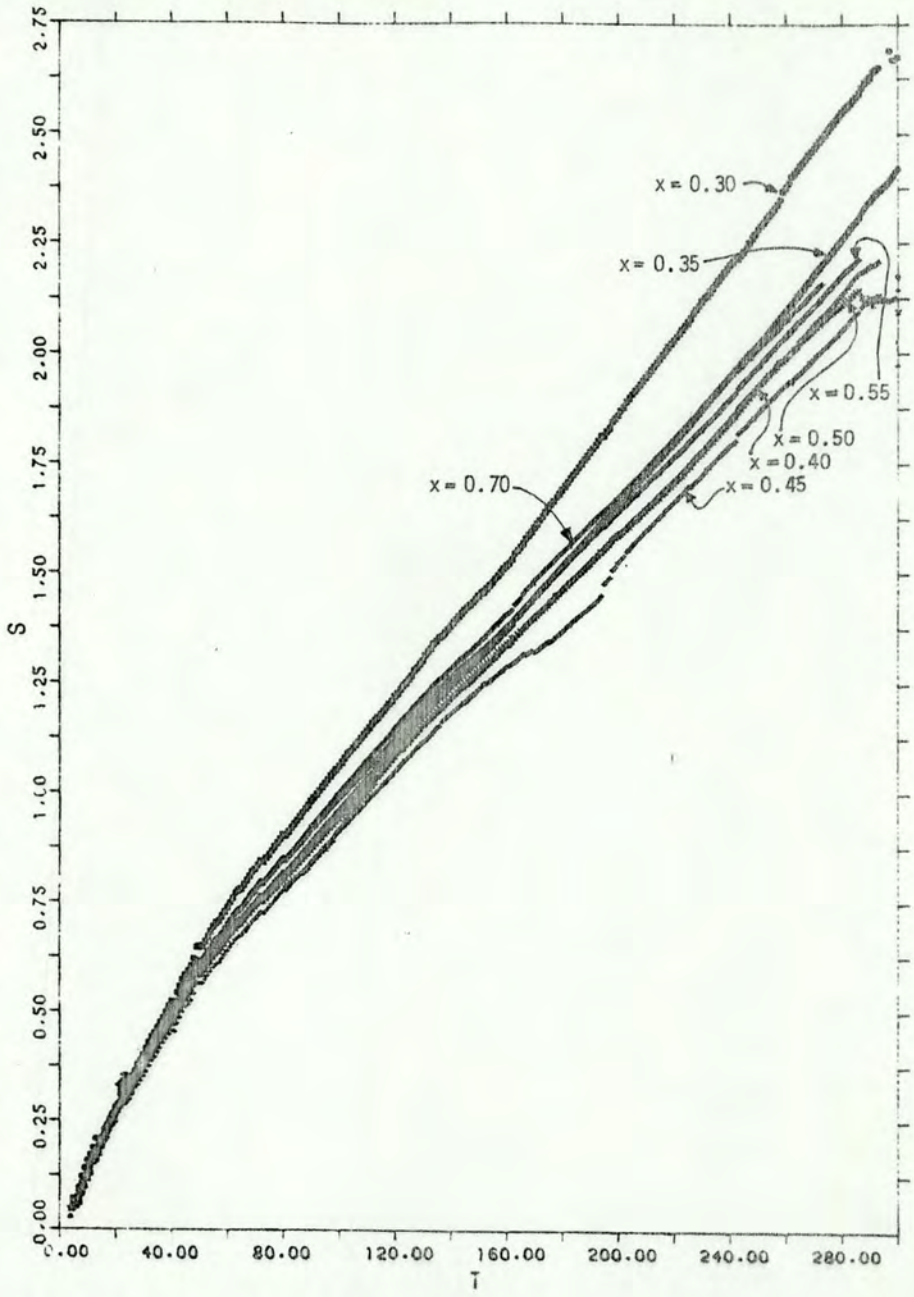

FIG. IV - 7 - Thermopower of 'as made' amorphous $Cu_{(1-x)}Zr_{(x)}$ alloys.

TABLE IV - 2

x	LOW TEMPERATURE		HIGH TEMPERATURE	
	INTERCEPT	SLOPE	INTERCEPT	SLOPE
0.30	-0.034	+0.0153	0.223	0.00823
0.35	-0.004	+0.0140	0.243	0.00711
0.40	-0.024	+0.0154	0.271	0.00661
0.45	-0.018	+0.0142	0.279	0.00628
0.50	-0.009	+0.0132	0.302	0.00644
0.55	+0.0006	+0.0134	0.337	0.00652
0.60	-0.015	+0.0145	0.337	0.00668
0.67	—	—	—	—
0.70	-0.036	+0.0164	0.342	0.00675

Linear regression parameters for the Thermopower of amorphous $Cu_{(1-x)}Zr_x$ (as made) alloys.

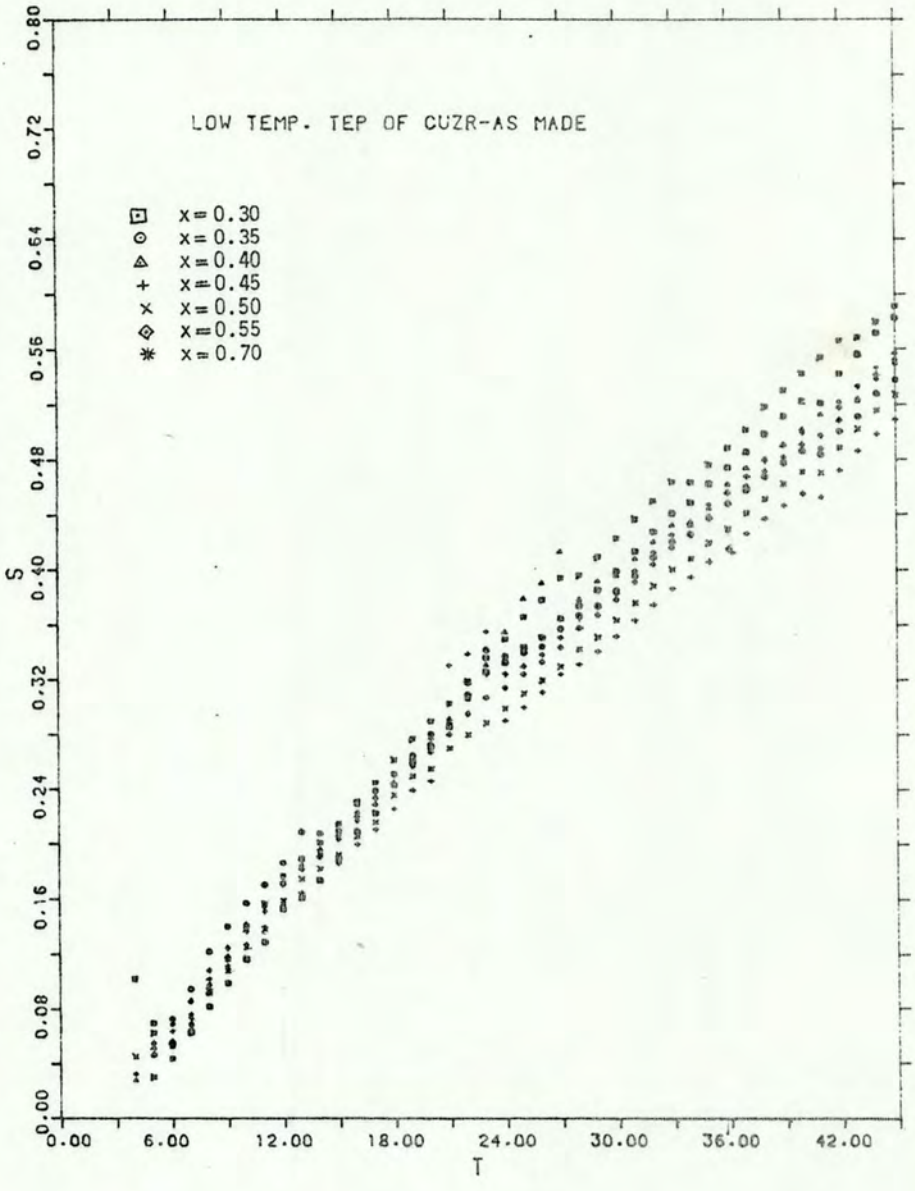

FIG. IV - 8 - Low temperature thermopower of 'as made' amorphous CuZr alloys.

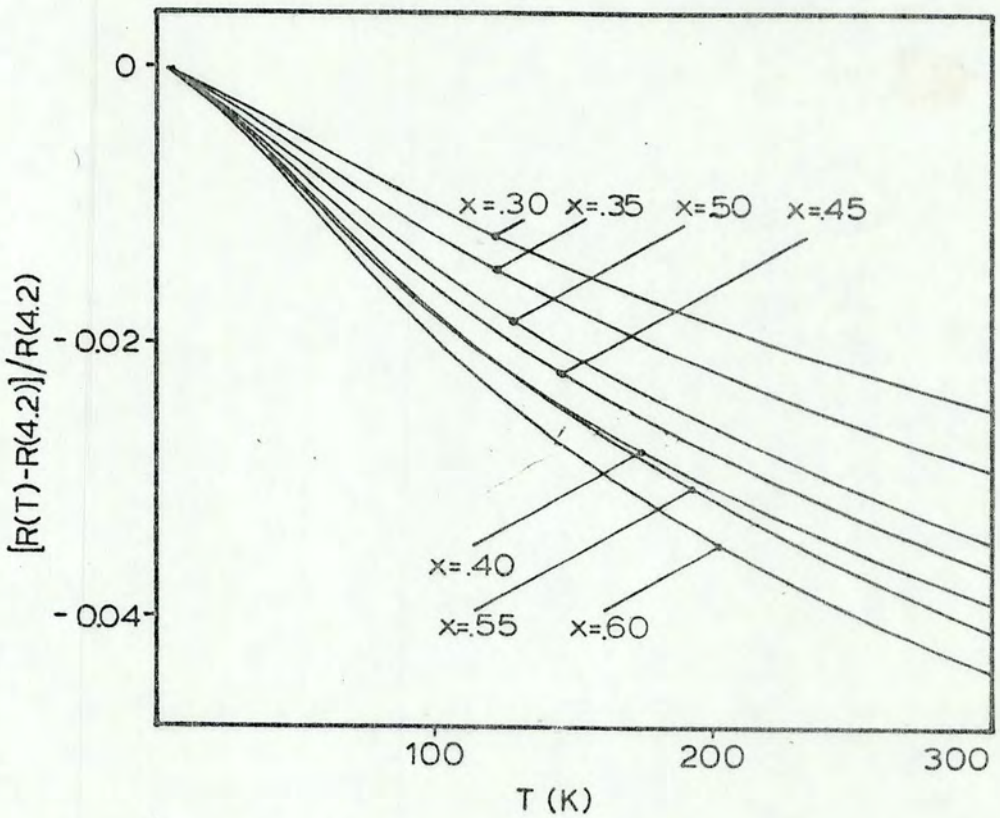

FIG. IV - 9 - Reduced resistance ratios of 'as made' amorphous CuZr alloys.

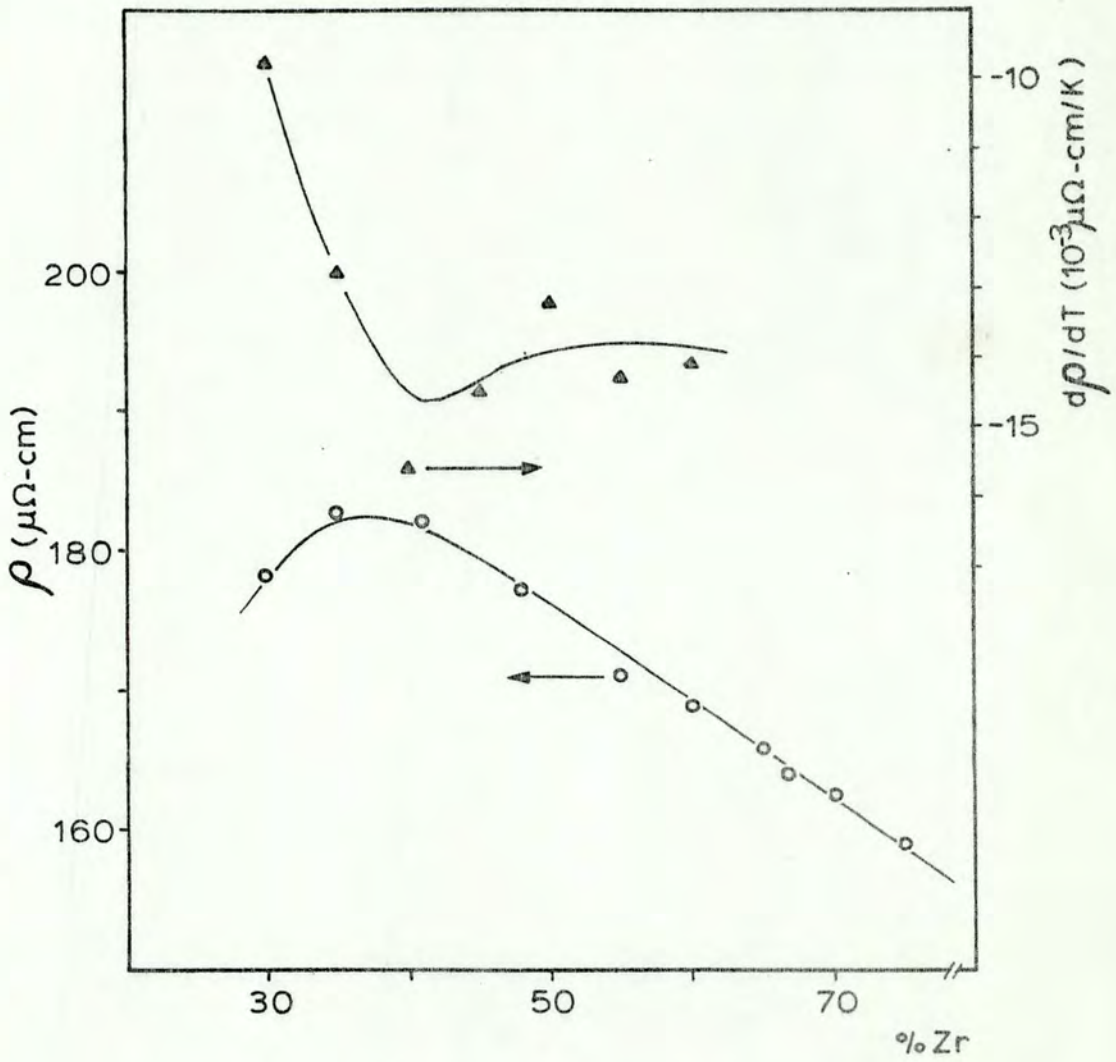

FIG. IV - 10 - Composition dependence of the room temperature resistivity of 'as made' amorphous CuZr alloys (o) and its temperature dependence at room temperature (▲).

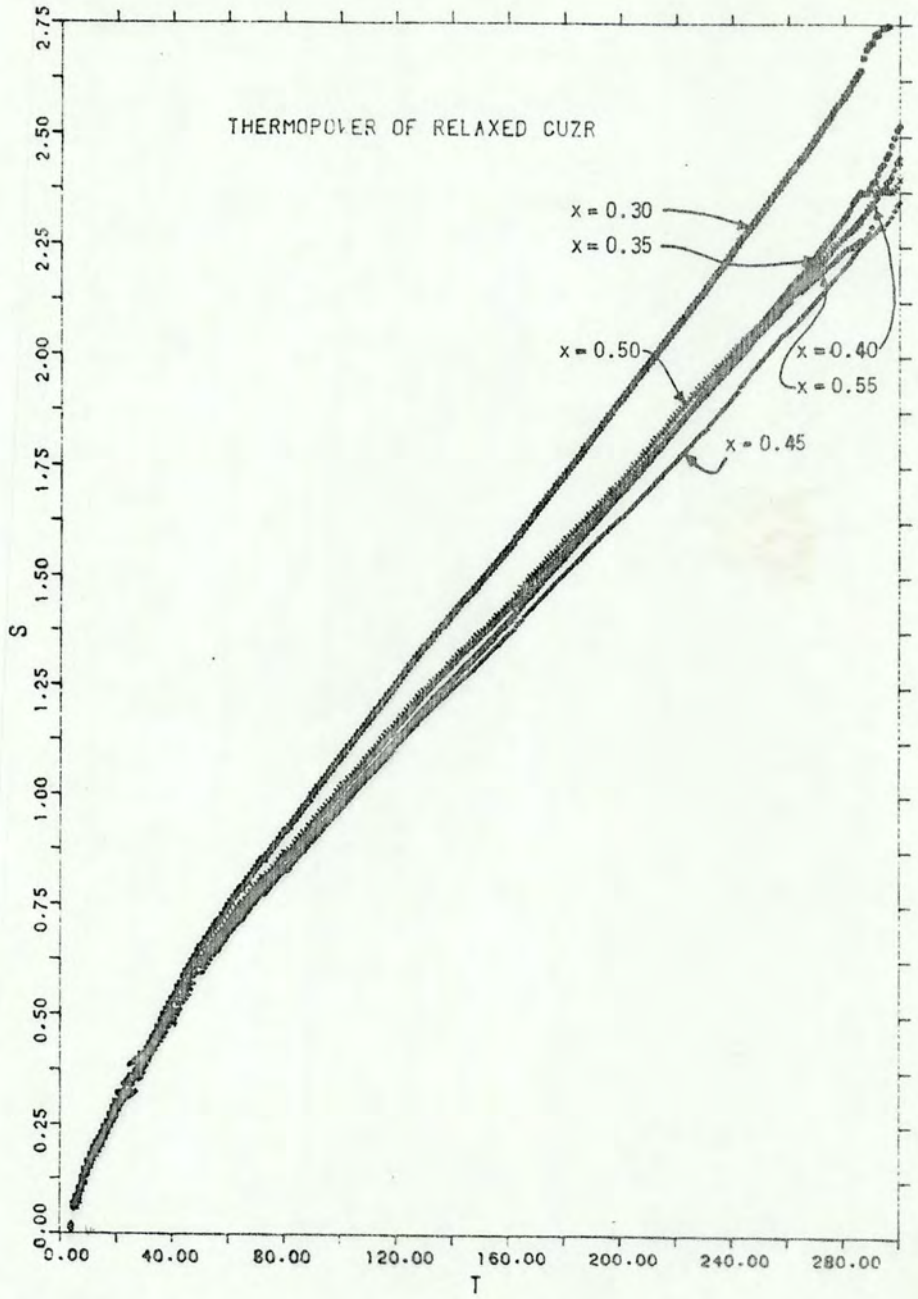

FIG. IV - 11 - Thermopower of 'relaxed' amorphous CuZr alloys.

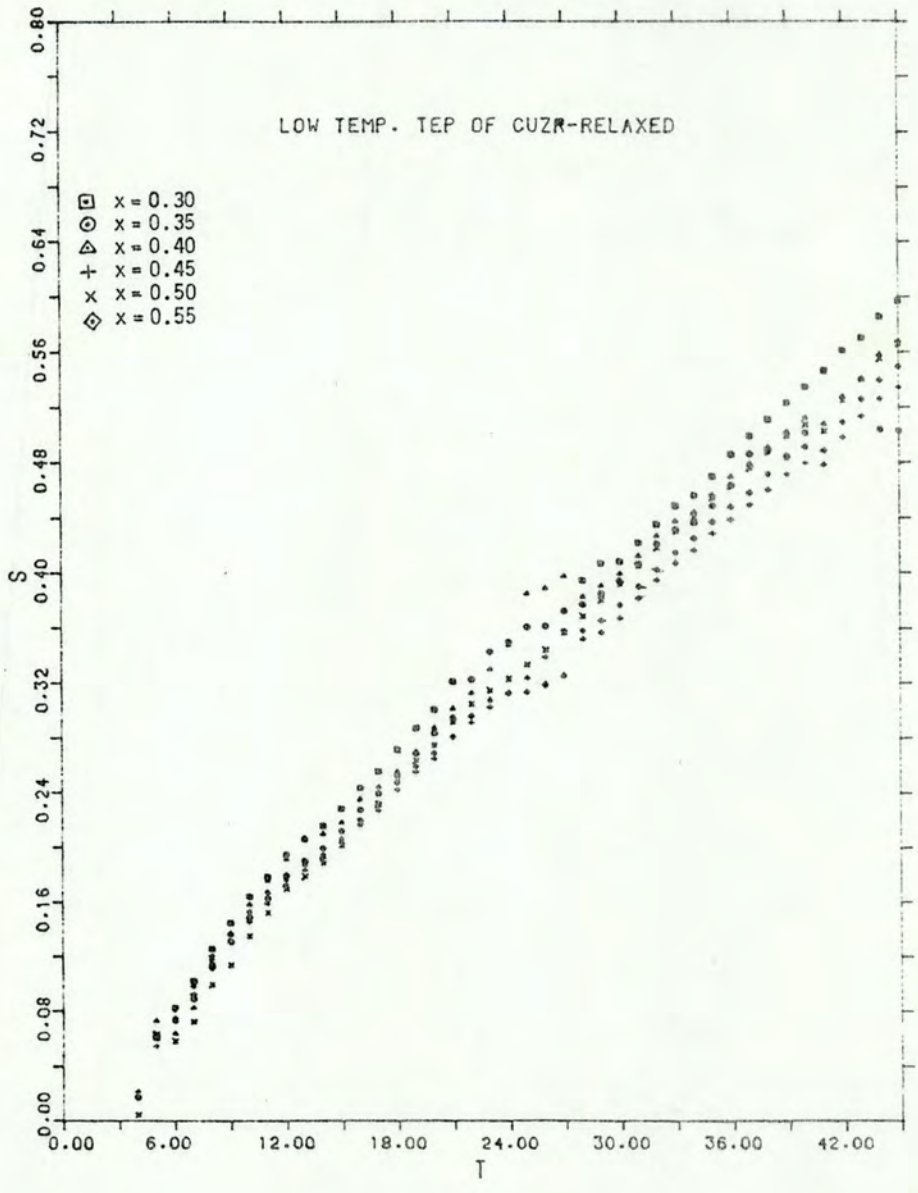

FIG. IV - 12 - Low temperature thermopower of 'relaxed' amorphous CuZr alloys.

reduced resistivities are displayed in Figure IV-13. The composition dependence of the room temperature resistivity and $d\rho/dT$ are shown in Figure IV-14.

Virtually the same observations can be verified in the 'relaxed' and 'as made' series. The thermopower measurements on the relaxed series show a somewhat larger slope, but still showing no significant increase in the separation between the different compositions. This can be verified in Table IV-3 which shows the results of a linear regression, similar to that applied to the 'as made' series.

The resistivity results are again similar to those found for the 'as made' series, with the exception of $Cu_{70}Zr_{30}$.

In order to facilitate direct comparisons between the 'as made' and 'relaxed' samples we present, for the same sample, the thermopower and reduced resistivity of $Cu_{60}Zr_{40}$, which is typical, in Figures IV-15 and IV-16 respectively.

In order to study the crystallization processes that take place in amorphous metals at temperatures below the glass transition temperature, we attempted a partial crystallization experiment similar to one recently reported by us on FeB amorphous alloys[39].

The results obtained for the thermopower and resistivity of partially crystallized amorphous $CuZr_2$ is shown in Figure IV-17 and IV-18 respectively. It can be observed that all of our results are concentrated in a region very near total crystallization.

As was described in Chapter II, we used the results of Altounian et al[22] to perform the partial crystallization experiment. The arrows in Figure IV-19 indicate the positions where we believed the partial

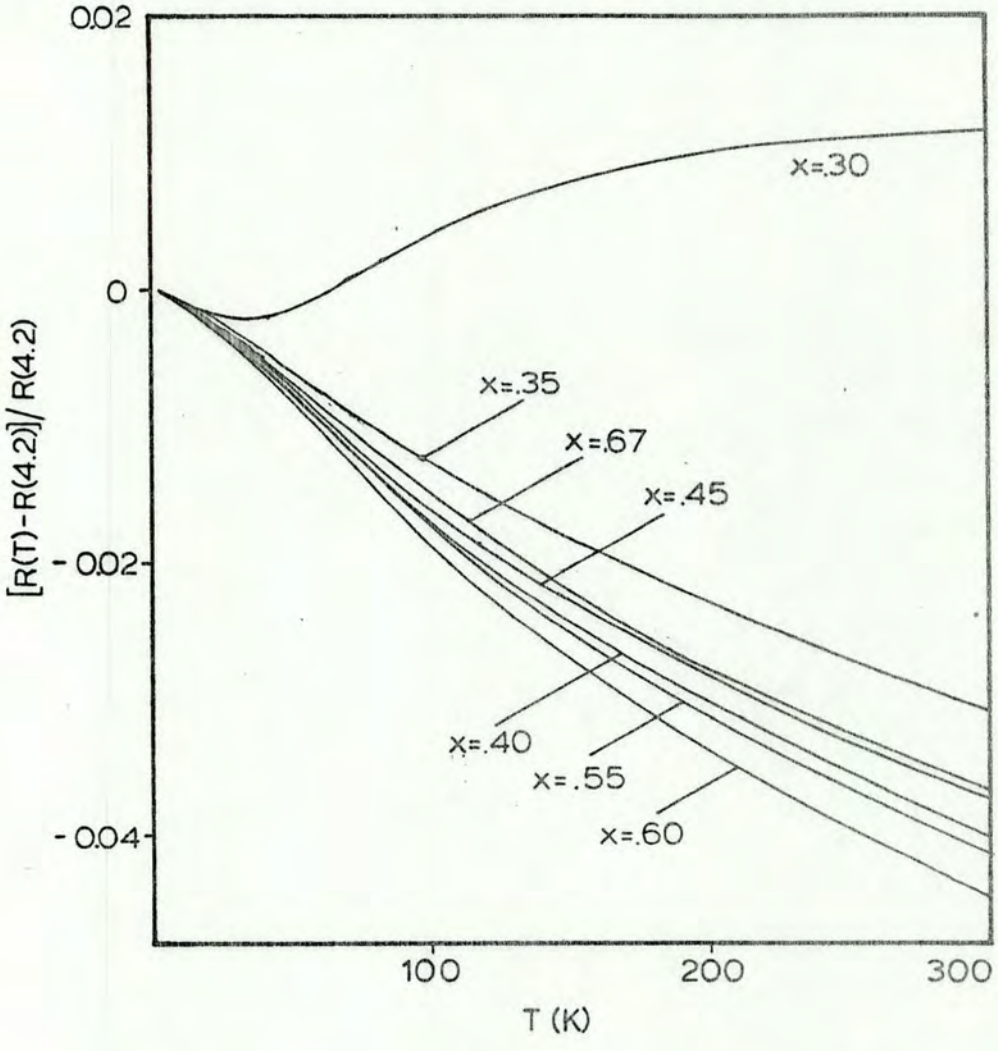

FIG. IV - 13 - Reduced resistance ratios of 'relaxed' amorphous CuZr alloys.

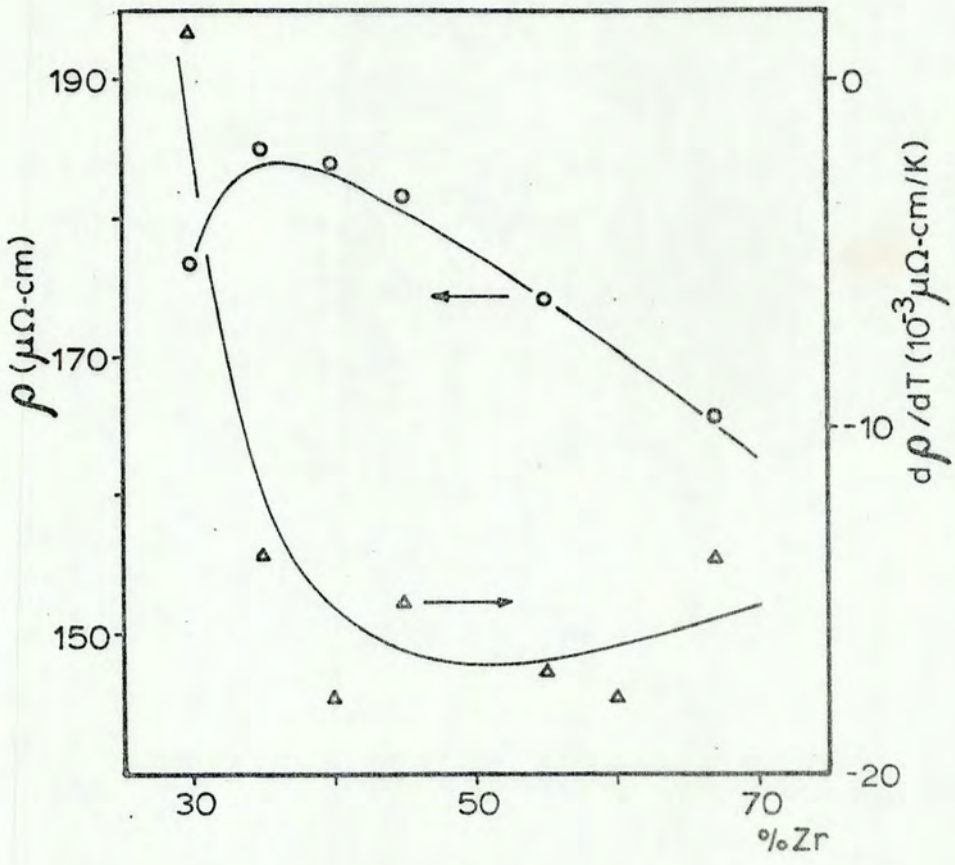

FIG. IV - 14 - Composition dependence of the room temperature resistivity of 'relaxed' amorphous CuZr alloys (○) and its temperature dependence at room temperature (△).

TABLE IV - 3

x	LOW TEMPERATURE		HIGH TEMPERATURE	
	INTERCEPT	SLOPE	INTERCEPT	SLOPE
0.30	-0.072	+0.0219	0.250	0.00828
0.35	-0.0076	+0.0148	0.238	0.00732
0.40	-0.0014	+0.0147	0.315	0.00695
0.45	+0.0081	+0.0129	0.288	0.00677
0.50	-0.013	+0.0143	0.314	0.00704
0.55	+0.017	+0.0125	0.315	0.00694

Linear regression parameters for the Thermopower of amorphous $Cu_{(1-x)}Zr_x$ (relaxed) alloys.

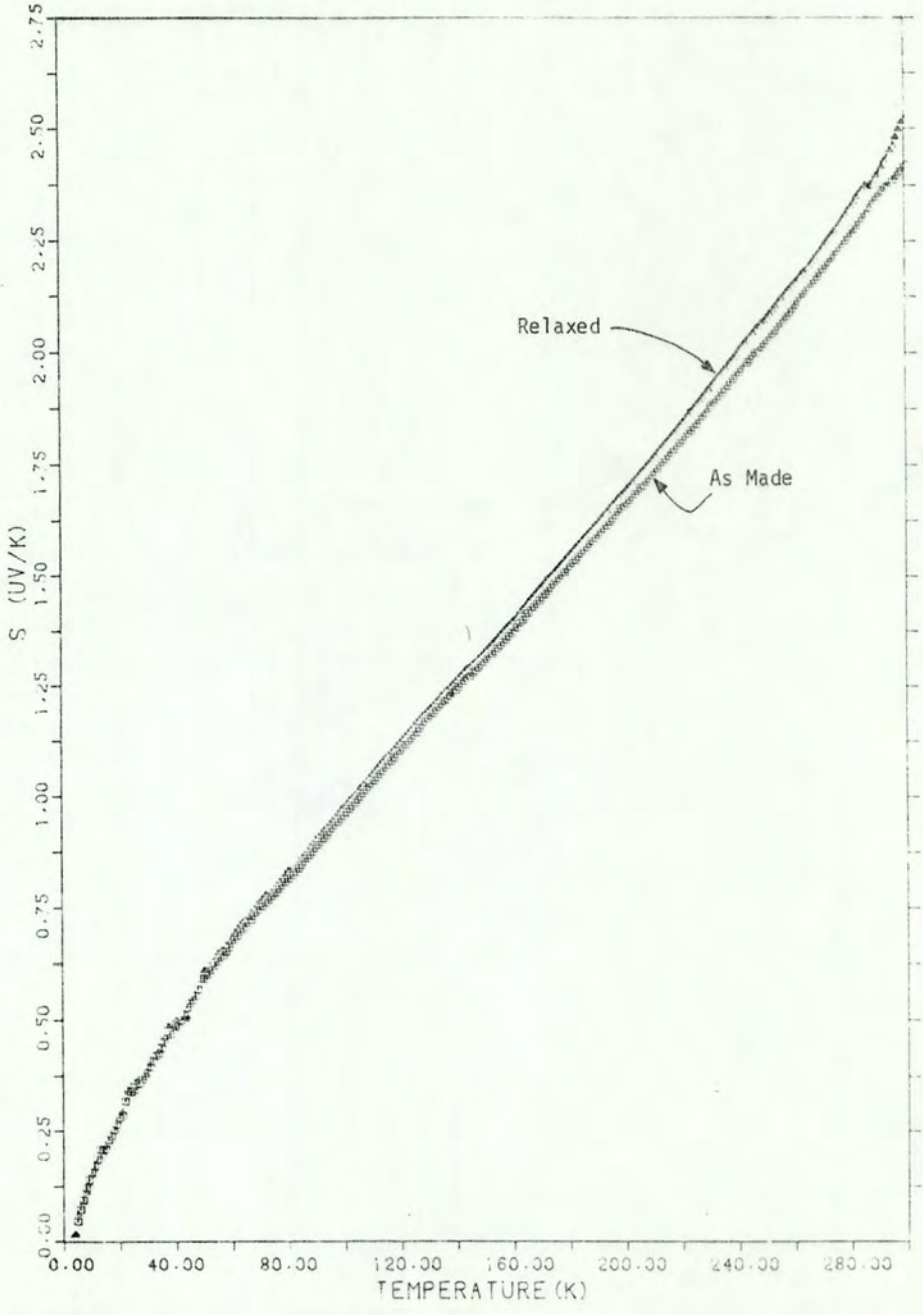

FIG. IV - 15 - Thermopower of amorphous $Cu_{60}Zr_{40}$ in the 'as made' and 'relaxed' states.

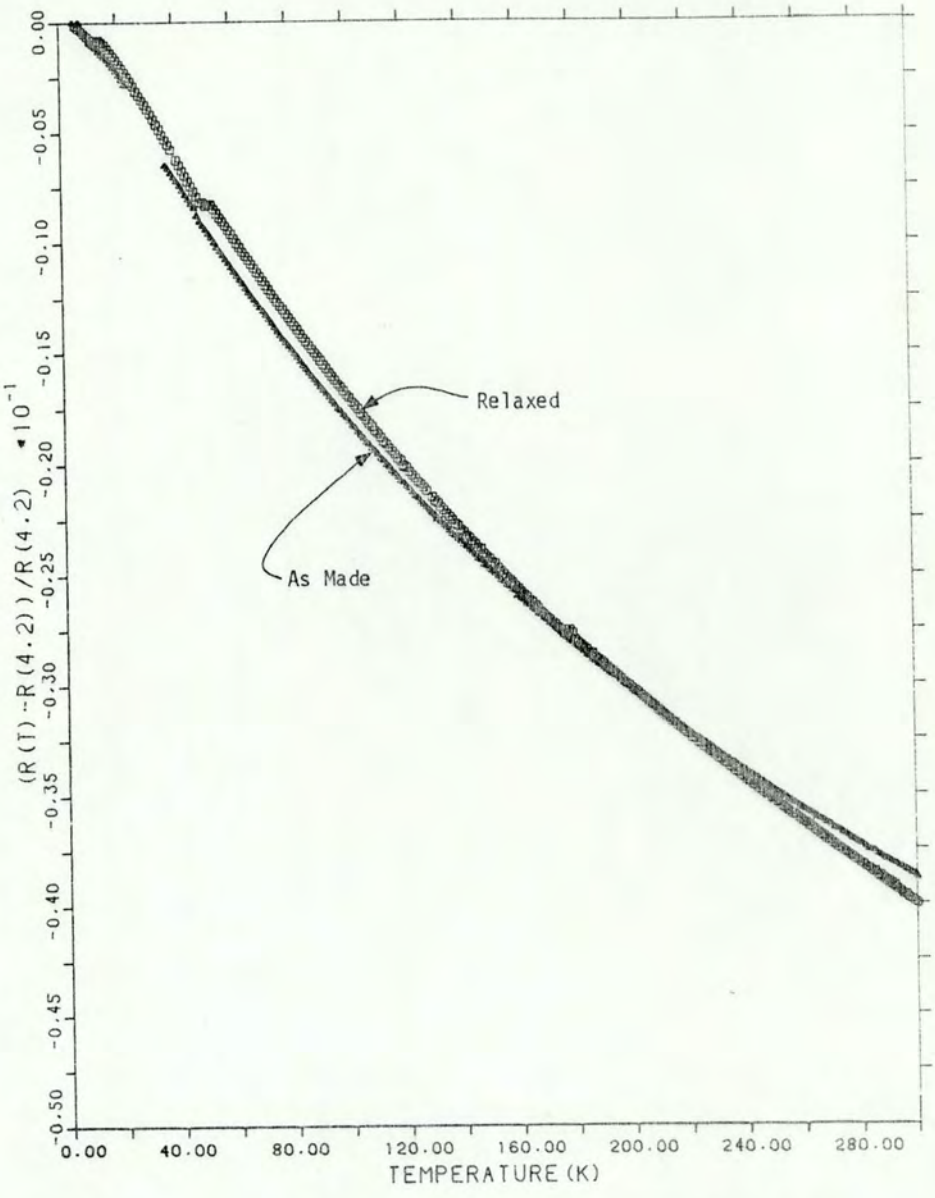

FIG. IV - 16 - Reduced resistance ratios of amorphous $Cu_{60}Zr_{40}$ in the 'as made' and 'relaxed' states.

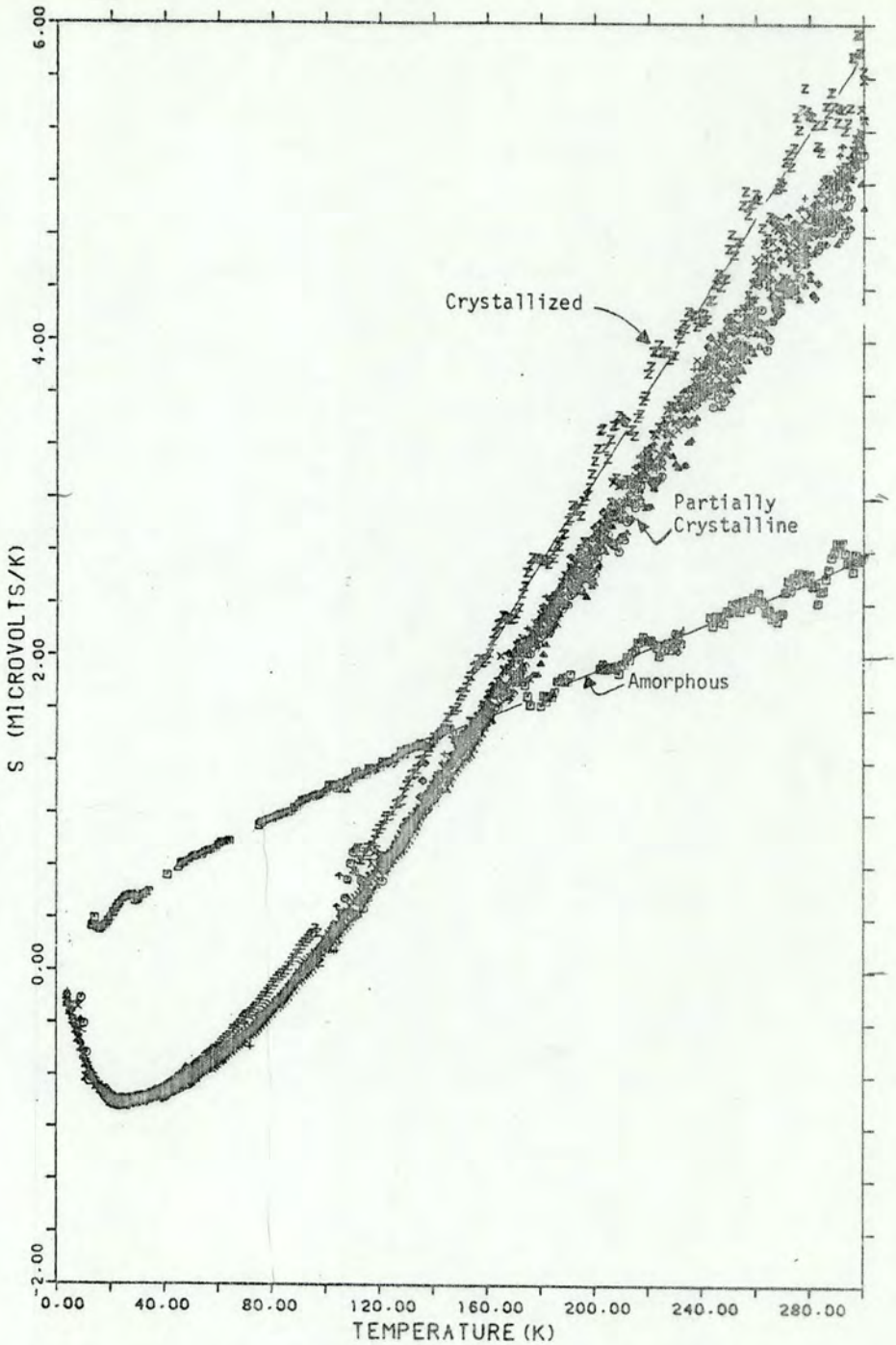

FIG. IV - 17 - Thermopower of $CuZr_2$ alloys in varying degrees of crystallivity.

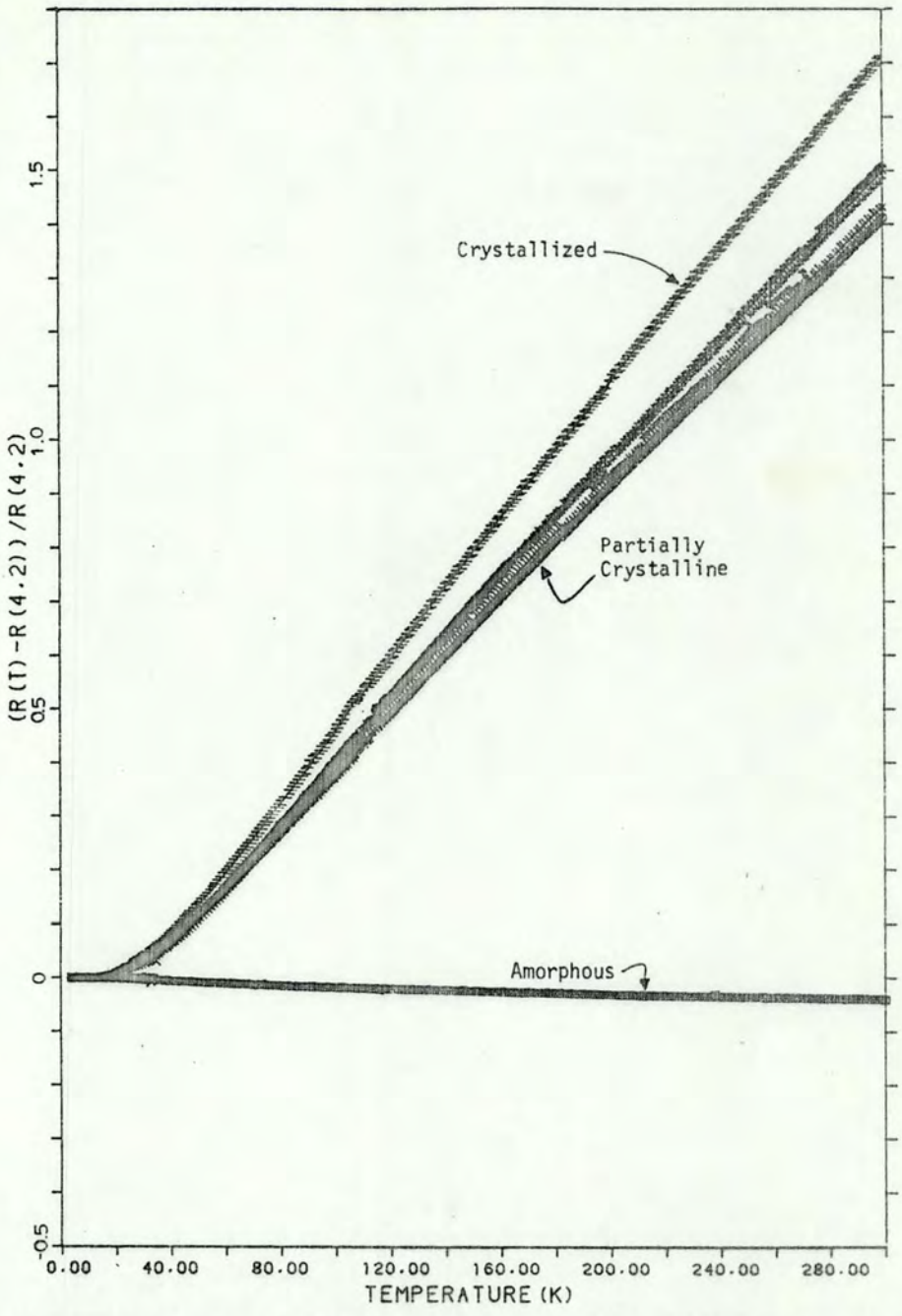

FIG. IV - 18 - Reduced resistance ratios of $CuZr_2$ alloys in varying degrees of crystallinity.

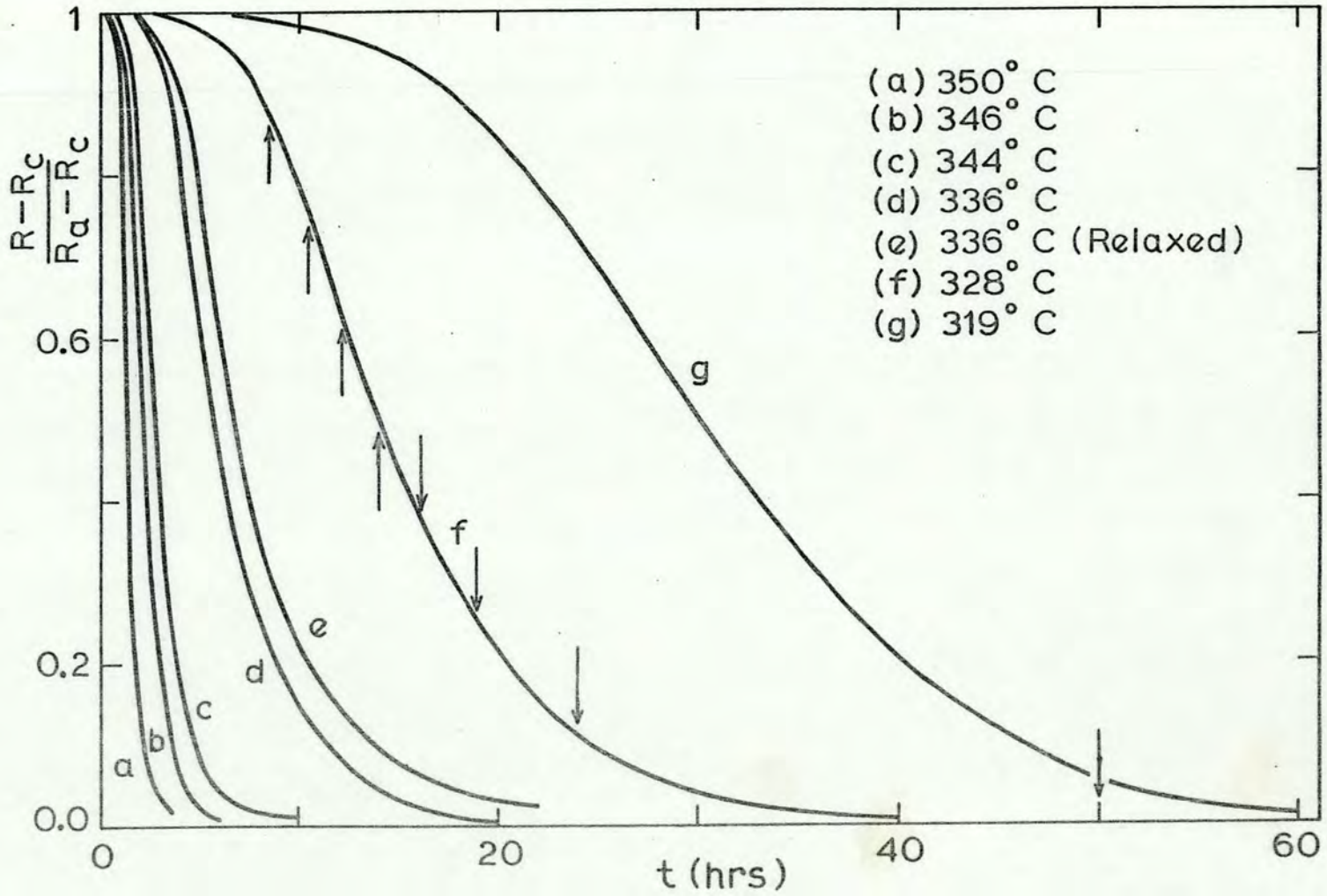

FIG. IV - 19 - Change in resistance during the crystallization of amorphous $CuZr_2$ (after Altounian et. al.[22]). The arrows indicate the positions chosen for partial crystallization.

crystallization was occurring (we monitored our experiment using time only). The samples were taken out of the furnace at those times but, as is evident, the crystallization was almost completed when the first sample was cooled. Applying the same effective medium analysis employed for $Mg_{0.70}Zn_{0.30}$ (program MBSAR.FOR in the Appendix) crystallization factors ranging from $\sim$ 99% to 100% are obtained. This leads us to believe that the crystallization characteristics of alloys near the $CuZr_2$ exact composition is extremely composition dependent, with small changes in the actual proportion of the constituents causing large changes in the activation energy, and therefore the time dependence of the isothermal crystallization.

V - DISCUSSION

V-1 Introduction

Any proposed theory of electron transport phenomena should at least be capable of correlating measurements of the various interdependent transport parameters. In this Chapter we will focus on the inherent ability of different models (or approximations) to correlate the measured values of resistivity and thermopower.

For amorphous metals this correlation is usually attempted in terms of the simple Ziman liquid metal model[7], where it is assumed that the free electron approximation is valid and that the effects of atomic disorder are taken into account using the average x-ray structure factor. This simple approximation does not include the influence of phonons on the electron scattering. Cote and Meisel[40] have evaluated the changes introduced by phonons in the electrical resistivity, but to date no extension of these results to the thermopower has been published.

In this Chapter the results for thermopower and resistivity of amorphous MgZn and CuZr alloys will be analyzed in terms of the simple Ziman model, and the limitations of this model exposed.

A simple model will be proposed which is essentially an extreme simplification of the Faber-Ziman model[19] for liquid metal alloys. This model is capable of fitting the data for both systems. A more rigorous approach in terms of an extension of the Faber-Ziman model to amorphous metal alloys requires the knowledge of the partial structure factors for the alloys. These partial structure factors have been measured for CuZr but unfortunately not for MgZn. Accordingly, the CuZr alloys are analyzed

in terms of the Faber-Ziman model and discrepancies are noted.

Recent suggestions[18,41,42] linking electron phonon mass enhancement effects to the behaviour of the thermopower and resistivity of amorphous metals are analyzed. Following Gallagher[18] the temperature dependence of the thermopower in the CuZr system is analyzed in terms of the value of λ (the electron-phonon mass enhancement term) obtained from superconductivity experiments. An attempt is also made to correlate the change in the enhancement as observed in the thermopower with that observed in the superconducting transition temperature when the alloy is thermally relaxed.

A correlation is also attempted between the high temperature derivative of the resistivity with respect to temperature and the mass enhancement term, as suggested by Rapp et al[42].

V - 2 The Simple Ziman Model

V - 2 - 1 MgZn Alloys

Recent experimental results on the heat capacity of amorphous $Mg_{70}Zn_{30}$ by Mizutani and Mizoguchi[43] indicate that this alloy behaves very nearly as a free electron system. The value found for the electronic heat capacity of this alloy (γ = 0.940 mV/g atom K^2) is within 1% of the calculated for free electrons (γ = 0.931 mV/g atom K^2). Also, Mizoguchi et al[44] have measured the Fermi wavevector (k_F) using positron annihilation and found a value of $1.46A^{-1}$, compared to the free electron value of $1.42A^{-1}$. This suggests that MgZn amorphous alloys are ideal for examining the applicability of the Ziman model to metallic glasses since this theory presupposes free electron behaviour for the materials under study.

Using the expressions developed in Chapter III, we write the thermopower as:

$$S = \frac{\pi^2 k^2 T}{3|e|\varepsilon_F}\,\xi \tag{1}$$

with

$$\xi = 3 - 2q - \frac{1}{2}\,r \tag{2}$$

where

$$q = \frac{|u(2k_F)|^2 a(2k_F)}{\langle |u(K)|^2 a(K)\rangle} \tag{3}$$

using the same notation as in Chapter III. The quantity r is expressed as:

$$r = \frac{k_F \langle \left(\frac{\partial |u(K)|}{\partial k}\right)_v a(K)\rangle}{\langle |u(K)|^2\, a(K)\rangle} \tag{4}$$

and is usually assumed to be small[13,16].

Using the expression for the resistivity

$$\rho = \frac{3\pi m \Omega_o}{8\hbar e^2 \varepsilon_F} \langle |u(K)|^2 a(K)\rangle \tag{5}$$

where m is the electron mass and Ω_o is the atomic volume, one can write the thermopower as a function of the experimental resistivity. Then

$$q = \frac{3\pi\, m\, \Omega_o}{8\hbar e^2\, \varepsilon_F}\;\frac{|u(2k_F)|^2 a(2k_F)}{\rho_{exp}} \tag{6}$$

and

$$r = \frac{3\pi\, m\, \Omega_o}{8\hbar e^2 \varepsilon_F} \; \frac{k_F \langle \left(\frac{\partial |u(K)|}{\partial k}\right)_v a(K) \rangle}{\rho_{exp}} \tag{7}$$

In order to calculate the thermopower for the different compositions of MgZn, we took the measured value of k_F (k_F = 1.46 $\mathring{A}^{-1}$) from Mizoguchi et al[44] for $Mg_{70}Zn_{30}$; for other compositions we assumed that a free electron model closely describes the system and scaled k_F to $\Omega_o^{1/3}$. The atomic volumes were obtained from density measurements[37] by taking

$$\Omega_o = \frac{(1 - x)\, M_{Mg} + x\, M_{Zn}}{0.602\, d}\, A^3 \tag{8}$$

where M_y is the atomic mass of element of y, and d is the density of the alloys expressed in g/cm^3.

The structure factor used in these calculations is that obtained by Mizoguchi et al[44] for $Mg_{0.70}Zn_{0.30}$. It is a total structure factor and we were forced to make the assumption that it did not change with composition. This is certainly not true for total structure factors in general and we estimate this introduced the largest errors in the analysis. By comparison with the variation of the total structure factors as a function of concentration in amorphous CuZr alloys one can estimate changes of the order of ± 4% in the value of the total structure factor of the extreme compositions in this series of MgZn alloys.

The values used for the pseudopotentials |u(K)| were obtained by linear interpolation between the published values for pure Mg and Zn[28] using the concentration as a weighting parameter:

$$|u_{alloy}(K)| = (1 - x)|u_{Mg}(K)| + x|u_{Zn}(K)| \tag{9}$$

All the parameters are presented in Table V-1, where the results of a calculation using equations (1),(2),(3),(5),(6),(8) and (9) at room temperature are also shown.

The experimental results as a function of concentration, at room temperature, are compared to the calculations in Figure V-1.

The agreement between the simple Ziman model and the experimental results for the thermopower is very poor even for this free electron alloy.

So far, we have considered that the term r in Eq.(2) is negligible. If one assumes that r is responsible for the difference between the experimental and calculated thermopowers, the quantity r should have a value ranging from 0 to -3. These values become large compared to the values for q and would indicate that in amorphous metals the thermopower is dominated by the energy dependence of the pseudopotential, the reverse of what is seen in liquid metals.

Unfortunately, a calculation of r from the Ziman model lies beyond our reach since the energy dependence of the pseudopotentials are unavailable.

V - 2 - 2 CuZr Alloys

The simple Ziman model can also be applied to CuZr amorphous alloys, where the total structure factors are known for different compositions.

A serious drawback to the application of this theory arises because there is evidence from both heat capacity[45] and thermal conductivity[46] experiments that amorphous CuZr alloys depart considerably from the free electron model.

TABLE V - 1

x	$a(2k_F)$	$\rho(\mu\Omega cm)$	$\varepsilon_F(eV)$	q	S(μV/K)
0.20	0.94	35	7.95	0.322	-2.17
0.25	0.89	43.1	8.04	0.245	-2.28
0.30	0.84	52.2	8.11	0.190	-2.36
0.33	0.83	47.8	8.19	0.201	-2.32
0.35	0.83	47.	8.20	0.206	-2.31

Parameters of a simple Ziman model calculation for the thermopower amorphous $Mg_{(1-x)}Zn_x$ alloys.

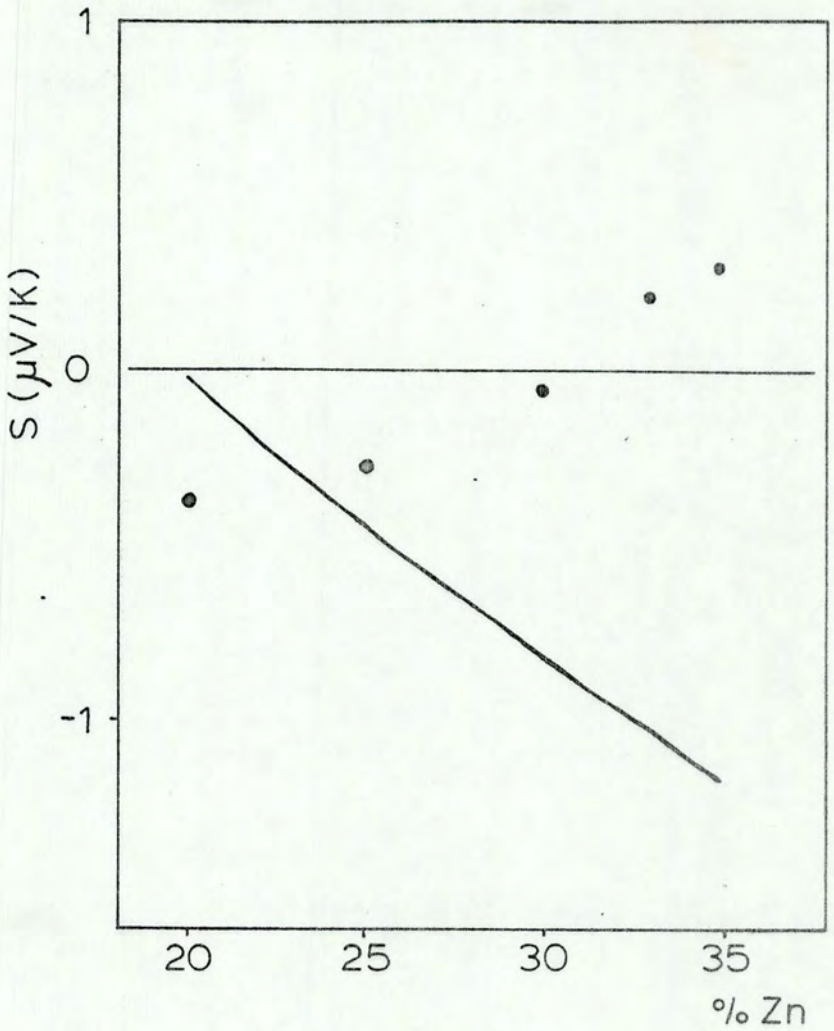

FIG. V - 1 - Thermopower of amorphous MgZn alloys at room temperature
(o) - experimental results
(□) - simple Ziman model calculation

On the basis of their x-ray determination of the structure factors Chen and Waseda[47] have suggested that there is charge transfer in CuZr. Other authors[48,42] have interpreted this as a reduction of the number of available electrons for transport.

This can be understood with the help of the photoemission results of Kübler et al[45]. In that study it was concluded that the bands reaching the Fermi energy are those of Zr and the effect of the charge transfer was to leave only s electrons available for transport.

This last assumption translates into using a valence $Z_{Zr} = 2$ instead of the usual $Z_{Zr}=4$ found for crystalline Zr. It also means that the electrons available for conduction are free electrons, which makes the free electron approximation more plausible.

We will thus assume that CuZr amorphous alloys are free electron-like with the number of electrons assigned as one for Cu and two for Zr. With this assumption we can apply the standard Ziman formalism to amorphous CuZr alloys.

To do this, the value of the pesudopotential for Zr must be determined. The value found in the literature has been established for crystalline Zr, which has valence 4. This value is not applicable in the present case where we have assumed that Zr has valence 2. We therefore resort to the scattering matrix formalism in order to calculate the needed pseudopotentials.

Using the t matrices published for CuZr[48] one can evaluate the pseudopotential for Cu and Zr in CuZr amorphous alloys and use the results to estimate $|u(2k_F)|_{alloy}$ using either one of the following approximations.

a) The definition of an effective pseudopotential related to the t

scattering matrices is given by[a]

$$u_{eff} \sim \frac{2}{3}\varepsilon_F \frac{2}{\pi}\frac{1}{Z}\sum_{\ell=0}^{\infty}(2\ell+1)\sin\eta_\ell \exp(i\eta_\ell)P_\ell(\cos\theta) \tag{10}$$

where ε_F is the Fermi energy of the alloy and Z is the valence of the ion.[a]

Upon evaluation of the sum in (10) the pseudopotential is obtained from the values of the Fermi energy of the alloy, the valence and the phase shifts (η_ℓ) associated with each of the elements.

Using the results of Waseda and Chen[48] for the phase shifts and $Z_{cu} = 1$; $Z_{Zr} = 2$; $\varepsilon_F \sim 7.05$eV[b] one obtains:

$$u_{eff}(2k_F)|_{cu} = 2.63\text{eV}$$
$$u_{eff}(2k_F)|_{Zr} = 10.63\text{eV} \tag{11}$$

b) Alternatively one takes the ratio of the values of $|t|^2$ at $2k_F$ as the square of the ratio of the pseudopotentials[c]

$$\frac{u(2k_F)|_{cu}}{u(2k_F)|_{Zr}} = \sqrt{\frac{|t_{cu}|^2}{|t_{Zr}|^2}} \tag{12}$$

(a) this expression is written following the normalization procedure of Dreirach[29] et al, using eq. (25), which results in t-matrices and pseudopotentials with the dimensions of energy.

(b) From density measurements[37] and a free electron model.

(c) This arises from the definitions of u_{eff} and t such that

$$u_{eff}{}^2 \sim |t|^2 = \frac{1}{2}(t^*t + tt^*) \tag{13}$$

Using the value found for crystalline Cu[28] at $2k_F$ as the value for Cu in amorphous CuZr one obtains[b]:

$$u(2k_F)|_{Cu} = 3.39\text{eV}$$
$$u(2k_F)|_{Zr} = 6.84\text{eV} \qquad (14)$$

Using any of the values obtained in a) or b), one can approximate the total pseudopotential at $2k_F$ by a concentration based linear interpolation:

$$u(2k_F)|_x = (1-x)\, u(2k_F)|_{Cu} + x\, u(2k_F)|_{Zr} \qquad (15)$$

With this information, and the values for $a(2k_F)$ interpolated between the measured total structure factor one can evaluate q in a simple Ziman model:

$$q = \left(\frac{3\pi N}{e^2 \hbar v_F^2 V}\right) \frac{[u(2k_F)]_x^2\, a_x(2k_F)}{\rho_{exp}} \qquad (16)$$

The results obtained with the values (11) and (13) are presented in Table V-2, along with the relevant parameters used for the calculation. In Figure V-2, we compare the calculated thermopowers to the experimentally measured ones as a function of concentration, at 300K.

TABLE V - 2

x	$a(2k_F)$	$u(2k_F)$ (a)	$u(2k_F)$ (b)	q (a)	q (b)	ρ	S(300K) (a)	S(300K) (b)
0.30	2.07	4.93	4.42	1.26	1.02	177.5	-0.50	-1.00
0.35	2.07	5.32	4.60	1.43	1.07	182.5	-0.15	-0.89
0.40	1.97	5.70	4.77	1.56	1.10	182.5	+0.12	-0.83
0.45	1.91	6.09	4.94	1.76	1.16	179.5	+0.54	-0.71
0.50	1.86	6.48	5.12	1.98	1.24	176	+1.00	-0.54
0.55	1.82	6.85	5.29	2.22	1.32	172	+1.50	-0.37
0.60	1.77	7.24	5.46	2.45	1.39	169	+1.98	-0.23
0.67	1.71	7.74	5.77	2.79	1.55	164	+2.68	+0.10
0.70	1.68	8.01	5.80	2.96	1.55	162.5	+3.00	+0.10

Parameters of a simple Ziman model calculation for the thermopower of amorphous $Cu_{(1-x)}Zr_x$ alloys

(a) - using method (a) to find the pseudopotential (page

(b) - using method (b) to find the pseudopotential (page

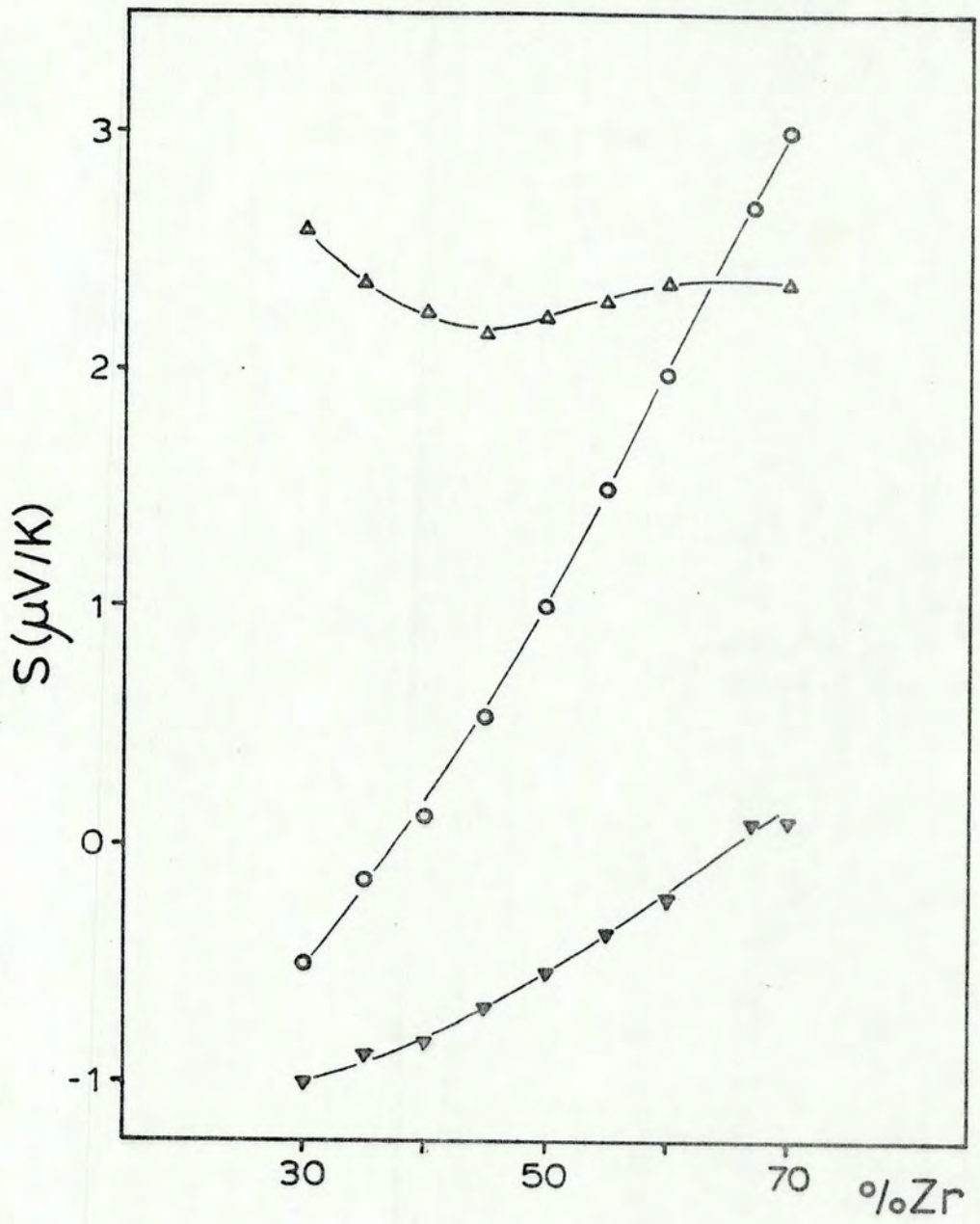

FIG. V - 2 - Thermopower of amorphous CuZr alloys

(△) - experimental results

(○) - simple Ziman model calculation with the pseudopotentials obtained in 4-2-2 (a)

(▽) - simple Ziman model calculation with the pseudopotentials obtained in 4-2-2 (b)

As it is clear from Figure V-2, one does not obtain a reasonable behaviour for the calculated thermopowers, irrespective of the set of pseudopotentials used.

The use of a simple Ziman model to explain the behaviour of the thermopower of amorphous metals, as proposed originally by Sinha[4] and subsequently advocated by Nagel[13] and others[16] is clearly not correct. This model is able to generate results that are linear in temperature (which is inherent in the model), but the absolute values it predicts, and most important, the composition dependence of the thermopowers are in disagreement with the experimental results.

A possible explanation of the observed effects comes from considering these amorphous metals as the alloys they really are. In this case one should use the theory developed by Faber and Ziman for liquid metal alloys. This theory was presented in Chapter III (page 27) and it can be seen in Eq. (III - 20,21) that the partial structure factors are needed for the calculation.

There exists in the literature two separate determinations of the partial structure factors for amorphous CuZr alloys[47,50]. Unfortunately there is considerable disagreement in these results. At the present time there is no determination of the partial structure factors for amorphous MgZn alloys. This lack of reliable information has lead us to propose a simple two component model which can be considered as a simplification of the Faber-Ziman approach.

V - 3 Simple two component model

The basic assumption in the Faber-Ziman theory of liquid metallic alloys is that there are two different scatterers participating in the transport phenomena of a binary alloy. In the simplest case each scatterin nechanism produces linear first order diffusion thermopower, then:

$$S_1 = aT$$
$$S_2 = bT \qquad (18)$$

where subscripts 1 and 2 refer to the scattering mechanisms.

Applying the Nordheim-Görter rule[31] to obtain the total diffusion thermopower of the alloy one has:

$$S_{alloy} = \frac{\rho_1}{\rho_1 + \rho_2} aT + \frac{\rho_2}{\rho_1 + \rho_2} bT \qquad (19)$$

where ρ_1 and ρ_2 are the resistivities associated with the scattering mechanisms

Upon assuming that ρ_i and ρ_2 vary linearly with the composition of the alloy one can write:

$$\rho_1 = (1 - x)\rho_a$$
$$\rho_2 = x\,\rho_b \qquad (20)$$

So the resistivity as a function of concentration is written as

$$\rho(x) = \rho_1 + \rho_2 = \rho_a + x(\rho_b - \rho_a) \tag{21}$$

Equation (12) can be written as

$$\frac{S(x)}{T} = \frac{(1 - x)}{\rho(x)} \rho_a(a - b) + b \tag{22}$$

and if our model is applicable a plot of $\frac{S(x)}{T}$ against $\frac{(1 - x)}{\rho(x)}$ should yield a straight line with intercept b and slope $\rho_a(a - b)$. Since the value of ρ_a can be found from an extrapolation of the resistivity results, all the parameters of the model can be determined.

V - 3 - 1 - MgZn Alloys

This model now can be applied to MgZn alloys. Figure IV - 3 shows that the resistivity is, within experimental error, linear in composition for MgZn in agreement with eq. (21). A plot of the experimentally obtained values for $S(x)/T$ vs. $(1 - x)/\rho(x)$ of MgAn alloys

is shown in Figure V.3. The rather large error bars result from the difficulty of measuring ρ.

Using Equation (14) and a value of ρ_a = 16 μΩ-cm we obtain $a = -10.3 \times 10^{-3}$ μV/K^2 , $b = 3.5 \times 10^{-3}$ μV/K^2 , and the characteristic thermopowers at 300K are S_1 = -3.1 μV/K and S_2 = + 1.05 μV/K.

The thermopower of the alloys can now be calculated by applying Eq. (22). This is done for T = 300 K and the results are shown in Figure V-4 where we also show the experimental results as a function of concentration.

This approach affords very good agreement with experiment despite its relative simplicity. Furthermore, the characteristic values found for the thermopowers S_1 and S_2 are not inconsistent with the measured thermopowers of amorphous metal alloys[15], and the resistivity ρ_a is remarkably close to what would be expected for supercooled liquid Mg[51].

V - 3 - 2 - CuZr Alloys

The same model can be applied to CuZr amorphous alloys in the region where the resistivity is very nearly a linear function of concentration ($x \geq 0.40$).

The characteristic parameters obtained using Eq. (22) and the extrapolation from the experimental resistivities are as follows: ρ_a the value of the resistivity of "pure amorphous" Zr is found to be equal to 141.8 μΩ-cm ; $a = 5.74 \times 10^{-3}$ μV/K^2 and $b = 8.70 \times 10^{-3}$ μV/K^2, giving characteristic thermopowers at 300K of S_1 = 1.72 μV/K and S_2 = 2.61 μV/K.

Figure V-5 shows the experimental resistivities with the linear extrapolation used to find ρ_a; Figure V-6 shows the experimental results as well as those calculated in this approximation for the thermopowers.

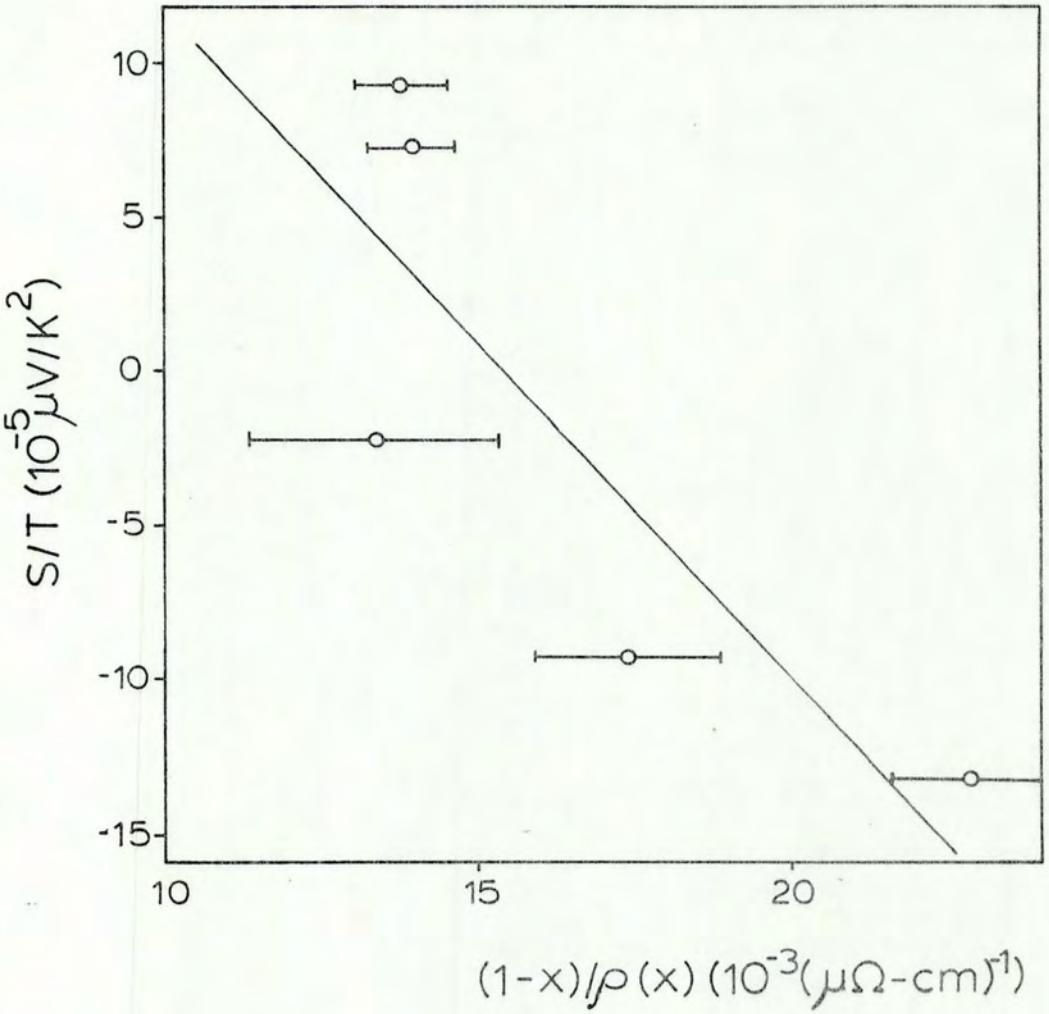

FIG. V - 3 - Plot of S/T vs. $(1 - x)/\rho(x)$ of amorphous MgZn alloys.

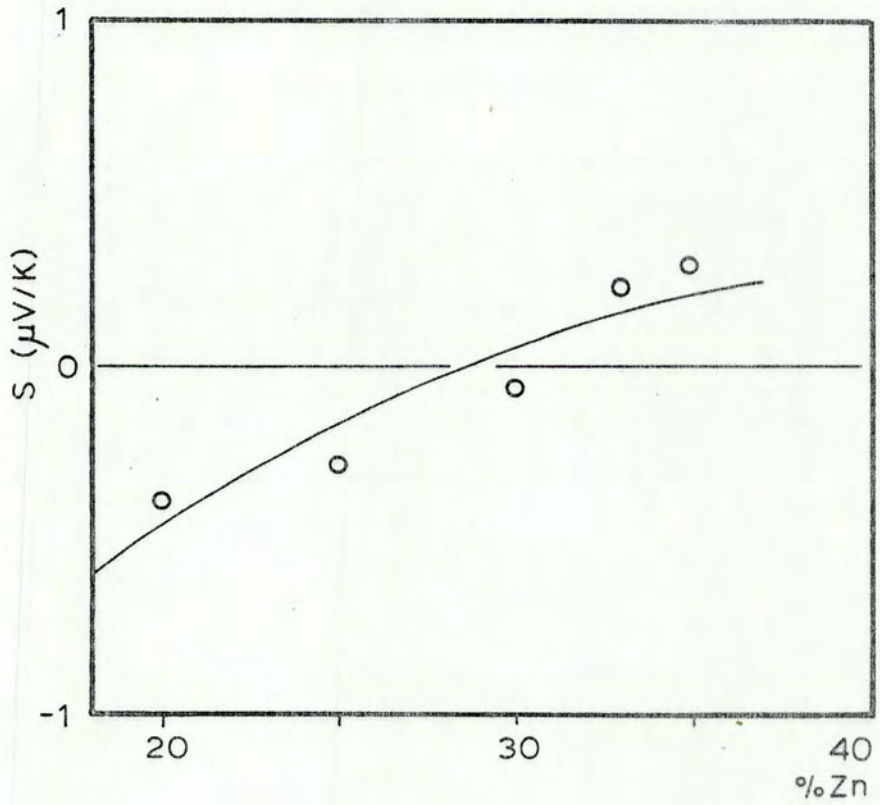

FIG. V - 4 - Thermopower of amorphous MgZn alloys. The experimental results are represented by (o) and the solid line is the result of a two component model calculation (see text).

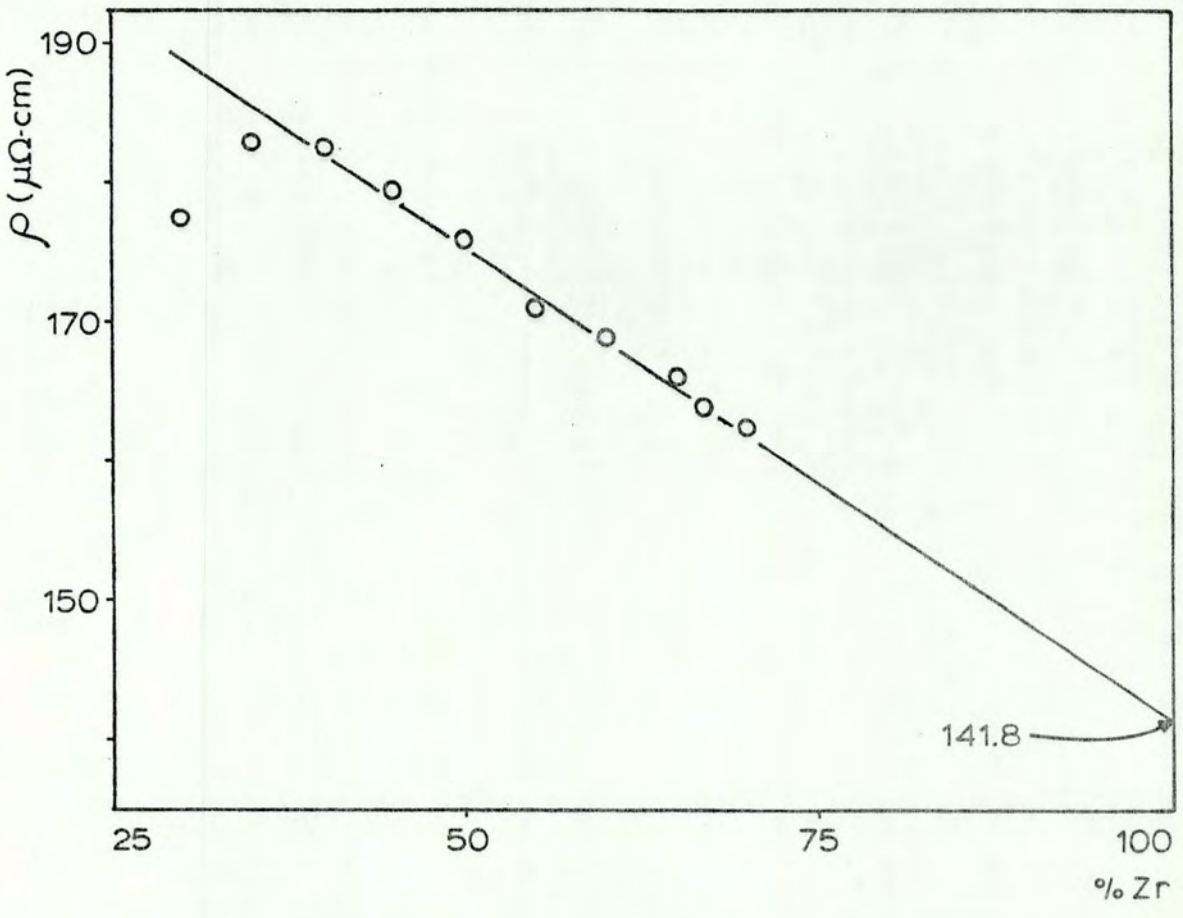

FIG. V - 5 - Resistivity of amorphous CuZr alloys showing the linear regression used for the two component model in (V 4-2).

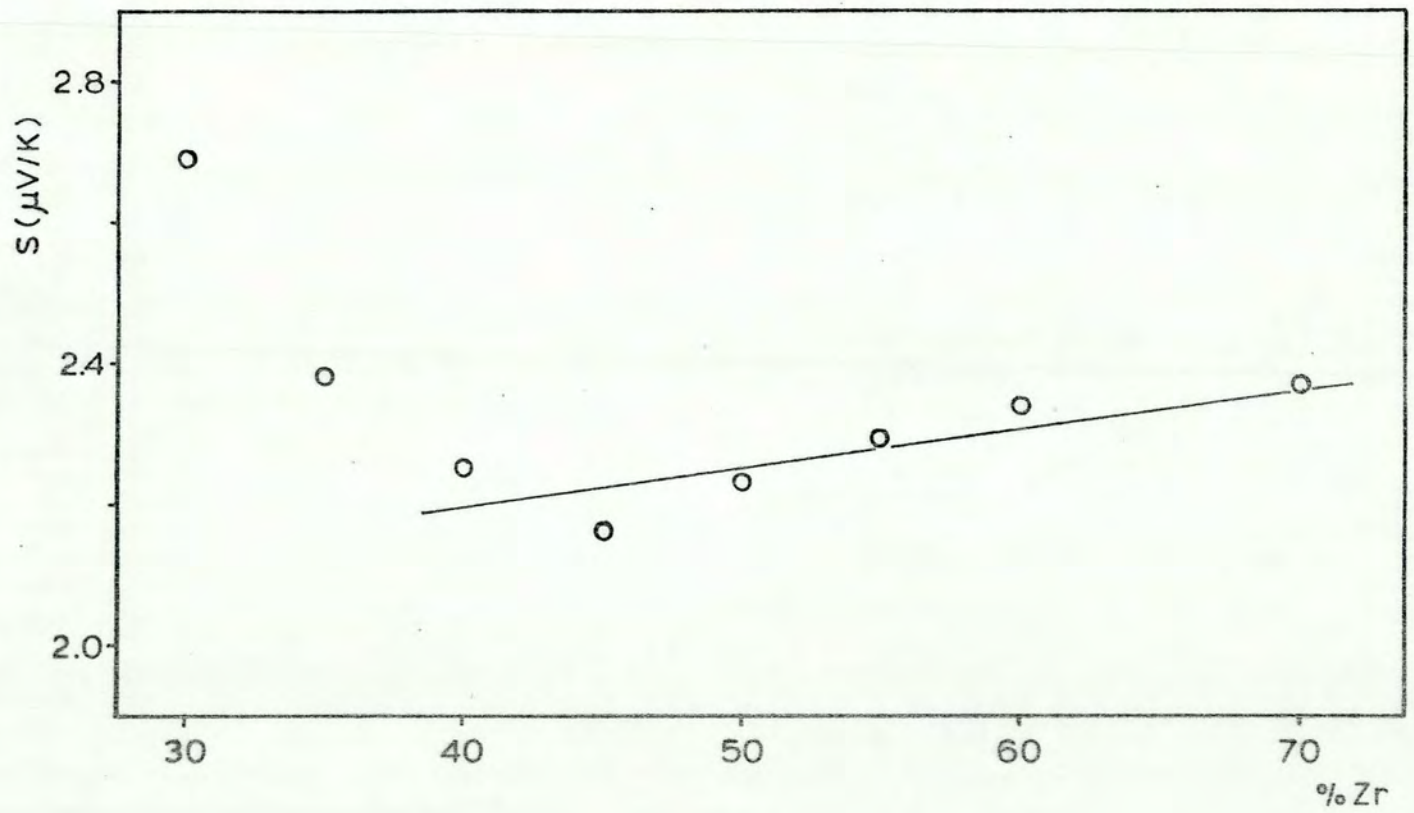

FIG. V - 6 - Thermopower of amorphous CuZr alloys. The experimental results are represented by (o) and the solid line is the result of a two component model calculation (see text).

It can be seen that, once again, relatively good agreement is obtained with this very simple model.

The results described above allow us to conclude that a simple Ziman approach produces results that are unrealistic (r varying from $\sim$ 0 to -3 as x goes from 0.2 to 0.35 while q only changes from 0.84 to 1.5) in contrast to a Faber-Ziman approach (since our calculation can be considered a simplification of it) where the contributions from each of the elements are counted in the calculation.

The results obtained in both alloy systems suggest that amorphous metals should be considered as the alloys they really are to obtain reasonable correlation between the various transport properties.

This should be tested further with the use of partial structure factors, where a more complete analysis of the problem can be obtained.

V - 4 Using Partial Structure Factors

Partial structure factors for MgZn amorphous alloys are, most regretably, unavailable. We therefore limit ourselves to studying CuZr amorphous alloys, where two sets of partial structure factors are available[47,50].

One of the essential parameters needed for the calculation of the electronic transport properties using the theory of Faber and Ziman is the value of the Fermi wavevector, k_F. Since no direct measurement of k_F for any of the CuZr alloys is found in the literature, we have used the measured densities and a free electron model to calculate it in the following manner:

The 'atomic' volume for the alloy was taken from Eq. (8), now written as

$$\Omega_o = \frac{(1 - x)M_{Cu} + x\, M_{Zr}}{0.602\ d} A^3 \tag{23}$$

From this and the effective valence, taken as being

$$Z_{alloy} = (1 - x)Z_{Cu} + x\, Z_{Zr} \tag{24}$$

for an alloy $Cu_{(1 - x)}Zr_x$ with $Z_{Cu} = 1$ and $Z_Zr = 2$, we calculated k_F in the free-electron approximation(52) :

$$k_F = (3\pi^2)^{1/3}\left(\frac{Z_{alloy}}{\Omega_o}\right)^{1/3} \tag{25}$$

Using the same assumptions developed for Eqs. (6) and (7), we write the integral $\langle a(K)|u(K)|^2\rangle$ as a function of the experimental resistivity. In the notation of Faber and Ziman this becomes:

$$q = \frac{F(2k_F)}{\langle F(2k_F)\rangle} = \left(\frac{3\ N}{e^2 \hbar v_F^2\ V}\right) \frac{F(2k_F)}{\rho_{exp}} \tag{26}$$

where

$$F(K) \equiv |u_{Zr}|^2\{x(1 - x) + x^2 a_{ZrZr}\} + |u_{Cu}|^2\{x(1 - x) + (1 - x)^2 a_{CuCu}\} + \tag{27}$$

$$+ 2u_{Cu}u_{Zr}\, x(1 - x)(a_{CuZr} - 1)$$

and a_{ij} are the experimental partial structure factors.

The pseudopotentials can be substituted by t scattering matrices, for which one writes[40]

$$F(K) = |t_{Cu}|^2\{x(1 - x) + (1 - x)^2 a_{CuCu}\} + |t_{Zr}|^2\{x)1 - x) + x^2 a_{ZrZr}\} + \tag{28}$$

$$+ |t^*_{Cu}t_{Zr} + t_{Cu}t^*_{Zr}|\{x(1 - x)(a_{CuZr} - 1)\}$$

In this formulation, we can use the results obtained by Waseda and Chen[48] for the amorphous $Cu_{60}Zr_{40}$ alloy. These authors have published the phase shifts η_ℓ describing the t matrices as:

$$t(E_F, K) = -\frac{2\pi}{\Omega_0(2E_F)^{1/2}} \Sigma_\ell (2\ell + 1)\sin \eta_\ell \exp(i\eta_\ell) P_\ell(\cos\theta) \tag{29}$$

We took the values of η_ℓ and the further assumption that the individual scattering matrices did not change with composition.

All relevant data, and the values of the parameters calculated are listed in Table V-3.

As mentioned before, two sets of partial structure factors were found in the literature for amorphous CuZr alloys. In view of the considerable disagreement in these results, and the lack of evidence for one of them being for some reason erroneous, we have done the calculations using both sets of partial structure factors.

As a matter of convenience, we present the structure factors used in these calculations in Figures V-7 to V-9.

As a first approximation we take the standard assumption that r is small (see Nagel[13,16]) and obtain values of q and S. The room

TABLE V - 3

x	ρ	q		S(300K)	
		(a)	(b)	(a)	(b)
0.30	177.5	2.46	1.20	2.01	+0.58
0.35	183	2.57	2.76	2.20	-2.42
0.40	182.5	3.10	2.52	3.32	-2.93
0.45	179.5	3.52	3.06	4.19	-2.99
0.50	176	4.01	3.73	5.22	-5.25
0.55	171	3.62	4.58	4.40	-6.89
0.60	169	3.07	5.51	3.27	-8.67
0.65	166	2.50	6.61	2.08	-12.71
0.67	164	2.26	7.06	1.58	-13.57
0.70	162.5	1.95	7.47	0.95	-14.37

Parameters of a Faber-Ziman calculation of the thermopower of amorphous $Cu_{(1-x)}Zr_{(x)}$ alloys.

(a) - using the partial structure factors of Chen and Waseda[47]

(b) - using the partial structure factors of Kudo et al[50]

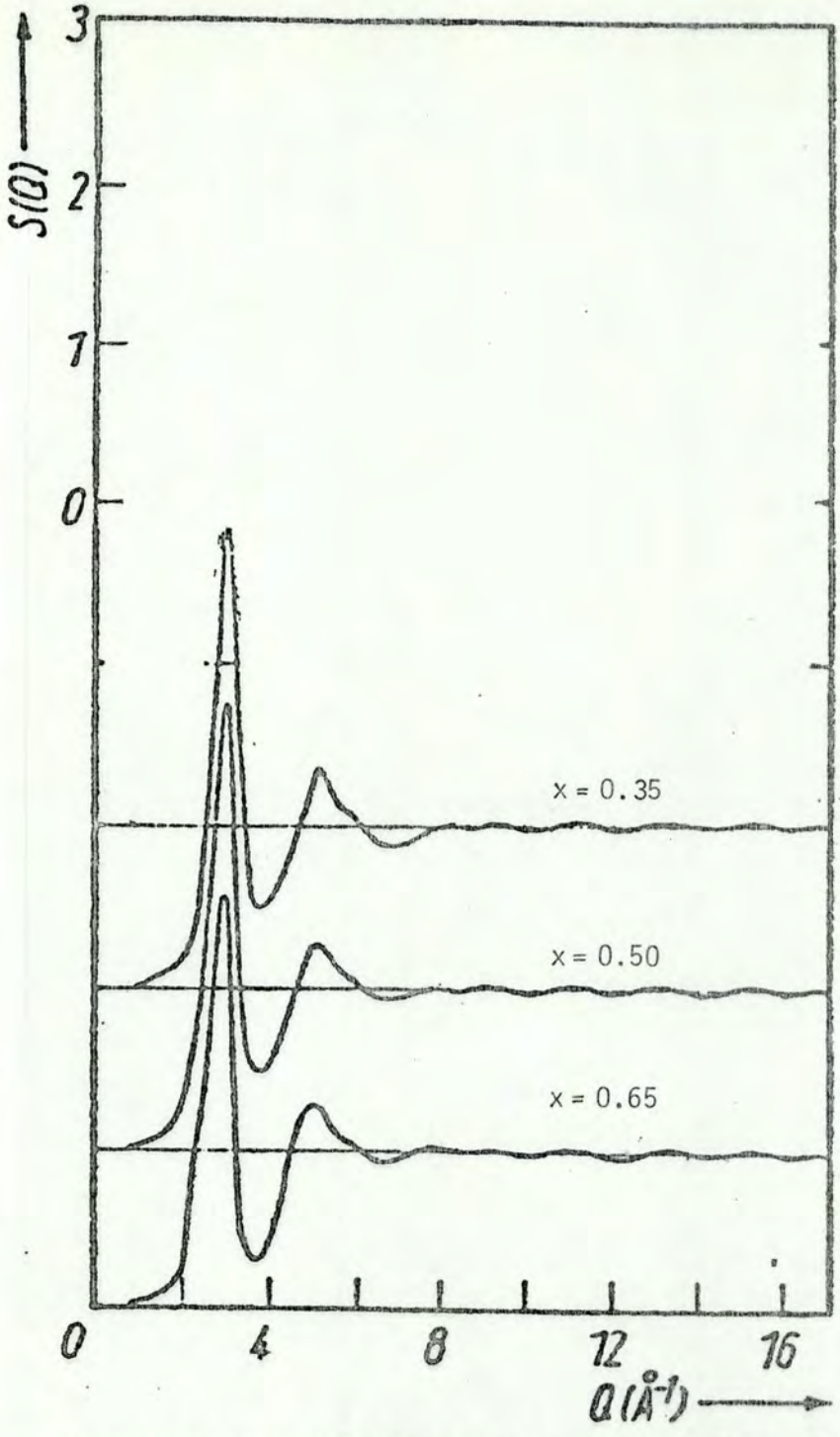

FIG. V - 7 - The total structure factors of amorphous CuZr alloys, after Chen and Waseda[47].

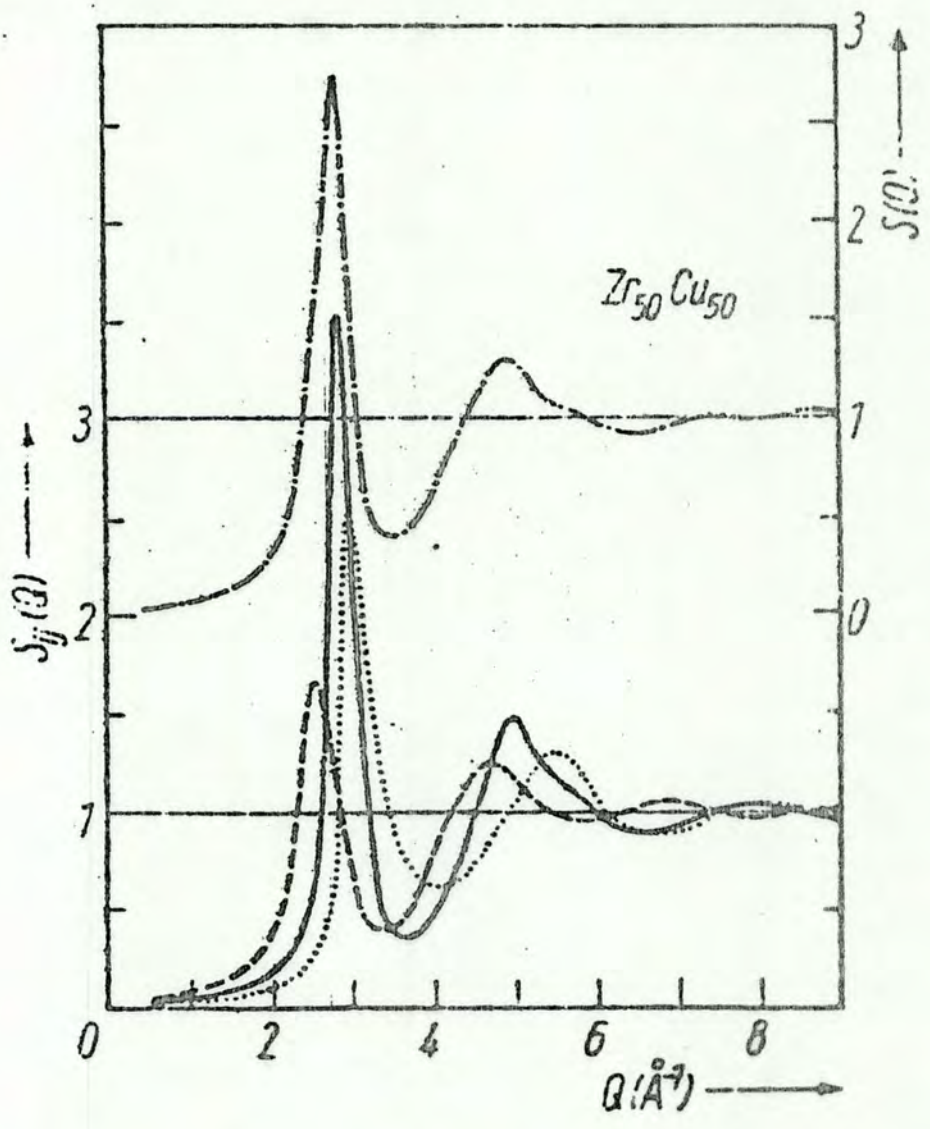

FIG. V - 8 - The partial structure factors of amorphous CuZr, after Chen and Waseda[47].

(_____ Zr-Cu).....Cu-Cu, -----Zr-Zr, ------ total)

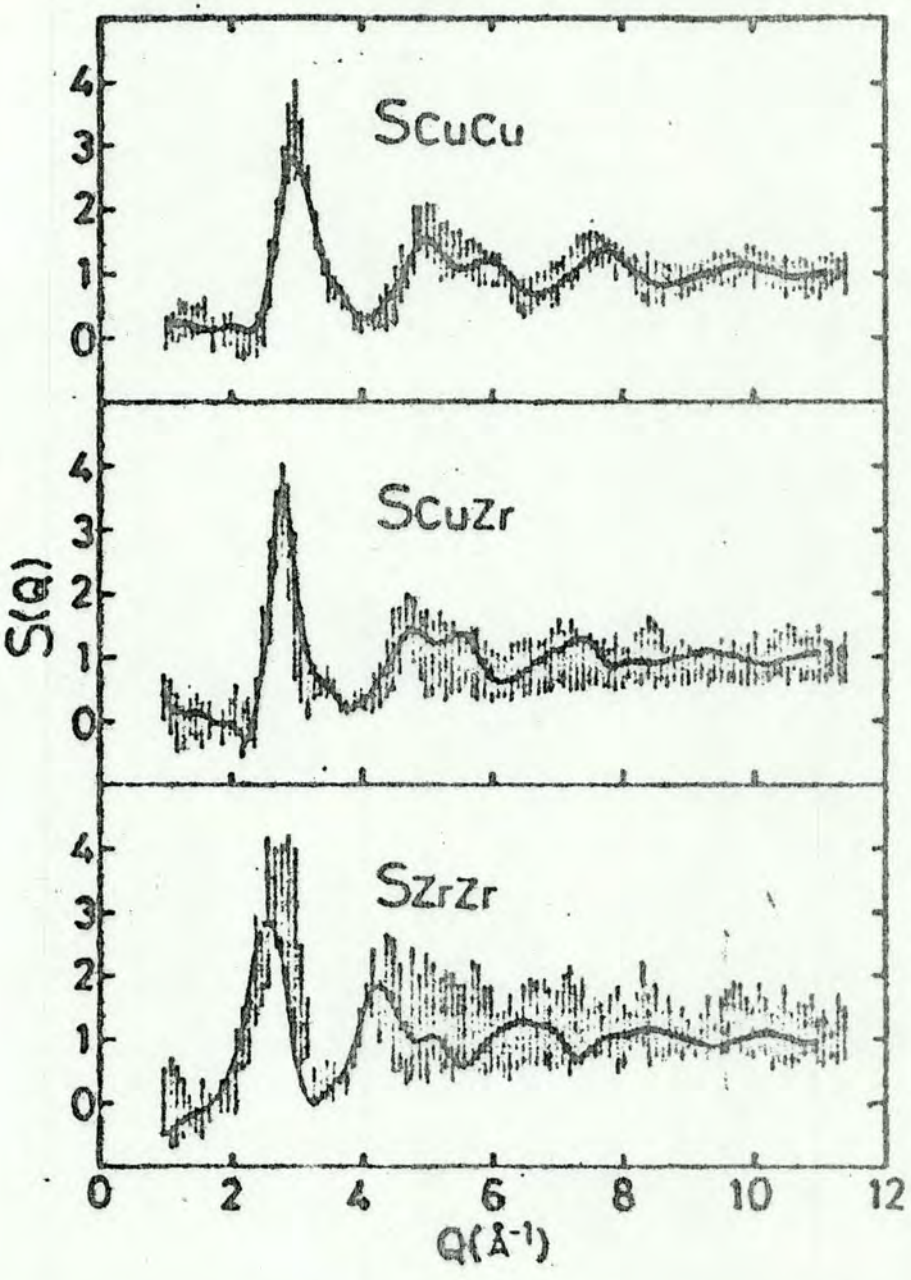

FIG. V - 9 - The partical structure factors of amorphous CuZr alloys, after Kudo et.al.[50].

temperature thermopowers obtained in this approximation are shown in Figure V-10 as a function of composition.

It is clear, only Chen and Waseda's[47] values for the partial structure factors give the correct sign and order of magnitude for the thermopowers.

We should point out that the disagreement between the q values calculated from Chen and Waseda's partial structure factors and those obtained by Kudo et al[50] is greatly reduced if one performs the integration $\langle|u|^2 a\rangle$ instead of assuming it proportional to the experimental resistivity[53]. But this is obviously begging the question since one does not thereby obtain the correct resistivities.

The difference between the measured and calculated thermopowers in this approximation is most probably due to the neglected energy dependent term r and this is plotted in Figure V-11.

A calculation of the quantity r could be attempted at this point, using the expression[31]:

$$r = k_F \frac{\langle|\frac{\partial F(k,K)}{\partial k}|^2_{k_F}\rangle}{\rho/C} \qquad (30)$$

where F is given by Eq. (28) and the integration indicated by the brackets performed between 0 and $2k_F$ as usual. The large number of approximation in this particular calculation, and the fact that we have two conflicting structure factors led us to conclude that, although all the parameters needed are known, the results obtained from this long procedure would contain errors much larger than would be needed for comparison with the experiments or with calculation of q. It should be pointed out never-

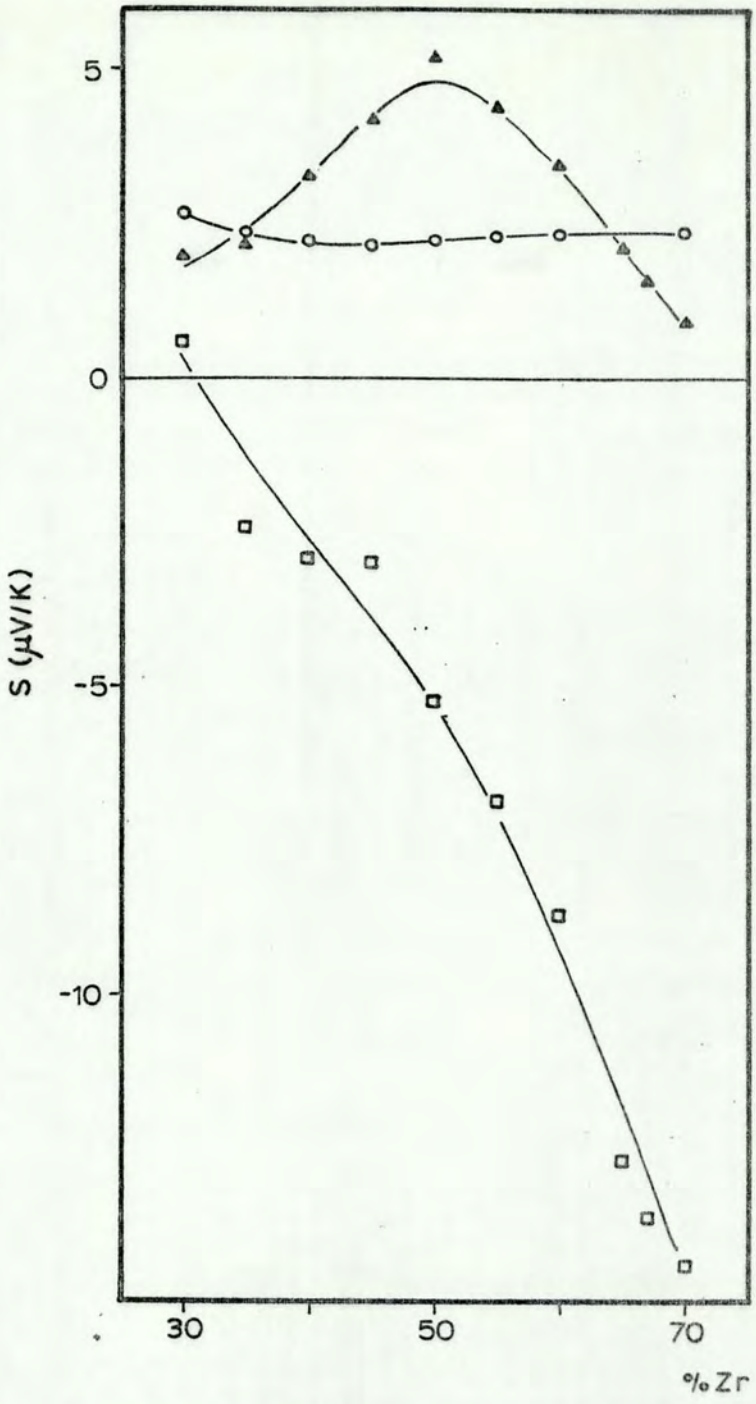

FIG. V - 10 - Thermopower of amorphous CuZr alloys at room temperature.
(O) - experimental results
(▲) - Faber-Ziman calculation using the partial structure factors of Chen and Waseda[47]
(□) - Faber-Ziman calculation using the partial structure factors of Kudo et.al[50]

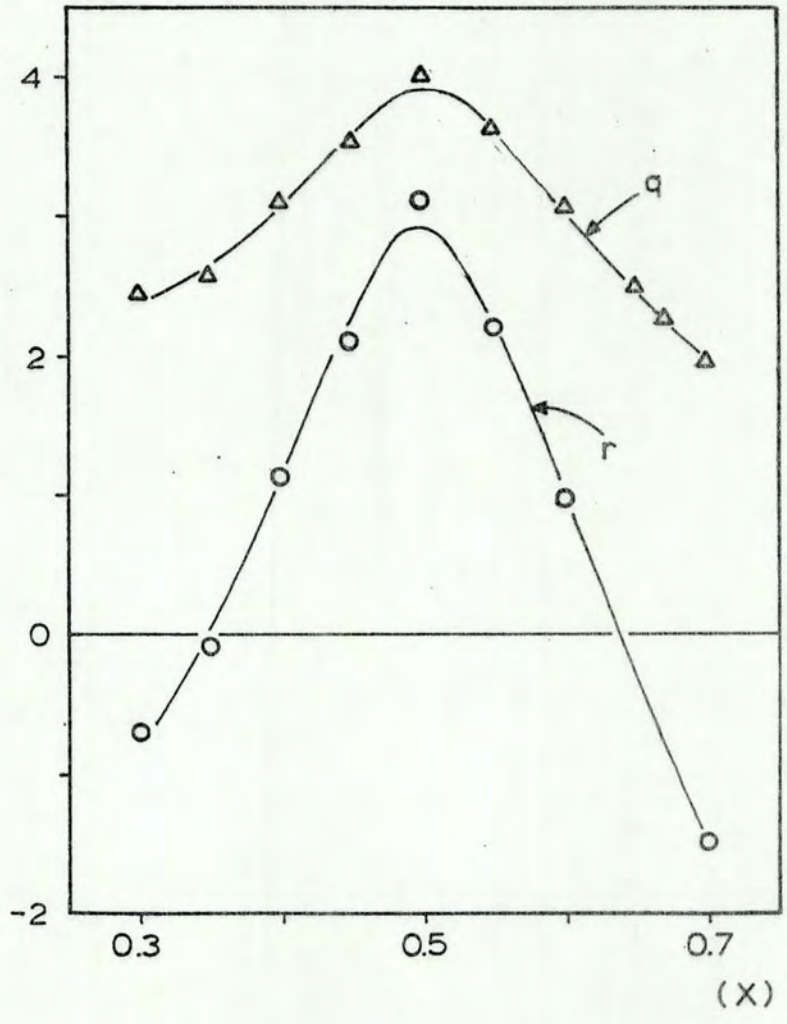

FIG. V - 11 - The parameters r and q as a function of composition, for amorphous CuZr alloys. These are calculated from a Faber-Ziman model and partial structure factors by Chen and Waseda[47] (see text)

theless that the larger contributions to r should come from the energy dependence of the phase shifts in Zr.

The results obtained using partial structure factors do not agree with the experiment if one supposes r, the term containing the energy dependence of the pseudopotential or scattering matrix, to be negligible as proposed by Nagel and others[13,16]. The results are, however, of the right order of magnitude and sign for the partial structure factors of Chen and Waseda.

This indicates that, as implied by Cote and Meisel[40], X-ray determined structure factors are closer to the true electron scattering structure factors (resistivity structure factors) than those determined by neutron scattering.

But, irrespective of which set of partial structure factors is used, we have shown that the energy dependence of the pseudopotential is central to the understanding of transport phenomena in amorphous CuZr alloys.

V - 5 - The Mass Enhancement Contribution to Electron Transport in CuZr Amorphous Alloys

On analyzing the high and low temperature behaviour of the thermopower of amorphous CuZr alloys one observes a distinct change in slope near 40K for all compositions. One of the possible explanations for this is the suggestion that electron-phonon mass enhancement effects could be the cause of the observed change in slope. This theory, advanced by Gallagher[18], suggests that at lower temperatures the thermopower is enhanced by $(1 + \lambda)$, where λ is the phonon mass enhancement parameter[54].

At high temperatures ($T \gtrsim \Theta_o$) the enhancement disappears, giving

$$\frac{(S/T)_{lowT}}{(S/T)_{highT}} = (1 + \lambda) \tag{31}$$

It is also suggested that the value of λ can be calculated from superconductivity experiments. To obtain λ, Gallagher proposed the use of the equation of McMillan[55]

$$T_c = \frac{<\omega>}{1.2} \exp\left(\frac{-1.04(1 + \lambda)}{\lambda - \mu^*(1 + 0.62\,\lambda)}\right) \tag{32}$$

where $<\omega>$ is an appropriate average phonon frequency and μ^* is a Coulomb potential describing the interaction between electrons.

We approximate $\hbar\omega = k_B\,\Theta_D$, as did Gallagher, and use an interpolation (or extrapolation) of the published values of Θ_D for the different compositions. The superconducting transition temperatures are those obtained by Altounian et al[56] on the same samples measured in this thesis.

Table V-4 summarizes all the parameters used, as well as the results obtained from the application of Eq. (32) with the values of $\mu^* = 0.13$ or the renormalized[57] $\mu^* = 0.225$, both used by Gallagher. The results obtained from the application of Eq. (31) are also shown in Table V-4 for comparison.

Figure V-12 shows values of λ obtained from superconductivity experiments along with those obtained from thermopower measurements as a function of composition. Clearly there is no agreement between the two sets of data in contradiction to Gallagher's claims.

TABLE V - 4

x	$\Theta_D^{(a)}$ (K)	$T_c^{(b)}$ (K)	λ (McMillan) $\mu^*=0.13$	$\mu^*=0.225$	$\lambda_{(TEP)}$
0.30	233	2.73	0.58	0.79	0.48
0.35	231.5				0.61
0.40	230	.31	0.34	0.56	0.85
0.45	228.5	.67	0.44	0.62	0.83
0.50	227	.93	0.41	0.65	0.78
0.55	225	1.27	0.49	0.68	0.73
0.60	224	1.73	0.52	0.72	0.67
0.65	222	2.25	0.56	0.77	
0.67	221.5	2.34	0.56	0.77	

The mass enhancement parameter λ as obtained from different experiments.

(a) - interpolation between published values[18]

(b) - measured in the same samples as this work by Altounian et.al[57]

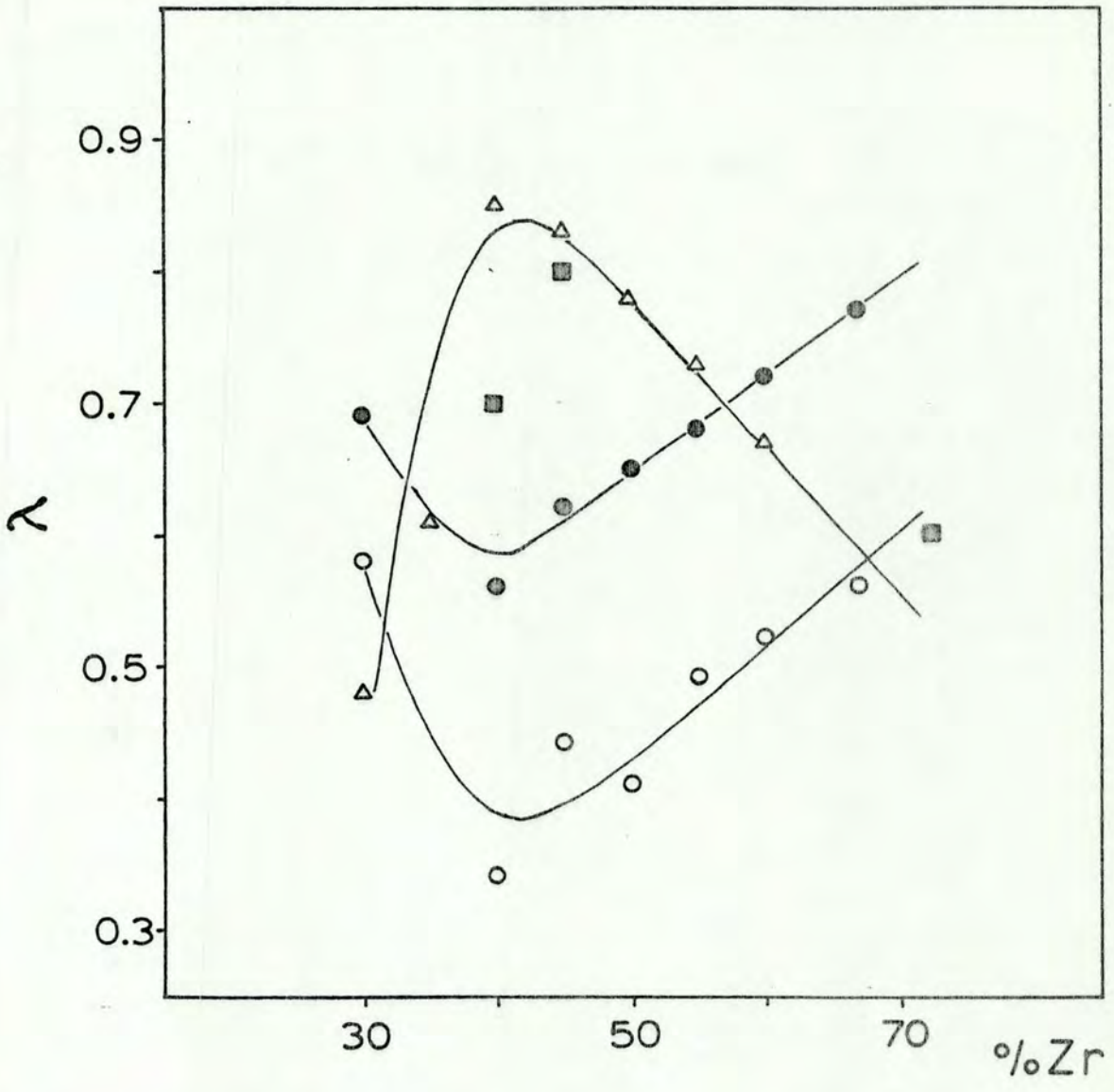

FIG. V - 12 - The mass enhancement parameter λ, as a function of composition, for amorphous CuZr alloys.

(△) - calculated using equation (31)

(○) - calculated using equation (32) with $\mu^* = 0.13$

(●) - calculated using equation (32) with $\mu^* = 0.225$

(■) - obtained by Gallagher[18] using equation (31)

The fact that the McMillan equation is so dependent upon the correct choice of parameters (like μ^* and Θ_D) might be one of the reasons for the lack of agreement between the two sets of measurements. As an alternative, one can write the superconducting transition temperatures in terms of the BCS equation[52].

$$T_c = 0.69\ \Theta_D \exp[-\frac{1}{N(0)V}] \tag{33}$$

or

$$T_c = 0.69\ \Theta_D \exp[-\frac{1}{\lambda_{BCS}}] \tag{34}$$

Again, the absolute values of λ obtained from this expression are dependent upon choice of the pertinent parameters. In order to avoid that, the ratio of the λ's obtained for the 'as made' samples to that for the 'relaxed' samples was taken for the superconductivity data. The same was done with the McMillan equation for comparison. The ratios of the λ's obtained from thermopower using expression (31) is shown, along with those using the BCS and McMillan equations, in Figure V-13 as a function of composition.

Both results for the superconductivity show ratios that are independent of composition, whereas the thermopower data is composition dependent.

One possible explanation for this disagreement is that the lowering of the local ground state in the relaxed sample has different effects on the thermopower and superconductivity which leads us to the conclusion that λ seen by superconductivity is not the same as that seen by thermopower.

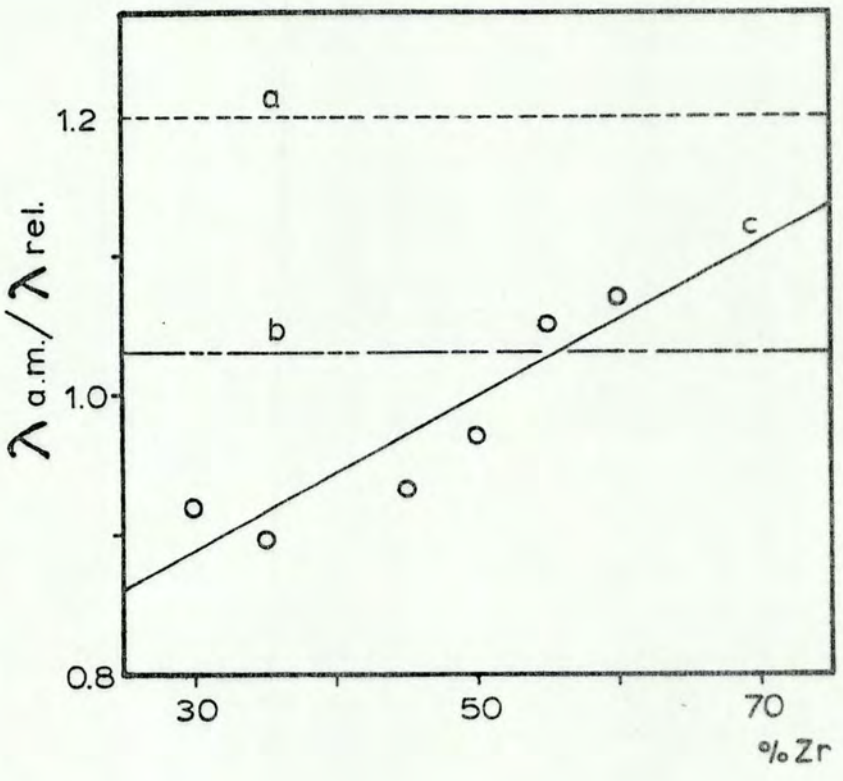

FIG. V - 13 - The ratio of mass enhancement parameters λ before and after relaxation

(a) - calculated using equation (34)

(b) - calculated using equation (32)

(c) - calculated using equation (31), as a linear regression over the experimental points (o).

Another correlation was suggested by Jäckle and collaborators[41,42], where the high temperature derivative of the resistivity is linked to the mass enhancement parameter λ by

$$\lambda = k \frac{d\rho}{dT} \tag{35}$$

where k is claimed to be a constant determined from Ziman's theory.

On attempting to verify the proposed correlation one obtains the results shown in Figure V-14, where λ is plotted as a function of $d\rho/dT$. These results were obtained by applying the McMillan equation as indicated in the preceding pages, and the results for $d\rho/dT$ presented in Chapter III. The lines obtained for λ determined from superconductivity experiments do not go through the origin, in clear contradiction to eq. (35). Curiously enough the λ obtained using eq. (31) correlate with the high temperature $d\rho/dT$ with a slope of -52.5 K/$\mu\Omega$cm.

Regrettably, the assumption that the resistivity for all samples at 275K is the same and equal to 200$\mu\Omega_{cm}$, and a constant Θ_D, as used by Rapp et al[42] renders any comparison between their experiments and ours meaningless. Also, the fact that their measurements were made on apparently two year old samples is an indication that the results obtained in that work should be regarded with reservations.

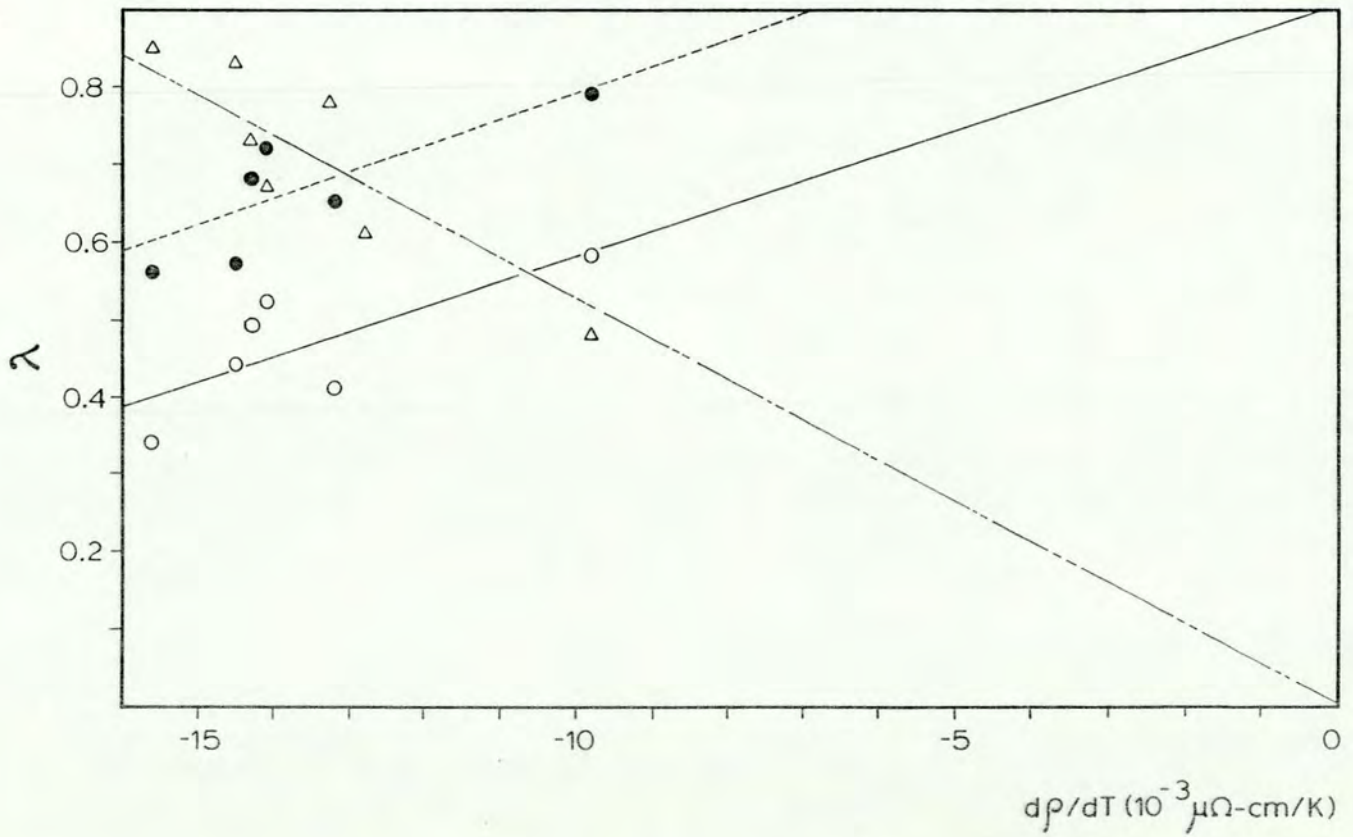

FIG. V - 14 - The suggested correlation between the mass enhancement parameter λ and the temperature dependence of the resistivity.

(△) - calculated from equation (31)

(○) - calculated from equation (32)($\mu^* = 0.13$)

(●) - calculated from equation (32)($\mu^* = 0.225$)

The lines correspond to linear regressions over the calculated data.

VI. CONCLUSIONS

We have measured the resistivities and thermopowers of a series of MgZn and CuZr alloys in various states ranging from the 'as made' to 'relaxed' amorphous, and different stages of partial crystallization.

The results for the resistivities of the amorphous alloys show negative temperature coefficients of the resistivity at high temperatures. The series of amorphous MgZn alloys shows a small maximum in the resistivities around 80K while the series of amorphous CuZr alloys does not show minima or maxima in the whole temperature range studied and $d\rho/dT$ remains negative everywhere. The CuZr alloys show positive, linear thermopowers above approximately 50K whereas the MgZn alloys range between small positive and small negative thermopowers.

The interpretation of the results for the thermopower using the simple Ziman model for liquid metals, as suggested by Sinha[4] and others[13,16] was shown to be incorrect for both alloys, even for MgZn, proven to be a free electron material; this is one of the suppositions used to develop the liquid metal model.

We have shown that only if these materials are treated as alloys by considering the different contributions to the thermopower, as is done in the Faber-Ziman approach[19], does one obtain reasonable agreement between the predictions of the theory and the experimental results.

A two component model is proposed for the thermopower of amorphous alloys, which is essentially an extreme simplification of the Faber-Ziman model, and is found to describe the data very well. More important, the values found for the parameters ('pure amorphous metal'

transport parameters) are very close to what would be expected from supercooled liquid metals.

A full Faber-Ziman calculation was performed for CuZr, where partial structure factors are known. The results of this calculation indicate that, although the correct order of magnitude is obtained for the thermopower, the term r containing the energy dependence of the pseudopotentials is essential to the proper description of the experimental results and should not be neglected as indicated by Nagel and others[4,13,16].

The proposed mass enhancement contributions to the low temperature thermopower and high temperature resistivity were tested by analyzing the transport parameters obtained in this thesis and the results for superconductivity of Altounian et al[56] who measured the very same samples studied here. The correlation between the mass enhancement parameter λ and the temperature dependence of the high temperature resistivity $d\rho/dT$, suggested by Jäckle and collaborators[41,42], was attempted with our experimental measurements. We have not found the proposed correlation to hold in a manner similar to that found by Rapp et al[42]. We could not pursue this matter further because of the great number of approximations used in Rapp et al's work, rendering any comparison between experiments essentially meaningless.

The characteristic behaviour of the thermopower of CuZr as a function of temperature, where a fairly localized 'knee' is produced by a change in slope between high and low temperatures, was tentatively explained by Gallagher[18] as an effect of mass enhancement at low temperatures. We have tested this idea and found no direct, linear correlation as was suggested in the proposed theory.

Moreover, we have tested both propositions by establishing the ratios of the different parameters for fresh and thermally relaxed samples. The composition dependence of these ratios was shown to be different for each of the proposed correlations, meaning that the enhancement seen by transport phenomena does not seem to correspond with that seen by superconductivity.

One might speculate at this point that ξ, the thermoelectric parameter, will change from low to high temperatures in a way analogous to crystalline materials. This could be verified by performing a calculation of the thermopower of amorphous alloys including the effects of phonons, similar to that presented by Cote and Meisel[40] for the resistivity.

We have shown the need for consistent, systematic work in order to achieve results that are compatible with the proposed theories. We suggest that not only the manufacture of the alloys be known, but essential parameters like the partial structure factors should be performed on the very same samples used for other transport phenomena experiments.

We have also shown the need for extended ranges of composition to understand the behaviour of those amorphous materials. To that end, we suggest that more work in liquid metals is needed and also that other techniques be used in the production of the amorphous solids.

We believe that we made clear the need for more extensive theoretical work in this field; in particular towards the understanding of the rôle of phonons in these materials and the effect of the different approximations used.

APPENDIX

In this appendix we present the FORTRAN programs used to treat the experimental data and the details of an effective medium calculation.

- A - 1 - Data processing

The data is collected by means of an automatic data collection system, operated by program PCMAIN, stored in disk for operation in the PDP-11/34 minicomputer in our laboratory. The untreated experimental results are stored in a file of the type MBRSXX.DAT. This file is translated by program MB0001.FOR into a formated file (type MBPLXX.DAT) containing the temperature of the measurment, the resistance ratio [R(T)-R(4.2)/R(4.2)], the value of the interpolation between the values of the integrated thermopower of Pb (from the calibration of Roberts[36] - file ATHPPB.DAT), the measured e.m.f. and the obtained integrated thermopower of the sample. A listing of program MB0001.FOR follows.

The files obtained from MB0001 are treated by program MB0002.FOR, where the resistivity ratios are averaged for each integer temperature. In the same program the differentiation of the integrated thermopower is performed. This differentiation is done by fitting a second degree polinomial to the integrated thermopower, over varying intervals. This procedure is repeated ten times and the average of the calculated derivatives is assigned to each integer temperature. In the same program the values of the resistivity (from an independent determination of the room temperature resistivity), S/T, $\rho S/T$, $\frac{1}{\rho} d\rho/dT$ and σ are calculated. The output of this program is found in a file type MBPLXX.TOT, which can be displayed graphically using MBDRA2 to operate the Calcomp Plotter linked

```
C*************************************************************
C       P R O G R A M   MB0001.FOR
C*************************************************************
        DIMENSION FILE(2)
        DATA FILE/6RDL1MB0,6R002SAV/
        DIMENSION TEMP0(79),VPB(79)
        DIMENSION DIFF(85,5)
        DATA DIFF/425*0./
        EQUIVALENCE (VPB(1),DIFF(1,1))
        DIMENSION XINSTR(3)
        DIMENSION EXPVAR(5),TEMP(94),RES(94)
        CALL SETERR(12,99)
        CALL SETERR(10,99)
        R0=0.
        CALL ASSIGN(3,'DK:TC1254.DAT',13,'RDO','NC',2)
        OPEN (UNIT=10,NAME='DL1:PCFT10.SCR',TYPE='SCRATCH')
C       CALL ASSIGN(10,'DK:PCFT10.TMP',13,'SCR','NC',2)
C
C       INTERPRETATION DES RESULTATS EXPERIMENTAUX.
C
        JFLAG=0
        CALL OPNDRK
1001    CONTINUE
        CALL READRK(EXPVAR,JFLAG)
        IF(JFLAG.EQ.-2)GO TO 3001
        CALL DRKTRA(XINSTR)
        XINSTR(2)=XINSTR(2)*10.**(-6)
        XINSTR(3)=XINSTR(3)**(-1)*10.**6
        WRITE(10,2)(XINSTR(I),I=1,3),(EXPVAR(I),I=1,5)
        GO TO 1001
3001    CONTINUE
        REWIND 10
C
C       CALCUL DE LA TEMPERATURE, DE LA RESISTIVITE,
C       ET DE L'INTEGRALE DU POUVOIR THERMOELECTRIQUE
C       TEMP1=TEMPERATURE R=RESISTIVITE INTTEP=INTEGRALE DU T.E.P.
C
        READ(3,1)(TEMP(I),RES(I),I=1,94)
1       FORMAT(F6.3,1X,F8.3)
        OPEN (UNIT=1,NAME='DL1:TINTIN.SCR',TYPE='SCRATCH')
1000    CONTINUE
        READ(10,2,END=999)(XINSTR(I),I=1,3),(EXPVAR(I),I=1,5)
2       FORMAT(3E13.6,1X,3E13.6/2E13.6/)
        DO 100 I=1,93
        J=I
        IF(XINSTR(3).LE.RES(I).AND.XINSTR(3).GT.RES(I+1))
        @GO TO 101
100     CONTINUE
        J=93
101     CONTINUE
        TEMP1=TEMP(J)+(TEMP(J+1)-TEMP(J))/(RES(J+1)-RES(J))*
        @(XINSTR(3)-RES(J))
        R=XINSTR(2)*EXPVAR(3)/EXPVAR(2)+EXPVAR(1)
        TEPINT=XINSTR(1)*EXPVAR(4)/EXPVAR(5)/1000.
        IF(R0.EQ.0.)R0=R
        R=(R-R0)/R0
        WRITE(1,3)TEMP1,R,TEPINT,XINSTR(3)
3       FORMAT(' ',1X,F7.3,1X,E13.6,1X,E13.6,1X,E13.6)
        GO TO 1000
999     REWIND  1
        CLOSE(UNIT=10)
C
C       SOUSTRACTION DU PLOMB DE L'INTEGRALE DU T.E.P.
```

```
C       EXPERIMENTAL
C
        CALL ASSIGN(12,'DL1:ATHPPB.DAT',14,'RDO','NC')
        READ(12,4)(TEMPO(N),VPB(N),N=1,79)
4       FORMAT(F7.3,1X,F8.3)
C
C       CALCUL DU TABLEAU DES DIFFERENCES NORMALISEES
C
        DO 2001 N1=2,5
        N=N1-1
        DO 2000 M=N1,79
        IF(TEMPO(M).EQ.TEMPO(M-1))GO TO 2000
        DIFF(M,N1)=(DIFF(M,N)-DIFF(M-1,N))/(TEMPO(M)-TEMPO(M-1))
2000    CONTINUE
2001    CONTINUE
C
C       CALCUL DU VPB CORRESPONDANT A LA TEMP. ACTUELLE
C
        WRITE(7,5)
5       FORMAT(1H$,1X,'ENTRER LE NOM DE MB0001.DAT:')
        CALL ASSIGN(11,'MB0001.DAT',-10,'NEW','NC')
1981    READ(1,33,ERR=1982,END=998)TEMP1,R,TEPINT,XINSTR(3)
33      FORMAT(1X,F7.3,1X,E13.6,1X,E13.6,1X,E13.6)
        GO TO 1983
1982    WRITE(7,*)TEMP1,R,TEPINT,XINSTR(3)
        GO TO 1981
1983    CONTINUE
        DO 2002 N=3,78
        J=N
        IF(TEMP1.GE.TEMPO(N).AND.TEMP1.LT.TEMPO(N+1))
        @GO TO 2003
2002    CONTINUE
        VEXP=TEPINT
        VPBO=0.
        GO TO 1989
2003    VPBO=VPB(J)
        A=ABS(TEMP1-TEMPO(N))
        VPBO=VPBO+A*DIFF(J+1,2)
        VPBO=VPBO+A*(A-1)*DIFF(J+2,3)/2.
        VPBO=VPBO+A*(A-1)*(A-2)*DIFF(J+3,4)/6.
        VPBO=VPBO+A*(A-1)*(A-2)*(A-3)*DIFF(J+4,5)/24.
        VEXP=VPBO+TEPINT
1989    WRITE(11,11)TEMP1,R,VPBO,VEXP,TEPINT
11      FORMAT(' ',5E16.6)
        GO TO 1981
        REWIND 11
998     CONTINUE
        CLOSE(UNIT=3)
        CLOSE(UNIT=11)
        CLOSE(UNIT=12)
        STOP
        END
```

to the computer.

A listing of MB0002.FOR is presented below:

```
C*************************************************************************
C         P R O G R A M   MB0002.FOR
C*************************************************************************
C       THIS PROGRAM CALCULATES ALL THE AVERAGED RESISTIVITIES
C       AND THERMOPOWERS, AND ALL REQUIRED COMBINATIONS
C       FROM THE FILES TRANSLATED BY MB0001.FOR
C*************************************************************************
        DOUBLE PRECISION ANAME,ANOME,CO
        DIMENSION RR(300),ICNT(300),CO(30)
        DIMENSION ANAME(2),RO(300),SOT(300),RSOT(300),ANOME(2)
        DIMENSION COND(300),S(300),DY(300),D2Y(300),ALFA(300),ICNT1(300)
        DIMENSION D3Y(300),D4Y(300),DYDT(300),YDDT(300),TT(300)
        COMMON ANAME,S,T,DERII,TT,ICNT1,RR,ICNT,NCOUNT,CO
        CALL SETERR(10,120)
        CALL SETERR(12,120)
        OPEN(UNIT=3,NAME='MBINFO.PRG',TYPE='OLD')
1       READ(3,3311,END=987)ANAME(1),ANAME(2),ANOME(1),ANOME(2),REX
3311    FORMAT(2A8,2A8,E15.5)
C1      WRITE(7,1133)
C1133   FORMAT(1H ,'INPUT FILE ?',/)
C       READ(5,1123)ANAME(1),ANAME(2)
C1123   FORMAT(2A8)
C       WRITE(7,1132)
C1132   FORMAT(1H ,'ROOM TEMPERATURE RESISTIVITY :',/)
C       READ(5,4411)REX
C4411   FORMAT(E15.5)
C       WRITE(7,1144)
C1144   FORMAT(1H ,'OUTPUT FILE ?',/)
C       READ(5,1123)ANOME(1),ANOME(2)
        OPEN(UNIT=1,NAME=ANOME,TYPE='NEW')
        WRITE(7,1818)ANOME
1818    FORMAT(1H ,'OUTPUT FILE : ',2A8,/)
        CALL INPUT
        WRITE(7,4444)
4444    FORMAT(1H ,'SUBROUTINE INPUT FINISHED',/)
        CALL TEP
        WRITE(7,2222)
2222    FORMAT(1H ,'SUBROUTINE TEP FINISHED',/)
        DO 9 ITEMP=1,300
        IF(ICNT(ITEMP))8,8,9
9       RR(ITEMP)=RR(ITEMP)/ICNT(ITEMP)
8       CONTINUE
        DO 1000 I=1,300
D       IF(I.LE.20)WRITE(7,*)FLOAT(I+3),RR(I)
        IF(ICNT(I))10,10,1000
10      N1=MIN0(I-1,5)
        N2=0
        DO 100 J=I+1,300
        IF(ICNT(J))100,100,11
11      N2=N2+1
100     CONTINUE
        N2=MIN0(N2,5)
        BS=0
        L=I-N1
        DO 500 K=I-N1,I+N2
59      IF(ICNT(L))60,60,61
60      L=L+1
        GO TO 59
61      L1=I-N1
        BB=1
        DO 400 K1=I-N1,I+N2
62      IF(ICNT(L1))63,63,64
63      L1=L1+1
```

```
      GO TO 62
64    IF(L-L1)66,65,66
65    BB=BB*RR(L)
      L1=L1+1
      GO TO 400
66    BB=BB*(I-L1)/(L-L1)
      L1=L1+1
400   CONTINUE
      BS=BS+BB
      L=L+1
500   CONTINUE
      RR(I)=BS
      ICNT(I)=1
1000  CONTINUE
      RO4=REX/(1.+RR(293))
D     WRITE(7,997)RO4
997   FORMAT(1H ,'HELIUM TEMP. RESISTIVITY=',F9.5,/)
      DO 111 I=1,300
      RO(I)=RO4*(RR(I)+1.)
      COND(I)=1./RO(I)
      SOT(I)=S(I)/FLOAT(I+3)
      RSOT(I)=RO(I)*SOT(I)
D     IF(I.LE.20)WRITE(7,*)FLOAT(I+3),RO(I)
111   CONTINUE
      DO 120 I=1,297
      J=I+1
      DY(I)=RO(J)-RO(I)
120   CONTINUE
      DO 121 I=1,296
      J=I+1
      D2Y(I)=(DY(J)-DY(I))/2
121   CONTINUE
      DO 122 I=1,295
      J=I+1
      D3Y(I)=(D2Y(J)-D2Y(I))/3
122   CONTINUE
      DO 123 I=1,294
      J=I+1
      D4Y(I)=(D3Y(J)-D3Y(I))/4
123   CONTINUE
      DO 124 I=5,297
      J=I-1
      K=I-2
      L=I-3
      M=I-4
      DYDT(I)=(DY(I)-D2Y(I)+D3Y(I)-D4Y(I))
      YDDT(I)=DY(J)+D2Y(K)+D3Y(L)+D4Y(M)
124   CONTINUE
      DO 125 I=1,4
      DYDT(I)=DY(I)-D2Y(I)+D3Y(I)-D4Y(I)
      YDDT(I)=DYDT(I)
125   CONTINUE
      DO 126 I=1,300
      ALFA(I)=COND(I)*(DYDT(I)+YDDT(I))/2
126   CONTINUE
      DO 56 K=1,297
      WRITE(1,2030)FLOAT(K+3),RR(K),S(K),RO(K),COND(K),SOT(K),RSOT(K),
     1ALFA(K)
2030  FORMAT(' ',8(E15.5))
56    CONTINUE
      CLOSE(UNIT=1)
      WRITE(7,696)ANOME
696   FORMAT(1H ,'FILE ',2A8,' CLOSED',/)
      GO TO 1
987   CLOSE(UNIT=3)
      WRITE(7,765)
```

```
765     FORMAT(1H ,'FILE MBINFO.PRG CLOSED',/)
        STOP
        END
C*************************************************************************
        SUBROUTINE INPUT
C*************************************************************************
        DOUBLE PRECISION ANAME,CO
        DIMENSION CO(30)
        DIMENSION RR(300),ICNT(300),S(300),TT(300),ICNT1(300),ANAME(2)
        COMMON ANAME,S,T,DERII,TT,ICNT1,RR,ICNT,NCOUNT,CO
        DATA ICNT/300*0/,RR/300*0./
        OPEN(UNIT=2,NAME=ANAME,TYPE='OLD',READONLY)
        DO 55 J=1,300
        ICNT(J)=0
        RR(J)=0.
55      CONTINUE
5       CONTINUE
        READ(2,2,END=5006)X,R
2       FORMAT(F7.3,1X,E13.6)
        ITEMP=X-2.5
        ICNT(ITEMP)=ICNT(ITEMP)+1
        RR(ITEMP)=R+RR(ITEMP)
        GO TO 5
5006    CONTINUE
        RETURN
        END
        SUBROUTINE TEP
C %%%%%%%%%%%%%%%%%%%%%%%%%%%%%%%%%%%%%%%%%%%%%%%%%%%%%%%%%%%%%%%%%%%%%%%
C THIS SUBROUTINE PERFORMS LEAST SQUARE FIT OVER A SET OF DATA STORED
C IN AN INPUT FILE,THE LENGHT OF THE INTERVAL OVER WHICH THE FIT
C IS TO BE MADE IS DETERMINED BY 'TINCR',THE DERIVATIVE IS CALCULA
C TED OVER A SUBSET OF THIS INTERVAL
C %%%%%%%%%%%%%%%%%%%%%%%%%%%%%%%%%%%%%%%%%%%%%%%%%%%%%%%%%%%%%%%%%%%%%%%
      DOUBLE PRECISION CO,ANAME
      DIMENSION CO(30),TT(300),ICNT1(300),S(300),ANAME(2)
      DIMENSION RR(300),ICNT(300)
      COMMON ANAME,S,T,DERII,TT,ICNT1,RR,ICNT,NCOUNT,CO
      DATA ICNT1/300*0/,TT/300*0./
      DO 567 J=1,300
      ICNT1(J)=0
      TT(J)=0.
567   CONTINUE
      NCO=3
C %%%%%%%%%%%%%%%%%%%%%%%%%%%%%%%%%%%%%%%%%%%%%%%%%%%%%%%%%%%%%%%%%%%%%%%
C SELECT THE INTERVAL OVER WHICH THE FIT IS TO BE DONE,THE SUBSET
C OF THIS INTERVAL OVER WHICH THE DERIVATIVE IS TO BE CALCULATED,
C THE INITIAL TEMPERATURE AND THE MAX TEMPERATURE (LIMIT OF FIT
C DOMAIN).
C %%%%%%%%%%%%%%%%%%%%%%%%%%%%%%%%%%%%%%%%%%%%%%%%%%%%%%%%%%%%%%%%%%%%%%%
      REWIND 2
      DO 5 KK=1,10
      TINIT=3.9+.1*KK
      WIDTH=7.*KK
      TINCR=8.*KK
      TMAX=300.
      IF(KK.GT.3)GO TO 111
      TINCR=4.*KK
      WIDTH=2.5*KK
      TMAX=50.
 111  MEND=0
D       WRITE(7,*)KK
 1093 CALL DEV(NCO,CO,TINIT,TINCR,MEND)
      IF(CO(1).EQ.0.0.AND.CO(2).EQ.0.0)GO TO 1949
      T=TINIT+(TINCR-WIDTH)/2.
1094  IF(T.GT.TMAX)GO TO 1096
      IF(T.GT.TINIT+(TINCR+WIDTH)/2.) GO TO 1097
```

```
      CALL DERIV(NCO,CO)
      IF(NCOUNT.LE.2) GO TO 1099
      ITEMP=T-2.5
      TT(ITEMP)=TT(ITEMP)+DERII
      ICNT1(ITEMP)=ICNT1(ITEMP)+1
D     AMED=TT(ITEMP)/ICNT1(ITEMP)
D     IF(ITEMP.GT.(TMAX-10))WRITE(7,*)TT(ITEMP),ICNT1(ITEMP),
D    @(ITEMP+2),AMED
      T=T+1.
      GO TO 1094
 1097 IF(MEND.EQ.1) GO TO 1099
 1949 TINIT=TINIT+TINCR
 1096 IF(MEND.EQ.1) GO TO 1099
      GO TO 1093
 1099 REWIND 2
        WRITE(7,1122) KK
 1122   FORMAT(1H ,'ITERATION NUMBER',I2,' COMPLETED')
 5    CONTINUE
        CLOSE(UNIT=2)
      CALL AVER
        WRITE(7,556)
D       WRITE(7,*)(FLOAT(I+3),S(I),I=1,20)
 556    FORMAT(1H ,'AVERAGE PERFORMED')
      RETURN
      END
C*************************************************************
      SUBROUTINE DEV(NCO,CO,TINIT,TINCR,MEND)
C*************************************************************
      DOUBLE PRECISION CO,A,B,U,ANAME
      DIMENSION CO(30),A(31,30),B(30),ANAME(2)
      DIMENSION S(300),TT(300),ICNT1(300),RR(300),ICNT(300)
      COMMON ANAME,S,T,DERII,TT,ICNT1,RR,ICNT,NCOUNT,CO
      DO 993 JI=1,30
      DO 994 JJ=1,31
 994  A(JJ,JI)=0.0D-10
      CO(JI)=0.0D-10
 993  B(JI)=0.0D-10
      NCOUNT=0
      NCOP1=NCO+1
D       WRITE(7,77)
 77     FORMAT(1H ,'IN SUBROUTINE DEV:',/)
 992  READ(2,990,END=991) X1,Y1
 990  FORMAT(F7.3,25X,F9.3)
      NCOUNT=NCOUNT+1
C %%%%%%%%%%%%%%%%%%%%%%%%%%%%%%%%%%%%%%%%%%%%%%%%%%%%%%%%%%%%
C SELECT INTERVAL FOR FIT
C %%%%%%%%%%%%%%%%%%%%%%%%%%%%%%%%%%%%%%%%%%%%%%%%%%%%%%%%%%%%
D       IF(NCOUNT.LE.5)WRITE(7,*)X1,Y1
      IF(X1.LT.TINIT-1.0.OR.X1.GT.TINIT+TINCR) GO TO 995
      DO 1 I=1,NCO
      DO 2 J=1,NCO
      AJ=J-.999999
      AI=I-.999999
 2999 A(I,J)=A(I,J)+((X1**(AI))*(X1**(AJ)))
 2    CONTINUE
 1    CONTINUE
      DO 6 J=1,NCO
      AJ=J-.999999
 3999 A(NCOP1,J)=A(NCOP1,J)+(X1**(AJ))*Y1
 6    CONTINUE
      GO TO 992
 991  CONTINUE
      MEND=1
 995  IF(NCOUNT.LE.2) GO TO 996
C %%%%%%%%%%%%%%%%%%%%%%%%%%%%%%%%%%%%%%%%%%%%%%%%%%%%%%%%%%%%
C     GAUSS METHOD
```

```
C %%%%%%%%%%%%%%%%%%%%%%%%%%%%%%%%%%%%%%%%%%%%%%%%%%%%%%%%%%%%%%%%%%%%%%%
      DO 8 J=1,NCO
      IF(DABS(A(J,J)).GT.1.D-16) GO TO 15
      N1=NCO-J
      GO TO 11
 15   J1=1-J
      N1=NCO-J
      U=A(J,J)
      DO 9 I=1,NCOP1
      A(I,J)=A(I,J)/U
      DO 10 K=J1,N1
      IF(K.EQ.0) GO TO 10
      N=J+K
      IF(I.GT.1) GO TO 50
      B(N)=A(J,N)
 50   A(I,N)=A(I,N)-B(N)*A(I,J)
 10   CONTINUE
 9    CONTINUE
 8    CONTINUE
      DO 16 L=1,NCO
 16   CO(L)=A(NCOP1,L)
      GO TO 17
 996  MEND=1
 17   RETURN
 11   DO 12 L=1,N1
      N2=J+L
      IF(DABS(A(J,N2)).GE.1.D-16) GO TO 13
 12   CONTINUE
      WRITE(7,18)
 18   FORMAT(1H ,'NO SOLUTION')
      GO TO 17
 13   DO 14 I=1,NCOP1
      U=A(I,N2)
      A(I,N2)=A(I,J)
 14   A(I,J)=U
      GO TO 15
      RETURN
      END
C %%%%%%%%%%%%%%%%%%%%%%%%%%%%%%%%%%%%%%%%%%%%%%%%%%%%%%%%%%%%%%%%
C CALCULATE THE DERIVATIVE
C %%%%%%%%%%%%%%%%%%%%%%%%%%%%%%%%%%%%%%%%%%%%%%%%%%%%%%%%%%%%%%%%
      SUBROUTINE DERIV(NCO,CO)
C*****************************************************************
      DOUBLE PRECISION CO,ANAME
      COMMON ANAME,S,T,DERII,TT,ICNT1,RR,ICNT,NCOUNT,CO
      DIMENSION CO(30),S(300),ANAME(2),TT(300),ICNT1(300)
      DIMENSION RR(300),ICNT(300)
      DERII=0.0
      DO 999 I=2,NCO
      AI=I-0.999999
      DERII=DERII+AI*CO(I)*(T**(I-1.9999999))
 999  CONTINUE
      RETURN
      END
C************************************************************************
        SUBROUTINE AVER
C************************************************************************
        DOUBLE PRECISION ANAME
        COMMON ANAME,S,T,DERII,TT,ICNT1,RR,ICNT,NCOUNT,CO
        DIMENSION ICNT1(300),TT(300),S(300),ANAME(2),RR(300),ICNT(300)
        DIMENSION CO(30)
        DO 8 J=1,300
        IF(ICNT1(J))8,8,9
9       TT(J)=TT(J)/ICNT1(J)
8       CONTINUE
        DO 1000 I=1,300
```

```
      IF(ICNT1(I))10,10,1000
10    N1=MIN0(I-1,5)
      N2=0
      DO 100 J=I+1,300
      IF(ICNT1(J))100,100,11
11    N2=N2+1
100   CONTINUE
      N2=MIN0(N2,5)
      AS=0
      BS=0
      L=I-N1
      DO 500 K=I-N1,I+N2
59    IF(ICNT1(L))60,60,61
60    L=L+1
      GO TO 59
61    L1=I-N1
      A=1
      B=1
      DO 400 K1=I-N1,I+N2
62    IF(ICNT1(L1))63,63,64
63    L1=L1+1
      GO TO 62
64    IF(L-L1)66,65,66
65    B=B*TT(L)
      L1=L1+1
      GO TO 400
66    B=B*(I-L1)/(L-L1)
      L1=L1+1
400   CONTINUE
      BS=BS+B
      L=L+1
500   CONTINUE
      TT(I)=BS
      ICNT1(I)=1
1000  CONTINUE
      DO 1001 I=1,300
      S(I)=TT(I)
1001  CONTINUE
      RETURN
      END
```

Program MB0002 being relatively large causes some problems concerning memory space. These problems are solved by employing the command file MB0002.COM to LINK in OVERLAY:

```
**********
  MB0002.COM
  This command file
  is used for the
  overlay LINK
  (LINK @MB0002)
**********
MB0002/PROMPT
INPUT/O:1
TEP/O:1
AVER/O:2
DEV/O:2
DERIV/O:2
//
```

- A - 2 - Effective medium calculation

The transport parameters of partially crystalline amorphous metals can be calculated using the expressions developed for composite materials[39]. On account of the greater accuracy of the measurements of the resistivity ratio ([R(T)-R(4.2)]/R(4.2)) it is desirable to obtain the standard expressions for the conductivity and thermopower of mixtures in terms of the known $\Delta\rho/\rho$ and the ratio of the resistances of

the sample before and after annealing (Q).

We assume that the size of the sample remains unchanged upon annealing and write:

$$Q \equiv \frac{R(296)}{R_o(296)} \simeq \frac{\rho(296)}{\rho_o(296)} \tag{A1}$$

where the subscript o indicates the fresh amorphous values.

The crystallized fraction (x_c) can be written in terms of the conductivity as[58]:

$$x_c = \frac{\sigma - \sigma_o}{\sigma_o + 2\sigma} \left[\frac{\sigma_c - \sigma}{\sigma_c + 2\sigma} + \frac{\sigma - \sigma_o}{\sigma_o + 2\sigma}\right]^{-1} \tag{A2}$$

where the subscript c represents the values associated with the totally crystalline material. Expression (A2) can be written in terms of the ratios (Q) after some simple algebra as:

$$x_c = \frac{1 - Q}{Q + 2} \left[\frac{Q - Q_c}{Q + 2Q_c} + \frac{1 - Q}{Q + 2}\right]^{-1} \tag{A3}$$

or

$$x_c = \frac{\xi}{\xi - \xi_c} \tag{A4}$$

where

$$\xi = \frac{1 - Q}{Q + 2} \tag{A5}$$

and

$$\xi_c = \frac{Q_c - Q}{Q + 2Q_c} \tag{A6}$$

The thermopower of a mixture is written as[38]:

$$S = \frac{\sum_i S_i \sigma_i \gamma_i}{1 - 2\sigma \sum_i \gamma_i} \tag{A7}$$

where

$$\gamma_i = \frac{3x_i \kappa}{(2\sigma + \sigma_i)(2\kappa + \kappa_i)} \tag{A8}$$

and κ is the heat conductivity.

Using the Wiedemann-Franz relation[52]

$$L = \frac{\kappa}{\sigma T} \tag{A9}$$

expression (A8) reduces to:

$$\gamma_i = \frac{3x_i \sigma}{(2\sigma + \sigma_i)^2} \tag{A10}$$

We then rewrite (A7) as:

$$S = \frac{\sum_i S_i \sigma_i \frac{3x_i}{(2\sigma + \sigma_i)^2}}{1\text{-}6\ \sigma^2 \sum_i \frac{x_i}{(2\sigma + \sigma_i)^2}} = \frac{A}{B} \tag{A11}$$

Since $x_o = 1 - x_c$, we write:

$$A = 3\sigma\{\frac{(1-x_c)\sigma_o S_o}{(2\sigma + \sigma_o)^2} + \frac{x_c\ c S_c}{(2\sigma + \sigma_c)^2}\} \tag{A12}$$

and

$$B = 1 - 6\sigma^2 \{ \frac{(1 - x_c)}{(2\sigma + \sigma_o)^2} + \frac{x_c}{(2\sigma + \sigma_c)^2} \} \tag{A13}$$

The conductivities can be written as a function of the resistivity ratios ($\Delta\rho/\rho$):

$$\sigma = \frac{1}{\rho} = \frac{\gamma}{Q\ \rho_o(296)\alpha} \tag{A14}$$

where

$$\gamma = \frac{\Delta\rho}{\rho}(296) + 1 \tag{A15}$$

and

$$\alpha = \frac{\Delta\rho}{\rho}(T) + 1 \tag{A16}$$

Substituting (A14) into (A12) and (A13) one obtains after some more simple algebra:

$$A = 3\Delta[\frac{(1 - x_c)S_o\Delta_o}{(2\Delta + \Delta_o)^2} + \frac{x_c S_c \Delta_c}{(2\Delta + \Delta_c)^2}] \tag{A17}$$

and

$$B = 1 - 6\Delta^2[\frac{1 - x_c}{(2\Delta + \Delta_o)^2} + \frac{x_c}{(2\Delta + \Delta_c)^2}] \tag{A18}$$

where

$$\Delta = \frac{\gamma}{Q\alpha} \tag{A19}$$

The program MBSAR is written using equations (A1) through (A6), (A11), (A17) and (A18) and a listing of it is presented below:

```
C*********************************************************
C       P R O G R A M  MBSAR.FOR
C*********************************************************
      DOUBLE PRECISION ANAME,ANOME,ANOM,ANAM
      DIMENSION ANAME(2),ANOME(2),ANOM(2),ANAM(2)
      DIMENSION DELTA(300),DELTAA(300),DELTAC(300)
      DIMENSION ALFA(300),ALFAA(300),ALFAC(300)
      DIMENSION R(300,3),T(300,3),DDT(300,3)
      DIMENSION RR(300),TT(300),DTTDT(300),RRA(300),TTA(300)
      DIMENSION DTTDTA(300),RRC(300),TTC(300),DTTDTC(300)
      DIMENSION SA(300),SC(300),SAR(300)
      EQUIVALENCE (R(1,1),RR(1)),(R(1,2),RRA(1)),(R(1,3),RRC(1))
      EQUIVALENCE (T(1,1),TT(1)),(T(1,2),TTA(1)),(T(1,3),TTC(1))
      EQUIVALENCE (DDT(1,1),DTTDT(1)),(DDT(1,2),DTTDTA(1)),
     @(DDT(1,3),DTTDTC(1))
      EQUIVALENCE (SA,DTTDTA),(SC,DTTDTC)
      WRITE(7,2000)
 2000 FORMAT(1H ,'ENTER INPUT FILENAME')
      READ(5,2005) ANAME(1),ANAME(2)
 2005 FORMAT(2A8)
      OPEN(UNIT=1,NAME=ANAME,TYPE='OLD',READONLY)
      WRITE(7,2001)
 2001 FORMAT(1H ,'ENTER FILENAME AMORPHOUS')
      READ(5,2005) ANOME(1),ANOME(2)
      OPEN(UNIT=3,NAME=ANOME,TYPE='OLD',READONLY)
      WRITE(7,2002)
 2002 FORMAT(1H ,'ENTER FILENAME CRYSTALLINE')
      READ(5,2005) ANOM(1),ANOM(2)
      OPEN(UNIT=3,NAME=ANOM,TYPE='OLD',READONLY)
      WRITE(7,2003)
 2003 FORMAT(1H ,'ENTER OUTPUT FILENAME')
      READ(5,2005) ANAM(1),ANAM(2)
      OPEN(UNIT=9,NAME=ANAM,TYPE='NEW')
      WRITE(7,7)
    7 FORMAT(1H ,'ENTER R(RT)')
      READ (5,*)R296
      WRITE(7,8)
    8 FORMAT(1H ,'ENTER RA(RT)')
      READ(5,*)RA296
      WRITE(7,9)
    9 FORMAT(1H ,'ENTER RC(RT)')
      READ (5,*) RC296
      WRITE (7,6)
    6 FORMAT(1H ,'ENTER RAC(RT)')
      READ (5,*) RAC296
      DO 71 L=1,3
      READ(L,70)(T1,R(I,L),DDT(I,L),I=1,300)
   70 FORMAT(3(E15.5))
   71 CONTINUE
      Q=R296/RA296
      QC=RC296/RAC296
      CSI=(1.-Q)/(Q+2.)
      CSIC=(QC-Q)/(2.*QC+Q)
      XFR=CSI/(CSI-CSIC)
      GAMMA=R296+1.
      GAMMAA=RA296+1.
      GAMMAC=RC296+1.
      DO 72 L=1,300
      ALFA(L)=RR(L)+1.
      DELTA(L)=GAMMA/(Q*ALFA(L))
      ALFAA(L)=RRA(L)+1.
      DELTAA(L)=GAMMAA/ALFAA(L)
      ALFAC(L)=RRC(L)+1.
      DELTAC(L)=GAMMAC/(QC*ALFAC(L))
      B(L)=1.-(6.*DELTA(L)**2)*((1.-XFR)/(2.*DELTA(L)+DELTAA(L))**2+
     @XFR/(2.*DELTA(L)+DELTAC(L))**2)
      AA(L)=(1.-XFR)*SA(L)*DELTAA(L)/(2.*DELTA(L)+DELTAA(L))**2
      AB(L)=XFR*SC(L)*DELTAC(L)/(2*DELTA(L)+DELTAC(L))**2
      A(L)=3.*DELTA(L)*(AA(L)+AB(L))
      SAR(L)=A(L)/B(L)
      WRITE(9,2004)FLOAT(L+3),SAR(L)
 2004 FORMAT(' ',2(E15.5))
   72 CONTINUE
      STOP
      END
```

BIBLIOGRAPHY

1. R.W. Cochrane, Journal de Physique, Colloque C6, supp. au no 8, 39, 1540 (1978).

2. J.J. Gilman, Phys. Today, May 1975, pp 46-53.
P. Chaudhari, B.C. Giessen and D. Turnbull, Scientific American 242, no. 4, 98 (April 1980).

3. W. Klement Jr., R.H. Willens and P. Duwez, Nature 187, 869 (1960).

4. A.K. Sinha, Phys. Rev. B 1, 4541 (1970).

5. R.W. Cochrane and J.O. Ström-Olsen, J. Phys. F. 7, no. 9, 1799 (1977).

6. J. Kondo, Solid State Physics 23, 184 (1969).

7. J.M. Ziman, Phil. Mag. 6, 1013 (1961).

8. C.C. Tsuei and R. Hasegawa, Solid State Comm. 7, 1581 (1969).

9. G.S. Grest and S.R. Nagel, Phys. Rev. B 19, 3517 (1978).

10. R.W. Cochrane, R. Harris, J.O. Ström-Olsen and M.J. Zuckermann, Phys. Rev. Letters 35, 676 (1975).

11. S.R. Nagel and J. Tauc, Phys. Rev. Letters 35, 380 (1975).

12. D. Korn and W. Mürer, Z. Physik B27, 309 (1977).

13. S.R. Nagel, Phys. Rev. Letters 41, 990 (1978).

14. P.J. Cote and L.V. Meisel, Phys. Rev. B20, 3030 (1979).

15. M.N. Baibich et. al., Phys. Letters 73A, 328 (1979).

16. S. Basak, S.R. Nagel and B.C. Giessen, Phys. Rev. B21, 4049 (1980).
J.P. Carini, S. Basak and S.R. Nagel, Journal de Physique Colloque C8, supp. au no. 8, 41, C8-463 (1980).

17. R.W. Cochrane et. al., Physica 107B, 131 (1981).

18. B.L. Gallagher, J. Phys. F11, L207 (1981).

19. T.E. Faber and J.M. Ziman, Phil. Mag. 11, 153 (1965).

20. R.W. Cochrane, J. Kastner and W.B. Muir, J. Phys. E. to be published

21. G.J. Edwards, J. Phys. E4, 299 (1971).

22. Z. Altounian, Tu Guo-hua, J.P. Ström-Olsen and W.B. Muir, Phys. Rev. B24, no. 2, 505 (1981).

23. Z. Altounian, Tu Guo-hua and J.O. Ström-Olsen, to be published.

24. M.N. Baibich and W.M. Muir - unpublished results.

25. J.M. Ziman, Advances in Physics 16, no. 64, 551 (1967).

26. T.E. Faber, Advances in Physics 16, no. 64, 637 (1967).

27. C.C. Bradley, T.E. Faber, E.G. Wilson, and J.M. Ziman, Phil. Mag. 7, 865 (1962).

28. Pseudopotentials in the theory of metals, W.A. Harrison, W.A. Benjamin inc., New York, Amsterdam (1966).

29. O. Dreirach, R. Evans, H.-J. Guntherodt and J.-U. Künzi, J. Phys. F 2, 709 (1972).

30. J.E. Enderby, J.B. Zytveld, R.A. Howe and A.J. Mian, Phys. Letters 20A, no. 2, 144 (1968).

31. Thermoelectricity in metals and alloys, R.D. Barnard, Taylor and Francis Ltd., London (1972).

32. T. Masumoto, Y. Waseda, H. Kimura and A.Inoue, Sci Rep. Res. Inst. Tohoku Univ. 26A, 21 (1976).

33. Y. Waseda, H. Okazaki and T. Masumoto, Journal of Material Science 12, 1927 (1977).

34. M. Banville and R. Harris, Phys. Rev. Letters 44, no. 17, 1136 (1980).

35. Electrical resistance of metals, G.T. Meaden, The International Cryogenics Monograph Series, Plenum Press, New York (1965).

36. R.B. Roberts, Phil. Mag. 36, 91 (1977).

37. Z. Altounian and Tu Guo-hua - private communication.

38. S.C. Airapetiants - J. Tech. Phys. (USSR) 27, no. 3, 478 (1957).

39. M.N. Baibich, W.B. Muir and D.R. Van Wyck, J. Appl. Phys. 52, no. 3, 1886 (1981).

40. P.J. Cote and L.V. Meisel, in Glassy Metals I, (ed. Guntherodt and Beck) Springer-Verlag, Berlin (1981).

41. J. Jäckle, J. Phys. F 10, L43 (1980).
J. Jäckle and K. Froböse, J. Phys. F10, 471 (1980).

42. Ö. Rapp, J. Jäckle and K. Froböse, J. Phys. F 11, 2359 (1981).

43. U. Mizutani and T. Mizoguchi, J. Phys. F 11, 1385 (1981).

44. T. Mizoguchi, N. Shiotani, U. Mizutani, T. Kudo and S. Yamada, Journal de Physique, Colloque C8, supp. au no. 8, 41, C8-183 (1980).

45. P. Garoche, Y. Calvayrac and J.J. Veyssie, Journal de Physique, Colloque C8, supp. au no. 8, 41, C8-766 (1980).

46. H.V. Löhneysen et.al., Journal de Physique, Colloque C8, supp. au no. 8, 41, C8-745 (1980).

47. H.S. Chen and Y. Waseda, Phys. Stat. Sol. (a) 51, 593 (1979).

48. Y. Waseda and H.S. Chen, Phys. Stat Sol. (b) 87, 777 (1978).

49. J. Kübler et.al., Phys. Rev. B, 23, no. 10, 5176 (1981).
P. Oelhafen et.al., Phys. Rev. Lett., 43, no. 15, 1134 (1979).

50. T. Kudo et.al., J. Phys. Soc. Japan 45, no. 5, 1773 (1978).

51. G. Busch and H.-J. Güntherodt, in Solid State Physics, vol. 29, (ed. H. Ehrenreich, F. Seitz and D. Turnbull) Academic Press, New York and London (1974).

52. Introduction to solid state physics, C. Kittel, John Wiley & Sons, Inc., New York, 4th ed.

53. C.L. Foiles - private communication

54. P.J. Scalapino, in Superconductivity, vol. 1 (ed. R.D. Parks) Marcel Dekker, Inc., New York (1969).

55. W.L. McMillan, Phys. Rev. 167, no. 2, 331 (1968).

56. Z. Altounian, Tu Guo-hua and J.O. Ström-Olsen, Solid State Comm. 40, 221 (1981).

57. J.M. Daams, B.Mitriovic and J.P. Carbotte, Phys. Rev. Lett. 46, no. 1, 65 (1981).

58. R. Landauer, J. Appl. Phys. 23, no. 7, 779 (1952).